Functional Analysis of the Murine Genes, *MOCS1*

and *Sox15*

Dissertation

vorgelegt von

Heon-Jin Lee

aus Pusan, Korea

Göttingen 2003

D7

Referent: Prof. Dr. W. Engel

Korreferentin: PD Dr. S. Hoyer-Fender

Tag der mündlichen Prüfungen: 02. 07. 2003

INDEX

ABBREVIATIONS

ABI	Applied Biosystem Instrument
APS	Ammonium peroxodisulfate
ATP	Adenosintriphosphate
BAC	Bacterial Artificial Chromosome
BCP	1-bromo-3-chloropropane
bp	base pair
BSA	Bovine serum albumin
°C	Degree Celsius
cDNA	complementary DNA
Cy3	indocarbocyanine
dATP	Desoxyriboadenosintriphosphate
dH2O	distil Water
DAPI	Diamidino-2-phenylindole dihydrochloride
dCTP	Desoxyribocytosintriphosphate
DMSO	Dimethyl sulfoxide
DEPC	Diethylpyrocarbonate
DNA	Deoxyribonucleic acid
DNase	deoxyribonuclease
dNTP	deoxynucleotidetriphosphate
dpc	day post coitus
dT	deoxythymidinate
DTT	Dithiothreitol
EDTA	Ethylene diamine tetraacetic acid
EGL	External granular layer
ES	Embryonic stem
F	Filial generation
FCS	Fetal calf serum
FITC	Fluorescein isothiocyanate
g	gravity
gm	gram
HEPES	N-(-hydroxymethyl)piperazin,N'-3-propansulfoneacid

Abbreviation

HPLC	High performance liquid chromatograpy
hr(s)	hour(s)
IGL	Internal granular layer
IPTG	Isopropyl-ß-thiogalactopyranoside
IVF	In vito fiterlisation
JL	Jackson Laboratory
kb	kilobase
LB	Luria-Bertrani
LIF	Recombinant leukaemia inhibitory factor
LPS	lipopolysaccharides
M	molarity
Mb	Mega base pair
MEF	Mouse embryonic fibroblast
ML	Molecular layer
MoCo	Molybdenum cofactor
MOCS	*Molybdenum cofactor synthesis step*
MOPS	3-[N-Morpholino]-Propanesulfate
mRNA	messenger Ribonucleic acid
mg	milligram
ml	millileter
µl	microliter
µm	micrometer
min	minute
NaAc	Sodium acetate
NBT	Nitro-blue tetrazolium
NCBI	National Center for Biotechnology Information
Neo	*Neomycin*
ng	nanogram
NLS	Nuclear localisation sequence
nm	nanometer
NTP	Nucleotidetriphospate
OD	Optimal density
ORF	Open Reading Frame
PAC	Bacteriophage P1 Artificial Chromosome

Abbreviation

PAGE	Polyacrylamide Gel Electrophoresis
PCR	Polymerase chain reaction
pH	Prepondirance of hydrogen ions
pmol	picomol
PBS	Phosphatebuffersaline
PBT	Phosphatebuffersaline + Tween 20
PMSF	Phenylmethylsulfonyl fuoride
RNA	Ribonucleic acid
Rnase	Ribonuclease
Rnasin	Ribonuclease inhibitor
rpm	revolution per minute
RT	Room temperature
RT-PCR	Reverse transcriptase-PCR
SDS	Sodium Dodecylsulfate
SDS-PAGE	SDS-Polyacrylamide Gel Electrophoresis
sec	second
Sox	<u>S</u>ry b<u>ox</u>
SV 40	Simian Virus 40
Taq	*Thermus aquaticus*
TBE	Tris-Borate-EDTA-Electrophoresis buffer
TE	Tris-EDTA buffer
TEMED	Tetramethylethylene diamine
Tris	Trihydroxymethylaminomethane
U	Unit
UV	Ultra violet
V	Voltage
w/v	weight/volume
X-Gal	5-bromo-4-chloro-3-indolyl-ß-galactosidase

Symbol of amino acids

A	Ala	Alanine
B	Asx	Asparagine or Asparatic acid
C	Cys	Cysteine
D	Asp	Asparatic acid
E	Glu	Glutamic acid
F	Phe	Phenylalanine
G	Gly	Glycine
H	His	Histidine
I	Ile	Isoleucine
K	Lys	Lysine
L	Leu	Leucine
M	Met	Methionine
N	Asn	Asparagine
P	Pro	Proline
Q	Gln	Glutamine
R	Arg	Arginine
S	Ser	Serine
T	Thr	Threonine
V	Val	Valine
W	Trp	Tryptophan
Y	Tyr	Tyrosine
Z	Glx	Glutamine or Glutamic acid

Symbols of nucleic acid

A	Adenosine
C	Cytidine
G	Gaunosine
T	Tymidine
U	Uridine

1. INTRODUCTION

1.1 The *MOCS1* gene

The molybdenum cofactor (MoCo) is an absolute requirement for all molybdoenzymes except nitrogenase of all organisms (Rajagopalan and Johnson 1992). The biosynthetic pathway of MoCo has first been discovered in bacteria (Rajagopalan and Johnson 1992), in plants (Mendel 1997), and finally in humans (Reiss et al. 1998b). Disease-causing mutations have been identified in the conserved genes *MOCS1* (Molybenum cofactor synthesis-step 1) (Reiss et al. 1998a; Reiss et al. 1998b) and *MOCS2* (Molybdenum cofactor synthesis-step 2) (Reiss et al. 1999; Johnson et al. 2001) as well as in the gene for gephyrin (Reiss et al. 2001), a protein that, besides its role in MoCo biosynthesis (Reiss 2000), has an additional function in neurotransmitter receptor clustering (Kirsch et al. 1993). Human genes involved in the MoCo biosynthesis pathway are summarized in Figure 1.1.

Both *MOCS1* and *MOCS2* have a bicistronic architecture that only for a few cellular mammalian genes have been described so far. Bicistronic genes are able to produce a bicistronic transcript with the potential to encode two independent proteins from adjacent open reading frames (ORFs). *MOCS1* and *MOCS2* genes have an identical and very low expression profile, and show extremely conserved C-terminal ends in their 5' ORFs (Reiss 2000).

The *MOCS1* gene is expressed in various tissues. However, it shows relatively high expression in the liver. Increased expression in the liver coincides with high sulfite oxidase activity in this organ (Reiss et al. 1998b).

The *MOCS1* gene has been reported to produce two proteins (MOCS1A and MOCS1B) from non-overlapping ORFs within a bicistronic transcript (Fig. 1.2). These two proteins are involved in the first MoCo biosynthesis step leading to "precursor Z". That is this bicistronic gene encodes the two MoCo biosynthesis enzymes, MOCS1A and MOCS1B, in two consecutive open reading fames and their expression involves a conserved splicing pattern leading to a functional MOCS1A protein without MOCS1B domain and activity and a fusion protein with MOCS1B activity and a non-functional MOCS1A domain (Gray and Nicholls 2000; Hanzelmann et al. 2002)
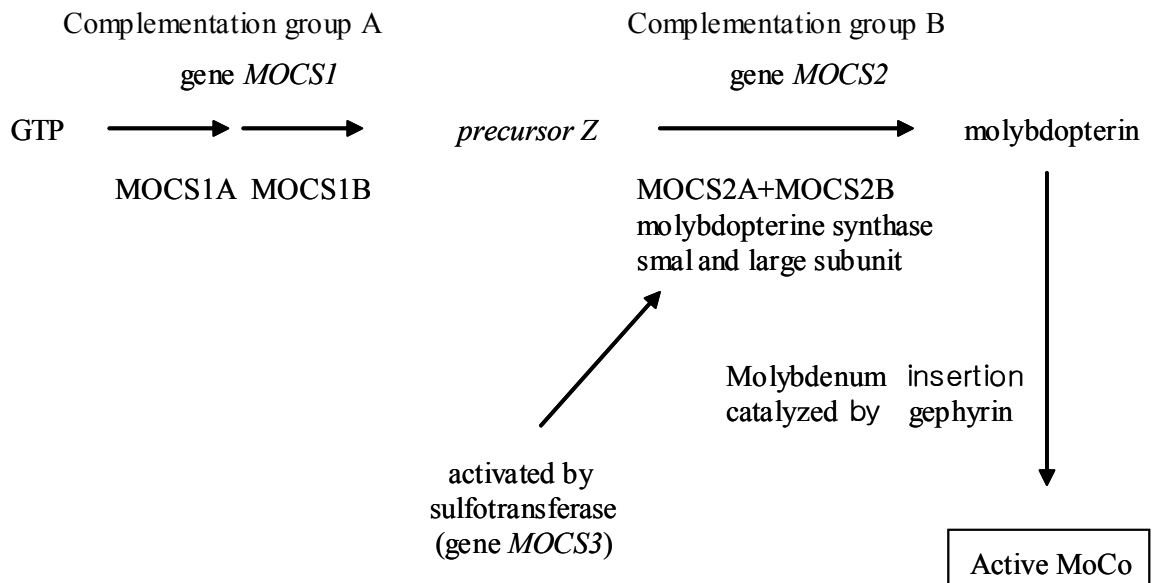
Figure 1.1: Summary of the roles of human genes involved in the MoCo biosynthesis pathway (adapted by Reiss et al., 2000)
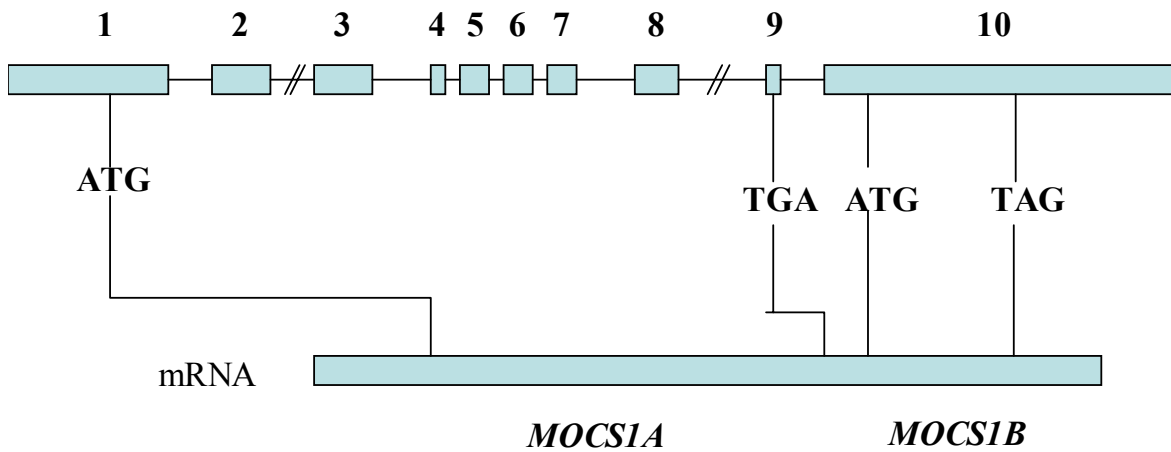
Figure 1.2: Genomic structure of human and murine *MOCS1*. The exons are numbered in the upper line. Exons and introns are not drawn to scale. Start and stop codons for MOCS1A and MOCS1B are indicated.

MoCo deficiency (OMIM, 252150; http://www.ncbi.nlm.nih.gov) is an autosomal recessive disease and results in a fatal neurological disorder similar to the isolated form of sulfite oxidase deficiency (Johnson 2001). Although the clinical spectrum may show variations among patients, the most prominent features are neonatal seizures that do not respond to therapy, axial hypotonia, peripheral hypertonicity, lens dislocation, abnormal facial features, feeding difficulties, urinary calculi, and mental retardation (Hansen et al. 1993). Neurological damage due to sulfite toxicity, sulfate deficiency, or a combination of both, is irreversible, and most patients die between two and six years of age. Biochemically, there are decreased uric acid levels in serum and increased excretion of sulfite, thiosulphate, S-sulfocysteine, taurine, xanthine, and hypoxanthine in urine (van Gennip et al. 1994). MoCo replacement seems to be not suitable because isolated molybdenum cofactor is unstable. Dietary methionine restriction, cysteine and sulfate supplementation, and low sulfur-containing amino acids have been used for treatment. However, besides having a positive biochemical response, they do not change the neurodevelopmental outcome and prognosis (Boles et al. 1993).

Studies of cell cultures derived form MoCo deficient patients suggest the existence of two complementation groups that are thought to represent two steps of molybdopterin synthesis (i) formation of precursor Z from GTP (defective in type A cells); and (ii) conversion of the precursor by a heterodimeric molybdopterin synthase (defective in type B cells) (Johnson et al. 1989).

Table 1.1 shows the distribution of identified mutations among MoCo-deficient patients. *MOCS1* mutations in case of complementation group A are responsible for two-third of cases. Three mutations are found quite frequently: (1) 418+1G$\rightarrow$A, affecting the MOCS1A protein, (2) R319Q, also affecting MOCS1A protein, and (3) 1523del AG, affecting the MOCS1B protein. These findings have been used for prenatal diagnosis using DNA obtained from chorionic villi sampling (Reiss et al. 1998a). It was pointed out that all described *MOCS1* and *MOCS2* mutations affect one or several highly conserved motifs. No missense mutations of a less conserved residue were identified. This mirrors the absence of mild or partial forms of MoCo deficiency and supports the hypothesis of a qualitative 'yes or no' mechanism rather than quantitative kinetics for MoCo functions, i.e., this function is either completely abolished or sufficient for a normal phenotype. The minimal expression of the *MOCS* genes concurs with this theory and would predict a low level of transfected or expressing cells that would be adequate for somatic biochemical or

gene therapy (Reiss 2000). Furthermore, precursor-producing cells seem to be capable of feeding their precursor-deficient neighbour cells (Johnson et al. 1989).

Affected protein	Number of patients (n)	Frequency (%)
MOCS1 A	21	51
MOCS1 B	6	15
MOCS2 A	2	5
MOCS2 A/B	1	2
MOCS2 B	9	22
Undelected	2	5

Table 1.1: Mutation distribution among 41 patients with combined MoCo deficiency (adapted by Reiss 2000).

Prenatal diagnosis for MoCo deficiency may be performed by assay of sulfite oxidase activity in cultured amniotic cells of chorionic villus biopsy (Gray et al. 1990; Johnson et al. 1991). Interestingly, however, low activity of MoCo was found in amniotic fluid of *MOCS1-/-* mouse embryos. This observation implies that a heterozygous mother can supplement the materials for MoCo activity to the homozygous embryos or fulfil a clearance function. In addition, this effect is to be considered for the prenatal diagnosis to avoid false positive patient.

To determine the function of the *MOCS1* gene and to establish an animal model for MoCo deficiency, the exon 3 of the murine *MOCS1* gene was removed by homologous recombination with a targeting vector. *MOCS1-/-* mice show a severe phenotype comparable to that of human MoCo-deficient patient and die 1 to 10 days after birth.

1.2 The *Sox15* gene

The Sox family of transcription factors was first identified in mammals in 1990 with the isolation and characterization of the gene for mammalian testis-determining factor Sry, which is located on the Y chromosome of mouse and man (Gubbay et al. 1990). Sry was found to contain a domain with similarity to the DNA-binding domain of the abundant non-histone chromosomal proteins HMG-1 and HMG-2. This so called HMG domain is present in a large number of proteins which all belong to the HMG box superfamily. There are few amino acid positions within the 70-80 amino acid long domain which are conserved throughout the HMG box superfamily (Laudet et al. 1993). Thus HMG domains can be highly diverse. However, in subgroups of the superfamily, strong conservation of HMG box sequence is observed. Such a subgroup is the Sox protein family. Proteins are grouped into the Sox family if they contain an HMG domain with strong amino acid similarity (usually >50%) to the HMG domain of SRY, which is also known as the <u>SRY</u> b<u>ox</u>. It is this box that gave the Sox protein family its name. *Sox* genes belong to a multigenic family classified into nine groups according to their amino acid sequence and genomic organization (Wegner 1999) (Fig. 1. 3)

Sox proteins bind to specific DNA sequence. Among HMG box proteins, this ability for sequence-specific DNA recognition is unique to Sox proteins. The consensus motif for Sox proteins has been defined as the heptameric sequence 5'-(A/T)(A/T)CAA(A/T)G-3' (Harley et al. 1994).
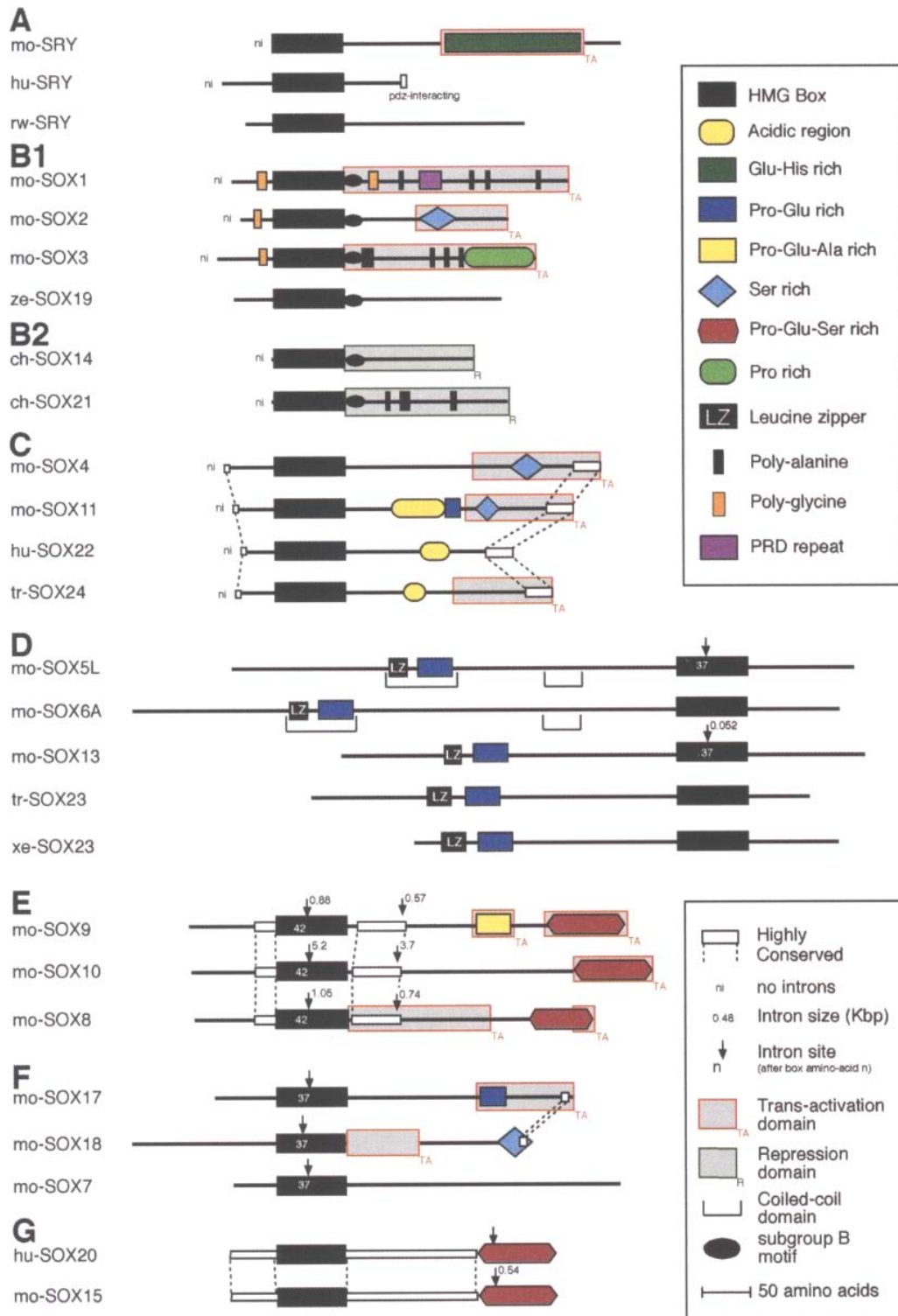
Figure 1.3: Schematic representation of Sox proteins highlighting conservation within Sox family groups. Proteins are arranged in groups as defined by HMG domain sequence. Various structure features, motifs, and functional regions (demonstrated or putative) are shown along with intron positions and sizes where known. Genomics structures are known in some cases-"ni" (no intron) indicates that an intronless structure has been reported. ch, chicken; hu, human; mo, mouse; rw, tammar wallaby; tr, rainbow trout; xe, frog; ze, zebrafish. (adapted by Bowles et al. 2000).

Most Sox proteins were originally identified not as full-length proteins, but as PCR-derived partial sequences corresponding to their HMG domains. Between 15 and 20 different Sox proteins have already been identified in both mouse and man. If partially cloned Sox proteins are taken together, it has to be assumed that the number of Sox proteins in any given vertebrate species will be >20 (Wegner 1999). Therefore, most tissues and cell types express a Sox protein during at least one stage of their development. This indicates that Sox proteins are widely distributed throughout the animal kingdom. Although it is conceivable that co-expressed Sox proteins perform different functions, especially when belonging to different subgroups and being distantly related, their recognition of similar DNA motif suggests that they might influence each other's activity or function redundantly (Wegner 1999).

The increasing number of cases in which mutations in Sox proteins are associated with human disease further highlights the importance of this group of transcription factors. Although some of *Sox* genes have not been characterized in detail, all studies indicated that *Sox* genes, like *SRY*, have roles in the regulation of development. *Sox4* is expressed in T and pre-B lymphocytes and participates in cardiac development and lymphocyte differentiation (van de Wetering et al. 1993; Schilham et al. 1996). Inactivation of a single *Sox9* allele in human is the cause of a severe skeletal malformation syndrome called campomelic dysplasia. In male patients, campomelic dysplasia is often associated with XY sex reversal (Wagner et al. 1994; Foster 1996; Meyer et al. 1997). It is known that *Sox9* is required for chondrogenesis as well (Ng et al. 1997). *Sox1*, *Sox2* and *Sox3* are involved in the development of the central nervous system in chicken and regulate δ-crystalline gene expression in the eyes (Kamachi et al. 1998; Nishiguchi et al. 1998). *Sox10* is essential for the peripheral nervous system development and has been identified as causative gene for Hirschsprung-Waardenburg syndrome (Bondurand et al. 1998; Pingault et al. 1998). However some *Sox* genes doesn't have clear function, for example, *Sox8* knock-out mice show only idiopathic reduction in weight, despite strong expression of the genes in many tissues (Sock et al. 2001).

Murine *Sox15* and its human orthologue *SOX20* gene were identified as the group G of *Sox* gene family. The two proteins share 74% homology in their coding sequence. Although most of the Sox proteins are encoded from a single exon, murine *Sox15* and human *SOX20* are the only members of the Sox family having an intron located 3' end and not interrupting the HMG domain(Beranger et al. 2000). Existing reports on *SOX20* expression are partially controversial. Northern blot analysis failed to detect *SOX20* specific transcript

in many adult and fetal tissues (Meyer et al. 1996). However, using the RT-PCR assay, the human *SOX20* gene transcript was detected in a wide variety of tissues, including fetal brain, spinal cord, thymus, heart, adrenal, and in all adult tissues tested including adult brain, lung, heart, liver, spleen, gut, small intestine, kidney, and testis (Vujic et al. 1998). In addition, another group (Hiraoka et al. 1998) has analysed the expression of human *SOX20* in different fetal and adult tissues and found that the expression of the gene is restricted to fetal testis. In case of *Sox15*, by RT-PCR, *Sox15* transcripts were detected, in a wide variety of adult tissues, as well as in early mouse embryos. However, *Sox15* transcript appeared to be most abundant in skeletal muscle and brain (Beranger et al. 2000).

In this study, we found the *Sox15* expression in the ES cells and myoblasts by using Northern blot.

A recent study has revealed that *Sox15* is involved in skeletal muscle differentiation. This in vitro study suggested that *Sox15* is an inhibitor of myoblast differentiation, as revealed by experiments involving cultured myoblasts (Beranger et al. 2000). Muscle differentiation is characterized by withdrawal of myoblasts from the cell cycle, induction of muscle-specific gene expression and cell fusion into multinucleated myotubes. All these events are coordinated by members of the MyoD family of myogenic proteins (Yun and Wold 1996; Miller et al. 1999).

To determine the exact function of *Sox15*, we have generated *Sox15* deficient mice by homologous recombination of targeting vector and investigated the role of *Sox15* gene in muscle differentiation and regeneration concerning with myogenic genes.

1.3 Objectives in this work

The aims and experimental approaches devised in this study can be placed in several categories, which are described below:

1) We generated a mouse model for MoCo-deficiency to find a suitable therapy for the human patients.
2) To elucidate the expression of the murine *MOCS1* gene, we studied expression pattern of *MOCS1* gene from different developmental stages of tissues.
3) We examined MoCo activity in the *MOCS1* homozygous embryos whether there is an effect from a healthy mother.

4) Generation of a specific anti-Sox15 antibody and expression analysis of *Sox15* in different tissues and cell types was performed.

5) To understand the role of *Sox15,* we decided to generate knock-out mice for *Sox15* by homologous recombination.

6) To search the function of *Sox15* during muscle differentiation, we isolated myoblasts from *Sox15*-/- mice and then, examined differentiation capacity and determined the expression of different myogenic factors in *Sox15*-/- myoblasts.

7) To determine the role of *Sox15* during muscle regeneration, crash-injured muscle of *Sox15*-/- mice was examined and possible role of the *Sox15* gene was postulated.

2. MATERIALS AND METHODS

2.1 Materials

2.1.1 Chemicals

Acrylamide	Serva, Heidelberg
Acetic acid	Merck, Darmstadt
Agar	Difco, Detroit, USA
Agarose	GibcoBRL, Karlsruhe
Ammonium acetate	Fluka, Neu Ulm
Ammonium persulfate	Sigma, Deisenhofen
Ampicillin	Sigma, Deisenhofen
Ampuwa	Fresenius, Bad Homburg
Bacto-tryptone	Difco, Detroit, USA
Bacto-Yeast-Extract	Difco, Detroit, USA
BCIP	Boehringer, Mannheim
bFGF	Boehringer Mannheim
Bisacrylamide	Serva, Heidelberg
Blocking powder	Boehringer, Mannheim
Bromophenol blue	Sigma, Deisenhofen
BSA	Biomol, Hamburg
Coomasie G-250	Sigma, Deisenhofen
Choloroform	Baker, Deventer, NL
DAPI	Vector, Burfingame
Dextran sulfate	Amersham, Freiburg
Diethyl pyrocarbonate (DEPC)	Sigma, Deisenhofen
Dimethyl sulfoxid (DMSO)	Merck, Darmstadt
Dithiothreitol	Sigma, Deisenhofen
DNA Markers	GibcoBRL, Karlsruhe
dNTPs (100 mM)	GibcoBRL, Karlsruhe
Dye Terminator Mix	Applied Biosystems
Ethanol	Baker, Deventer, NL
Ethidium bromide	Sigma, Deisenhofen

Ficoll 400	Amersham, Freiburg
FCS	Gibco/BRL, Karlsruhe
Formaldehyde	Gibco/BRL, Karlsruhe
Formamide	Fluka, Neu Ulm
Glutaraldehyde	Sigma, Deisenhofen
Glycerol	Gibco/BRL, Karlsruhe
Glycine	Biomol, Hamburg
Goat serum	Sigma, Deisenhofen
HCl	Merck, Darmstadt
H_2O_2	Merck, Darmstadt
HEPES	Merck, Darmstadt
Ionophore A23187	Calbiochem
IPTG	Biomol, Hamburg
Isopropanol	Merck, Darmstadt
IVF Medium	Medicult
KCl	Merck, Darmstadt
Lambda DNA	Boehringer, Mannheim
Liquemin N 25000 (Heparin)	Roche, Karlsruhe
Methanol	Merck, Darmstadt
$MgCl_2$	Merck, Darmstadt
MOPS	Merck, Darmstadt
Methyl benzoat	Fulka, Neu Ulm
β-Mercaptoethanol	Serva, Heidelberg
Mineral oil	Sigma, Deisenhofen
NaCl	Merck, Darmstadt
Na_2HPO_4	Merck, Darmstadt
NaH_2PO_4	Merck, Darmstadt
$NaHCO_3$	Merck, Darmstadt
NaN_3	Merck, Darmstadt
NaOH	Merck, Darmstadt
NBT	Boehringer, Mannheim
Orange G	Sigma, Deisenhofen
Osmium tetraoxide	Sigma, Deisenhofen
PBS	Gibco/BRL, Karlsruhe

Phosphoric acid	Merck, Darmstadt
Picric acid	Fulka, Neu Ulm
Poly [dI-dC]	Amersham, Freiburg
Phenol	Gibco/BRL, Eggenstein
Proteinase K	Boehringer, Mannheim
Protein marker	Biorad, Sigma
Radioactive substances:	
$[\gamma^{32}P]$-ATP, $[\alpha^{32}P]$-dCTP	Amersham, Braunschweig
Rediprime^{TM} II	Amersham, Freiburg
RNase Inhibitor	Boehringer, Mannheim
RNA length standard	Gibco/BRL, Eggenstein
RNase away	Biomol, Hamburg
Salmon sperms DNA	Sigma, Deisenhofen
SDS	Serva, Heidelberg
Select Peptone	Gibco/BRL, Eggenstein
Sodium acetate	Merck, Darmstadt
Sodium citrate	Merck, Darmstadt
TEMED	Serva, Heidelberg
Triton X-100	Serva, Heidelberg
Tris	Sigma, Deisenhofen
Tween-20	Sigma, Deisenhofen
X-Gal	Biomol, Hamburg
Xylencyanol	Bio-Rad, München
Cell culture media	Gibco/BRL

All those chemicals which are not mentioned above were bought from either Merck, Darmstadt or Roth, Karlsruhe.

2.1.2 Solutions, buffers and media

2.1.2.1 Agarose gel electrophoresis

5x TBE buffer	450 mM Trisbase
	450 mM Boric acid
	20 mM EDTA (pH 8)

Glycerol loading buffer -I	10 mM Tris/HCl (pH 7.5)
	10 mM EDTA (pH 8)
	0.025% Bromophenol blue
	0.025% Xylenecyanol
	30% Glycerol

Glycerol loading buffer -II	10 mM Tris/HCl (pH 7.5)
	10 mM EDTA (pH 8)
	0.025% Orange G
	30% Glycerol

2.1.2.2 SDS-PAGE

40% Acrylamide stock solution	Acrylamide 29.2% (w/w)
	Bis-acrylamide 0.8% (w/w)
	10% Ammonium persulfate solution in H_2O

Sample buffer (2x)	0.5 M Tris/HCl (pH 6.8)
	20% Glycerol
	4% SDS
	10% β-Mercaptoethanol

Running buffer (5x)	25 mM Tris/HCl (pH 8.3)
	192 mM Glycine
	0.1% SDS

Stacking gel buffer (4x)   0.5 M Tris/HCl (pH 6.8)

                                            0.4% SDS

Separating gel buffer (4x)   1.5 M Tris/HCl (pH 8.3)

                                            0.4% SDS

2.1.2.3 Electronic mobility shift assay

40% Acrylamide stock solution   Acrylamide 29.2% (w/w)

                                            Bis-acrylamide 0.8% (w/w)

5x TBE buffer   450 mM Trisbase

                                           450 mM Boric acid

                                           20 mM EDTA (pH 8)

2.1.2.4 Frequently used buffers and solutions

Denaturation solution   1.5 M NaCl

                                            0.5 M NaOH

Denhardt´s solution (50x)   1% BSA

                                            1% Polyvinylpyrrolidon

                                            1% Ficoll 400

Depurization solution   0.25 N HCl

E-buffer (10x)   300 mM $NaH_2 PO_4$

                                            50 mM EDTA

Elution buffer   1.5 M NaCl

                                            20 mM Tris/HCl (pH 7.5)

                                            1 mM EDTA

Bouin's solution   15 volume of picric acid (in H_2O)

	5 volume Formaldehyde
	1 volume Acetic acid
Hybridisation solution I	5x SSPE solution
	5x Denhardt´s solution
	0.1% SDS
Hybridisation solution II	5x SSC
	5x Denhardt´s solution
	10% Dextran sulfate
	0.1% SDS
Kinase buffer (10x)	100 mM Tris/HCl (pH 7.4)
	100 mM $MgCl_2$
	100 mM DTT
	1 mM ATP
Ligation buffer (10x)	600 mM Tris/HCl (pH 7.5)
	80 mM $MgCl_2$
	100 mM DTT
Lysis buffer I	100 mM Tris/HCl (pH 8.0)
	100 mM NaCl
	100 mM EDTA
	0.5% SDS
Lysis-buffer II	100 mM Tris/HCl (pH 8.0)
	5 mM EDTA
	200 mM NaCl
	0.2% SDS
	100 µg/ml proteinase K
10 X MOPS Buffer	41.8 g MOPS
	16.6 ml 3 M Sodium acetate

	20 ml 0.5 M EDTA
	in 1 liter of DEPC Water
	adjust pH to 6.75
Neutralisation solution	1.5 M NaCl
	1 M Tris/HCl (pH 7.0)
PBS buffer	130 mM NaCl
	7 mM $Na_2 HPO_4$
	4 mM $NaH_2 HPO_4$
PBT buffer	0.1% Tween-20 in PBS (1x)
SSC (20x)	3 M NaCl
	0.3 M Na_3 citrate (pH 7.0)
SSPE (20x)	0.02 M EDTA
	0.2 M $NaH_2 PO_4$
	3.6 M NaCl (pH 7.0)
Stop-Mix I	95% Formamide
	20 mM EDTA
	0.05% Bromphenol blue
	0.05% Xylene cyanol
Stop-Mix II	15% Ficoll 400
	200 mM EDTA
	0.1% Orange G
TE-buffer	10 mM Tris/HCl (pH 8.0)
	1 mM EDTA
Washing solution I	2x SSC
	0.1% SDS

Washing solution II   0.2x SSC

2.1.3 Laboratory materials

The laboratory materials, which are not listed here, were bought from Schütt and Krannich (Göttingen).

Whatman blotting paper   Schleicher and Schüll, Dassel
(GB 002, GB 003 and GB 004)

Cell culture flask   Greiner, Nürtingen

Culture slides   Falcon

Dialysis hoses   Serva, Heidelberg

Disposable filter Minisart NMI   Sartorius, Göttingen

Filter paper 0858   Schleicher and Schüll, Dassel

HPTLC Aluminum folio   Merck, Darmstadt

HiTrap NHS activated column   Amersham, Braunschweig

Hybond C   Amersham, Braunschweig

Hybond N   Amersham, Braunschweig

Petri dishes   Greiner, Nürtingen

Pipette tips   Eppendorf, Hamburg

Microcentrifuge tubes   Eppendorf, Hamburg

Transfection flask   Lab-Tek/Nalge, Nunc, IL, USA

X-ray films   Amersham, Braunschweig

Superfrost Slides   Menzel, Gläser

2.1.4 Sterilisation of solutions and equipments

All solutions that are not heat sensitive were sterilised at 121°C, 10^5 Pa for 60 min in an autoclave (Webeco, Bad Schwartau). Heat sensitive solutions were filtered through a disposable sterile filter (0.2 to 0.45 μm pore size). Plastic wares were autoclaved as above. Glasswares were sterilised overnight in an oven at 220°C.

2.1.5 Media, antibiotics and agar-plates

2.1.5.1 Media for bacteria

LB Medium (pH 7.5):   1% Bacto-trypton

0.5% Yeast extracts

1% NaCl

LB-Agar: 1% Bacto-trypton

0.5% Yeast extracts

1% NaCl

1.5% Agar

The LB medium was prepared with distilled water, autoclaved and stored at 4°C.

2.1.5.2 Media for cell culture

ES-cell medium:

DULBECCO´s MEM (DMEM)

0.1 mM   Non essential amino acids

1 mM   Sodium pyruvate

10 µM   ß-Mercaptoethanol

2 mM   L-Glutamine

20%   Fetal calf serum (FCS)

1000 U/ml   Recombinant leukaemia inhibitory factor (LIF)

Fibroblast cell medium (MEFs):

DULBECCO´s MEM (DMEM)

2 mM   L-Glutamine

10%   FCS

Myoblast cell medium

Ham's F-10

2mM   L-Glutamine

                              20%   FCS

For long time storage of the cells in liquid nitrogen, the following freezing media were used:

ES cell – freezing medium: 30%   ES cell medium

                                        50%   FCS

                                        20%   DMSO

MEFs cells – freezing medium: 30%   EmFi cell medium

                                        50%   FCS

                                        20%   DMSO

Myoblast cell-freezing medium   30%   Myoblast cell medium

                                        50%   FCS

                                        20%   DMSO

2.1.6 Antibiotics

Stock solutions were prepared for the antibiotics. The stock solutions were then filtered through sterile disposable filters and stored at –20°C. When antibiotics were needed, in each case, it was added after the autoclaved medium has cooled down to a temperature lower than 55°C.

	Master solution	Solvent	Final concentration
Ampicillin	50 mg/ml	H_2O	50 µg/ml
Kanamycin	25 mg/ml	H_2O	50 µg/ml
G 418	40mg/ml	PBS	400 µg/ml
Gancyclovir	100 mM	PBS	2 µM

2.1.7 IPTG / X-Gal plate

LB-agar with 50 µg/ml ampicillin, 100 µM IPTG and 0.4% X-Gal was poured into petri dishes. The dishes were stored at 4°C.

2.1.8 Bacterial strains

E. coli JM 109	(Promega, Wisconsin, USA)
E. coli DH5α	(GibcoBRL, Karlsruhe)
E. coli TOP10	(Invitrogen, Karlsruhe)

2.1.9 Eucaryotic strains

Swiss3T3, mouse embryonic fibroblast cell line, ATCC, Rockville, USA
        "NIH Swiss Mouse"
RI mouse embryonic stem cell line (Passage 11), Dr. A. Nagi, Toronto, Canada

2.1.10 Plasmids

pBluesript SK (+/-)	(Stratagene, La Jolla, USA)
pBluesript KS (+/-)	(Stratagene, La Jolla, USA)
pGEM-T	(Promega, Wisconsin, USA)
pGEM-T Easy	(Promega, Wisconsin, USA)
pTriEX-1.1 Neo	(Novagen, Darmstadt, Germany)
pPNT	Tybulewicz et al., 1991
pUC 18	Norander et al., 1983
pZERO-2	(Invitrogen, Karlsruhe, Germany)
Lawrist 7	RZPD, Berlin

2.1.11 Synthetic oligonucleotides

The synthetic oligonucleotide primers used in this study were obtained from Roth (Karlsruhe, Germany) and dissolved in water to a final concentration of 100 pmol/µl.

MOCS1 antisense (MGF1):	5' GGC AGA GGC TGT TCA ACA TGG 3'
MOCS1 sense (MOCS49):	5' CTG GGT TCC TGT GCC ATC TAG 3'
Pgk1:	5' TCT GAG CCC AGA AAG CGA AGG 3'

Sox15 antisense (SGF1):	5' GTG TCT GTA GTG AGA AGG AAG GC 3'
Sox15 sense (SGR1):	5' CCA TGC CTC CAA CCC ACG AAT 3'
WT antisense:	5' GTC ACT CAG ATA GTT GAA GCC ATT TAG 3'
MDX antisense:	5' GTC ACT CAG ATA GTT GAA GCC ATT TAA 3'
MDX –WT sense:	5' AAC TCA TCA AAT ATG CGT GTT AGT G 3'
MOCS27	5' CCA GTA TCA AAA CTC CCA TTG 3'
MOCS28	5' GTG ATC TCA GGG AGC CGG AC 3'
MOCS-F	5' GGC CGA CAA CAT AGT TAC CT 3'
MOCS-8	5' CGG TTC TTC ATC TGG GGC AA 3'
SupF1	5' CTT TCA AAG GGC TGC TGG TGC 3'
SupR2	5' CAG GGG CGA GTT CCA GGT CAG C 3'
SOXF4	5' CAA CTA TTC GAC AGC CTA CCT GCC 3'
SOXR3	5' GTG TTT AGT GTG CAT TCT GGT TCC 3'
MyoD-F	5' AGG CTC TGC TGC GCG ACC 3'
MyoD-R	5' TGC AGT CGA TCT CTC AAA GCA CC 3'
c-Met F	5' GAA TGT CGT CCT ACA CGG CC 3'
c-Met R	5' CAC TAC ACA GTC AGC ACA CTG C 3'
Myf5 F	5' TGC CAT CCG CTA CAT TGA GAG 3'
Myf5 R	5' CCG GGG TAG CAG CTG TCA GTT G 3'
Pax7 F	5' GTG GGG TCT TCA TCA ACG GTC 3'
Pax7 R	5' GCA GCG GTC CCG GAT TTC CA GC 3'
Myf5-1	5' GTG TCC AGC TTG GAT TGC TTG 3'
Myf5-2	5' GGG GCT TCA TTT ACC AGG CAT 3'
Hprt F:	5' CCT GCT GGA TTA CAT CAA AGC ACT G 3'
Hprt R:	5' GTC AAG GGC ATA TCC TAC AAC AAA C 3'
Mocs66	5' CCA GGG AGC CCT GAC TTT GCC 3'
Mocs29	5' GCA GGA TCA CAC TTG AGA CAG 3'
T7:	5' TAA TAC GAC TCA CTA TAG GG 3'
T3:	5' ATT AAC CCTT CAC TAA AG 3'
SP6:	5' AGG TGA CAC TAT AGA ATA C 3'
Poly T:	TTTTTTTTTTTTTTTTTTT
T-cell bindg factor:	5' GGAGA-CTGAGAACAAAGCGCTCTCA 3'
	3' CCTCT-GACTCTTGTTTCGCGAGAGT 5'
Mut 3-4:	5' GGAGACTGAGCACAAAG-CGCTCTCA 3'

31

<div align="center">3' CCTCTGACTCGTGTTTC-GCGAGAGT 5'</div>

2.1.12 cDNA probes

EF-2 cDNA	Hanes et al.1992
Murine *MOCS1* cDNA	In this study
Murine *Sox15* cDNA	In this study
β-actin cDNA	Clontech, Heidelberg, Germany

2.1.13 Mouse strains

Mice strains C57BL/6J, 129/Sv, and NMRI were initially ordered from Charles River Laboratories, Wilmington, USA and further inbred in Animal facility of Institute of Human Genetics, Göttingen.

The *mdx* mice were generously donated from Dr. Jockusch (Developmental Biology Unit, University of Bielefeld, Germany)

2.1.14 Antibodies

Mouse monoclonal against desmin, goat anti-rabbit-IgG-conjugated to alkaline phosphatase, FIFC-conjugated goat anti-mouse and Cy3-conjugated goat anti-rabbit antibodies were purchased from Sigma (Deisenhofen, Germany)

Rabbit anti-mouse Sox15 polyclonal antibody was generated in the present study.

2.1.15 Enzymes

Restriction enzymes (with supplied buffers)	(GibcoBRL, NEB)
Collangenase (Type II)	(Sigma, Deisenhofen)
DispaseII (grade II)	(Roche)
Klenow Fragment	(GibcoBRL, Karlsruhe)
Mung bean exonuclease	(GibcoBRL, Karlsruhe)
Proteinase K	(Sigma, Deisenhofen)
Platinum Taq polymerase	(GibcoBRL, Karlsruhe)
RNase A	(Qiagen, Hilden)
RNase H	(GibcoBRL, Karlsruhe)
RNase inhibitor	(GibcoBRL, Karlsruhe)

Superscript-II	(GibcoBRL, Karlsruhe)
Taq polymerase	(GibcoBRL, Karlsruhe)
T4 polynucleotide Kinase	(NEB)
T4 DNA ligase	(Promega)
Tyrpsin	(GibcoBRL, Karlsruhe)

2.1.16 Kits

Advantage-HF2 PCR kit	(CLONTECH)
BigDye Terminator Cycle Sequencing Ready Reaction Kit	(Applied Biosystems)
DYEnamic ET-Terminator mix	(Amersham Pharmacia)
Endo Free Plasmid Maxi Kit	(Qiagen, Hilden)
GST-Bind kit	(Novagen, Darmstadt)
JETsorb Gel Extraction Kit	(Genomed)
JETstar Plasmid MIDI Kit	(Genomed)
Large Construct Plasmid Kit	(Qiagen, Hilden)
Megaprime DNA Labeling Kit	(Amersham Pharmacia)
Maxi Plasmid Kit	(Qiagen, Hilden)
Mega Plasmid Kit	(Qiagen, Hilden)
Mini Plasmid Kit	(Qiagen, Hilden)
PCR Purification Kit	(Qiagen, Hilden)
QIAquick Gel Extraction Kit	(Qiagen, Hilden)
5`RACE Kit	(GibcoBRL, Karlsruhe)
5`and 3`RACE Kit	(Invitrogen, Karlsruhe)
RNA Easy Kit	(Qiagen, Hilden)
Rediprime^{TM} II Random Prime Labeling System	(Amersham Pharmacia)
SulfoLink Kit Trial Kit	(PIERCE, USA)

2.1.17 Instruments

ABI PRISM 377 DNA Sequencer	(Applied Biosystem)
ABI 3100 Genetic Analyzer	(Applied Biosystem)

Microscope BX60   (Olympus)

GeneAmp PCR System 9600   (Perkin Elmer)

Microtiterplate-Photometer   (BioRad)

Molecular Imager FX   (BioRad)

Phosphoimager Screen   (Kodak)

Semi-Dry-Blot Fast Blot   (Biometra)

Spectrophotometer Ultraspec 3000   (Amersham Pharmacia)

SpeedVac concentrator SVC 100H   (Schütt)

Thermomixer 5436   (Eppendorf)

Turboblotter^{TM} (Schleicher & Schüll)

UV Stratalinker^{TM} 1800   (Leica)

Video-Documentationsystem   (Herolab, Heidelberg)

X-Ray Automatic Processor Curix 60   (Agfa)

CASA system   (Hamilton Thorne Research)

2.2 Methods

2.2.1 Isolation of nucleic acids

2.2.1.1 Isolation of plasmid DNA
(Sambrook et al., 1989)

2.2.1.1.1 Small-scale isolation of plasmid DNA

A single *E.coli* colony was inoculated in 5 ml of LB medium with the appropriate antibiotic and incubated in a shaker for 16 hrs at 37°C with a speed of 160 rpm. 1 ml of this saturated culture was used for making glycerol stock and rest of the culture was centrifuged at 5000xg for 15 min. The pellet was resuspended in 150 µl of solution P1. The bacterial cells were lysed with 300 µl of P2 solution and than neutralised with 200 µl of solution P3. The precipitated solution was incubated on ice for 15 min, and centrifuged at 13000xg at 4°C. The supernatant was transferred into a new tube, and 1 ml of 100% ethanol was added to precipitate the DNA. It was then stored in ice for 15 min, centrifuged at full speed for 20 min, and finally the pellet was washed with 70% ethanol and after air-drying dissolved in 30 µl of TE buffer (adapted from Birnboim and Doly, 1979).

P1:	50 mM	Tris-Cl, pH 8.0
	10 mM	EDTA
	100 µg/ ml	RNase A
P2:	200 mM	NaOH,
	1%	SDS
P3:	3.0 M	Potassium acetate, pH 5.5

2.2.1.1.2 Large-scale preparation of plasmid DNA

A single clone was inoculated in 2 ml LB medium with appropriate antibiotic as a pre-culture for 8 hrs in 37°C shaker. In 100 ml LB medium with appropriate antibiotic, this pre-culture was added in a dilution of 1/100 fold and incubated overnight at 37°C with shaking. The saturated culture was centrifuged at 6000xg for 15 min. The pellet was resuspended in 5 ml of solution P1 and cells were lysed with P2 and P3 as described above. The precipitated solution was centrifuged at 20000xg for 30 min at 4°C. Meanwhile, the column (Qiagen-tip) that was provided with the midi preparation kit was equilibrated with 10 ml of QBT solution. After centrifugation, the lysate was poured into this equilibrated column to allow the DNA to bind with the resin present in the bed of the column. The column was then washed twice with 10 ml of solution QC. Finally, the DNA was eluted with 5 ml of QF solution. To precipitate the DNA, 3.5 ml of isopropanol was added and mixed thoroughly and centrifuged at 14000xg for 30 min at 4°C. The DNA pellet was washed with 70% ethanol and dissolved in 100 µl of TE.

QBT:	750 mM	Sodium chloride
	50 mM	MOPS pH 7.0
	15 %	Ethanol
	0.5 %	Triton X-100

QC:	1 mM	Sodium chloride
	50 mM	MOPS pH 7.0
	15 %	Ethanol

QF:	1.25 M	Sodium chloride
	50 mM	Tris/ HCl pH 8,5

2.2.1.1.3 Endotoxin free preparation of plasmid DNA

Endotoxins, also known as lipopolysaccharides or LPS, are cell membrane components of Gram-negative bacteria (e.g., *E.coli*). During lysis of bacterial cells, endotoxin molecules are released from the outer membrane into the lysate. Endotoxins strongly influence the transfection efficiency of cultured cells like embryonic stem (ES). Increased endotoxin

levels lead to sharply reduced transfection efficiencies. Endofree plasmid preparation kit integrates endotoxin removal into standard plasmid preparation procedure. The neutralised bacterial lysate was filtered through a QIA filter cartridge (provided in kit) and incubated on ice with a specific Endotoxin Removal buffer (patented by Qiagen). The endotoxin removal buffer prevents LPS molecules from binding to the resin in the columns (QIAGEN-tips) thus allowing purification of DNA containing less than 0.1 endotoxin units per µg plasmid DNA.

2.2.1.2 Isolation of genomic DNA from tissue samples
(Laird et al., 1991)

Lysis buffer I:	100 mM Tris/HCl (pH 8.0)
	100 mM NaCl
	100 mM EDTA
	0.5% SDS

The method employed was the same as that of Laird et al. (1991). 1 to 2 cm of the tail from a mouse was incubated in 700 µl of lysis buffer containing 35 µl proteinase K (10µg/µl) at 55°C overnight in Thermomixer 5436. To the tissue lysate, equal volume of phenol was added, mixed by inverting several times, and centrifuged at 8000xg for 5 min at room temperature. After transferring the upper aqueous layer into a new tube, the same procedure was repeated, first with 1:1 ratio of phenol and chloroform and then with chloroform. Finally, the DNA was precipitated with 0.7 volume of isopropanol, washed with 70% ethanol, and dissolved in 100-200 µl of TE buffer and incubated at 60°C for 15 min.

2.2.1.3 Isolation of genomic DNA from ES cells

Lysis-buffer II:	100 mM Tris-HCl (pH 8.5)
	5 mM EDTA
	200 mM NaCl
	100 µg /ml proteinase K
	0.2% SDS

To isolate the DNA from the ES cells, cells in a 24 well plate were washed with PBS and incubated overnight in 500 µl of lysis buffer II at 37°C. Equal volume of isopropanol was added and mixed for 15 min to precipitate the DNA. After washing with 70% ethanol, the DNA was transferred into a microcentrifuge cup containing 60 µl of TE buffer and incubated at 60°C for 15 min.

2.2.1.4 Isolation of total RNA from tissue samples and cultured cells

Total RNA isolation reagent is an improved version of the single-step method for total RNA isolation. The composition of reagent includes phenol and guanidine thiocyanate in a mono-phase solution. 100-200 mg of tissue sample was homogenised in 1-2 ml of TRI Reagent by using a glass-teflon homogeniser. The sample volume should not exceed 10% of the volume of reagent used for the homogenisation. To isolate total RNA from cultured cells, 350 µl of reagent was added to the petri dish (6 cm diameter). Cells were homogenised with a rubber stick and the lysate was transferred into a microcentrifuge tube. The homogenate was incubated at 4°C for 5 min to permit the complete dissociation of nucleoprotein complexes. Then, 0.2 ml of chloroform was added, mixed vigorously, and stored at 4°C for 10 min. After centrifugating at 12000xg for 15 min at 4°C, the colourless upper aqueous phase was transferred into a new tube. The RNA was precipitated by adding 0.5 ml of isopropanol. Finally, the pellet was washed twice with 75% ethanol and dissolved in 80-100 µl of DEPC-H_2O.

2.2.2 Determination of the nucleic acid concentration

The concentration of nucleic acids was determined spectrophotometrically by measuring absorption of the samples at 260 nm. The quality of nucleic acids i.e. contamination with salt and protein was checked by the measurements at 230, 280, and 320 nm. The concentration was calculated according to the formula:

$$C = (E\ 260 - E\ 320)fc$$

C	= concentration of sample ($\mu g/\mu l$)
E 260	= ratio of extinction at 260 nm
E 320	= ratio of extinction at 320 nm
f	= dilution factor
c	= concentration (standard) / absorption (standard)

for double stranded DNA : c = 0.05 $\mu g/\mu l$

for RNA : c = 0.04 $\mu g/\mu l$

for single stranded DNA : c = 0.03 $\mu g/\mu l$

2.2.3 Gel electrophoresis

Gel electrophoresis is the technique by which mixtures of charged macromolecules, especially nucleic acids and proteins, are separated in an electrical field according to their mobility which is directly proportional to macromolecule's charge to mass ratio.

2.2.3.1 Agarose gel electrophoresis of DNA

Agarose gels are used to electrophorese nucleic acid molecules from as small as 50 bases to more than 50 kb, depending on the concentration of the agarose and the precise nature of the applied electrical field (constant or pulse). Usually, 1 g of agarose was added in 100 ml of 0.5x TBE buffer and boiled in the microwave to dissolve the agarose, then cooled down to about 60°C before adding 3 μl of ethidium bromide (10 mg/ml). This 1% agarose gel was poured into a horizontal gel chamber.

2.2.3.2 Agarose gel electrophoresis of RNA
(Hodge, 1994)

Single-stranded RNA molecules often have complementary regions that can form secondary structures. Therefore, RNA was run on a denaturing agarose gel that contained formaldehyde, and before loading, the RNA was pre-treated with formaldehyde and

formamide to denature the secondary structure of RNA. 1.25g of agarose was added in 100 ml of 1x MOPS Buffer and dissolved by heating in microwave. After cooling it to about 50°C, 25 ml of formaldehyde (37%) was added, stirred and poured into a horizontal gel chamber.

RNA samples were treated as follows:

> 10 – 20 µg RNA
>
> 2 µl 10x MOPS Buffer
>
> 3 µl Formaldehyde
>
> 8 µl Formamide (40%)
>
> 1.5 µl Ethidium bromide

Samples were denatured at 65°C for 10 min and chilled on ice before loading into the gel. The gel was run at 40 V at 4°C for about 12 hrs.

2.2.3.3 Polyacrylamide gel electrophoresis (PAGE) for EMSA

Polyacrylamide gel electrophoresis was employed to separate and analyse small DNA fragment and protein binding. The percentage of acrylamide (7-12%) determines the resolving property of the gel. A 4% of gel was prepared as follows:

> 2.5 ml 40% stock solution
>
> 4.0 ml 5x TBE buffer
>
> 2.5 ml 80% glycerol
>
> 250 µl APS (10% w/v)
>
> 20 µl TEMED
>
> Up to 40 ml with water

APS in presence of TEMED generates free radicals, which initiate the polymerisation of acrylamide. The gel was poured vertically between two clean glass plates, ensuring no air bubbles.

2.2.3.4 SDS-PAGE for the separation of proteins
(Laemmli, 1970)

SDS gel electrophoresis is a method for separating proteins within a sample for analysis and molecular weight determination. The proteins are denatured and rendered monomeric by boiling in the presence of reducing agents (β-mercaptoethanol or dithiotheitol) and negatively charged detergent (SDS). The proteins, which normally differ according to their charges, are all coated with the SDS molecules, which are negatively charged. Hence, all the proteins in the sample become negatively charged and achieve constant charge to mass ratio. In this way, the separation is according to the size of the proteins. A SDS-PAGE consists of two gels; firstly, a 10-12 % separating gel was poured. In order to achieve a smooth boundary between separating and stacking gel, the separating gel was covered with a layer of water. After polymerisation of the separating gel, a 4 % stacking gel was poured over it. The samples were boiled in sample buffer for 10 min at 95°C before loading into the gel. The gel was run at 15 mA for 1 hr and then at a constant current of 30 mA.

2.2.4 Isolation of DNA fragments after agarose gel electrophoresis

2.2.4.1 Glass Silica Method
(Vogelstein and Gillespie, 1979)

For the isolation of DNA fragments of 300-4000 base pairs (bp) in length from agarose gels, the Geneclean kit from Biomol was used. The principle of this method depends on the binding capacity of DNA to silica in high salt concentrations and elution in low salt solutions. After separation of DNA on an agarose gel, the DNA fragment to be isolated was excised with a razor blade and weighed. 3 volumes of JETSORB solution was added and melted at 55°C. Depending on the DNA amount, required amount of GLASSMILK, which is an aqueous suspension of silica matrix, was added and the tube was placed on ice for 30 min. After centrifuging it at full speed for 2 min, the pellet was washed 2 times with "New Wash" and allowed to dry at room temperature. For elution of DNA, the pellet was resuspended in 30 μl of H_2O and incubated at room temperature for 10 min with continuous shaking. After the final centrifugation at 14000xg for 5 min, the supernatant containing the DNA was transferred into a new tube.

2.2.4.2 QIAquick Gel Extraction method

This method is designed to extract and purify DNA of 70 bp to 10 kilobase pairs (kb) in length from agarose gels. Up to 400 mg agarose can be processed per spin column. The principle of this method depends on selective binding of DNA to uniquely designed silica-gel membrane. To the excised DNA fragment from agarose, 3 volumes of QG buffer was added and incubated at 50°C for 10 min. After the gel slice was dissolved completely, it was applied over a QIAquick column and centrifuged for 1 min. The flow through was discarded and the column was washed with 0.75 ml of PE buffer. After drying the column, it was placed into a fresh microcentrifuge tube. To elute DNA, 50 µl of EB buffer was applied to the centre of the QIAquick membrane and centrifuged for 1 min.

2.2.5 Enzymatic modifications of DNA

2.2.5.1 Restriction of DNA

Restriction enzyme digestions were performed by incubating double-stranded DNA with an appropriate amount of restriction enzyme in its respective buffer as recommended by the supplier, and at the optimal temperature for the specific enzyme. Standard digestions include 2-10 U enzyme per microgram of DNA. These reactions were usually incubated for 1-3 hrs to ensure complete digestion at the optimal temperature for enzyme activity, which was typically 37°C. For genomic DNA digestion, the reaction solution was incubated overnight at 37°C.

2.2.5.2 Ligation of DNA fragments

The ligation of an insert DNA into a vector (digested with appropriate restriction enzyme) was carried out in the following reaction mix:

> 30 ng vector DNA (digested)
>
> 50-100 ng insert DNA (1:3, vector: insert ratio)
>
> 1 µl ligation buffer (10x)
>
> 1 µl T4 DNA ligase (5U / µl)
>
> in a total volume of 10 µl

Blunt-end ligations were carried out at 16°C for overnight, whereas overhang-end ligations were carried out at room temperature for 2-4 hrs.

2.2.5.3 TA-Cloning
(Clark, 1988; Hu, 1993)

Taq polymerase and other DNA polymerases have a terminal transferase activity that results in the non-template addition of a single nucleotide to the 3' ends of PCR products. In the presence of all 4 dNTPs, dATP is preferentially added. This terminal transferase activity is the basis of the TA- cloning strategy. For cloning of PCR products, the pGEM-T or pGEM-T Easy vector systems that has 5' T overhangs were used.

The followings were mixed:

> 50 ng of pGEM-T or pGEM-T Easy Vector
>
> PCR product (1:3, vector to insert ratio)
>
> 1 µl of T4 DNA Ligase 10x buffer
>
> 1 µl of T4 DNA Ligase
>
> in a total volume of 10 µl

The content was mixed by pipetting and the reaction was incubated overnight at 4°C.

2.2.5.4 Filling-up reaction
(Costa and Weiner, 1994)

0.1-4 µg of digested DNA was mixed with 0.05 mM dNTPs and 1-5 U of Klenow fragment with reaction buffer in a total volume of 50 µl. The reaction was incubated at 37°C for 15 min, and then stopped by heating at 75°C for 10 min.

2.2.6 Preparation of competent *E.coli* bacteria
(Dagert and Ehrlich, 1979)

The competent bacterial cells are generated by a physical cell wall modification that facilitates DNA uptake. LB medium (100 ml) was inoculated with a single colony of *E.coli* (strain DH5α) and the culture was grown at 37°C to OD 600 = 0.6. Bacteria were

centrifuged (10 min, 4°C, 3000xg) and the pellet was resuspended in 50 ml of sterile 50 mM CaCl$_2$ solution (4°C) and incubated on ice for 30 min. The suspension of bacteria was centrifuged (10 min, 4°C, 3000xg) and the pellet was resuspended in 10 ml of sterile 50 mM CaCl$_2$ (4°C) with 15% glycerol. The mixture was dispensed into aliquots of 100 µl and stored at -80°C. Mostly, competent DH5α were purchased from GibcoBRL.

2.2.7 Transformation of competent bacteria
(Ausubel et al., 1994)

Transformation of the bacteria was done by gently mixing one aliquot of competent bacteria (50 µl) with 10 µl of ligation reaction. After incubation for 30 min on ice, bacteria were heat shocked for 45 sec at 42°C, cooled down for 2 min on ice. After adding 450 µl of LB medium, bacteria were incubated at 37°C, 200 rpm for 1hr to allow recovery of heat shocked bacteria and were plated out on LB-agar plates containing appropriate antibiotic (50µg/ml) and whenever required, 1 mM IPTG and X-Gal 40mg/ml (X-Gal for "Blue-White" selection).

2.2.8 Polymerase Chain Reaction (PCR)

Without a doubt, the polymerase chain reaction (PCR) represents the single most important technique in the field of molecular biology. It is a very sensitive and powerful technique (Saiki et al., 1988) that is widely used for the exponential amplification of specific DNA sequences in vitro by using sequence specific synthetic oligonucleotides (primers). The general principle of PCR starts from a pair of oligonucleotide primers that are designed so that a forward or sense primer directs the synthesis of DNA towards a reverse or antisense primer, and vice versa. During the PCR, the *Taq* DNA polymerase (a heat stable polymerase) (Chien et al., 1976) catalyses the synthesis of a new DNA strand that is complementary to a template DNA from the 5' to 3' direction by a primer extension reaction, resulting in the production of the DNA region flanked by the two primers. It allows the rapid and unlimited amplification of specific nucleic acid sequences that may be present at very low concentrations in very complex mixtures.

2.2.8.1 PCR amplification of DNA fragments

The amplification cycles were performed in an automatic thermocycler. The PCR reaction contains in general, the following substances:

10 ng	DNA
1 µl	forward primer (10pmol)
1 µl	reverse primer (10pmol)
1 µl	10mM dNTPs
5 µl	10x PCR buffer
1.5 µl	50mM MgCl$_2$
1 µl	*Taq* DNA Polymerase (5U/µl)
Up to 50 µl	H$_2$O

The reaction mixture was placed in a 200 µl reaction tube and placed in thermocycler. A standard PCR program is shown here:

Initial denaturation	95°C	5 min
Elongation	95°C	30 sec (denaturation)
30-35 cycles	58°C	45 sec (annealing)
	72°C	1-2 min (extension)
Final extension	72°C	10 min

2.2.8.2 Genotyping of the knock-out mice by using PCR

The genotypes of all offspring of mutant mice were analysed by polymerase chain reaction (PCR). For amplification of the wild-type and the mutant allele, the DNA was extracted from mouse tails as described in 2.2.1.2 and pipetted to the following reaction mixture:

MOCS1 mice
1 µl DNA (300-500 ng)
1 µl MGF1 (10 pmol/µl)
1 µl MOCS49 (10 pmol/µl)
1 µl Pgk1 (10 pmol/µl)
1 µl dNTPs (10 mM)
5 µl *Taq* Polymerase buffer (10x)
0.5 µl *Taq* Polymerase (5 U/µl, Gibco)
Up to 50 µl H_2O

Sox15 mice
1 µl DNA (300-500 ng)
1 µl SGF1 (10 pmol/µl)
1 µl SGR (10 pmol/µl)
1 µl Pgk1 (10 pmol/µl)
1 ml dNTPs (10 mM)
5 µl *Taq* Polymerase buffer (10x)
0.5 µl *Taq* Polymerase (5 U/µl, Gibco)
Up to 50 µl H_2O

MDX mice
1 µl DNA (300-500 ng)
1 µl (10 pmol/µl)
1 µl MDX-WT sense (10 pmol/µl)
1 µl MDX or WT antisense (10 pmol/µl)
1 µl dNTPs (10 mM)
5 µl *Taq* Polymerase buffer (10x)
0.5 µl *Taq* Polymerase (5 U/µl, Gibco)
Up to 25 µl H_2O

The mixture was subjected to the following program in the thermocycler:

MOCS1 mice:

Denaturation	94°C for 5 min	
Elongation		
(for 35 cycle)	94°C for 45 sec	Denaturation
	60°C for 45 sec	Annealing
	72°C for 1 min 10sec	Elongation
Extension	72°C for 10 min	

Sox15 mice:

Denaturation	94°C for 5 min	
Elongation		
(for 35 cycle)	94°C for 45 sec	Denaturation
	57°C for 45 sec	Annealing
	72°C for 1 min	Elongation
Extension	72°C for 10 min	

MDX mice:

Denaturation	94°C for 5 min	
Elongation		
(for 35 cycle)	94°C for 1 min	Denaturation
	58°C for 1 min	Annealing
	72°C for 1 min	Elongation
Extension	72°C for 10 min	

2.2.8.3 High-fidelity PCR

To amplify genomic templeates with exceptionally high fidelity, Advantage®-HF 2 PCR kit (CLONTECH) was used. The fidelity of Advantage®-HF 2 was normalized by the company, CLONTECH (Table 2.1). The high level of fidelity delivered by the

Advantage®-HF 2 system increases confidence in sequence derived from PCR products and is beneficial in a variety of PCR applications, including expression studies of amplifed full-length cDNAs, generation of cDNA libraries, and analysis of homologous genes amplifed with degenerate primers

Enzyme	Error rate[a] (per 100 kb)
Taq	66[b]
Advantage®-2	24
Advantage®-HF 2	2.3

[a] detremined with individual clones after 25 PCR cyles.

[b] agrees with published data (Ling et al., 1991 ; Cariello et al., 1991)

Table 2.1 Fidelity of Advantage®-HF 2 based on sequencing data

The following reagents are mixed.

1 µl DNA (300-500 ng)

1 µl Forward primer (10 pmol/µl)

1 µl Reverse primer (10 pmol/µl)

5 µl 10X HF 2 dNTPs

5 µl 10X HF 2 PCR buffer

1 µl 50X Advantage-HF 2 Polymerase Mix

Up to 50 µl H_2O

The mixture was subjected to the following program in the thermocycler:

Denaturation   94°C for 4 min

Elongation

(for 35 cycle)   94°C for 60 sec   Denaturation

                            68°C for 4 min   Annealing/Elongation

Extension   68°C for 3 min

2.2.8.4 Reverse transcription PCR (RT-PCR)

RT-PCR generates cDNA fragments from RNA templates and is very useful to determine the expression of genes in specific tissues or in different development stages. 1-5 μg of total RNA was mixed with 1 μl of oligo $(dT)_{18}$ primer (10pmol/μl) in a total volume of 12 μl. To avoid the possible secondary structure of the RNA, which might interfere with the synthesis, the mixture was heated to 70°C for 10 min, and then quickly chilled on ice. After a brief centrifugation, the followings were added to the mixture:

> 4 μl 5x First strand buffer
>
> 2 μl 0.1 M DTT
>
> 1 μl 10mM dNTPs
>
> 1 μl Rnasin (10U/μl)

The content of the tube was mixed gently and incubated at 42°C for 2 min. Then, 1 μl of reverse transcriptase enzyme (Superscript II) was added and further incubated at 42°C for 50 min for the first strand cDNA synthesis. Next, the reaction was inactivated by heating at 70°C for 15 min. One μl of the first strand reaction was used for the PCR reaction (as described above).

2.2.8.5 One-Step RT-PCR

To obtain specific RT-PCR products, the QIAGEN OneStep RT-PCR kit was employed which contains optimized components that allow both reverse transcription and PCR amplification to take place in what is commonly referred to as a "one-step" reaction.

Master mix;	Per reaction
5 x Qiagen OneStep RT-PCR buffer	10 μl
dNTP mix (containing 10 mM of each dNTP)	2 μl
Forward primer (10 pmol)	1 μl
Reverse primer (10 pmol)	1 μl
Qiagen OneStep RT-PCR Enzyme Mix	2 μl
RNase inhibitor (20 units per l μl)	1 μl

RNase-free water   31 µl

2 µl (2 µg) of total RNA isolated from mouse tissues was added to 48 µl of prepared Master mix in a PCR tube, the sample was placed in the thermal cycler and the RT-PCR program run according to the user manual. After the amplification step, the sample was checked on an agarose gel.

Thermal cycler conditions:

Reverse transcription: 30 min   50 °C

Initial PCR activation step: 15 min   95 °C

35 cycles

Denaturation: 30 sec   94 °C

Annealing: 40 sec   56- 60 °C (depending on primers)

Extension: 1 min   72 °C

2.2.9 Protein and biochemical methods

2.2.9.1 Isolation of total proteins

100 mg of tissue was homogenized in 500 µl of 0.25 M Tris/HCl, pH 7.8, with a Teflon-glass headed pestle. The cell membrane was destroyed by freezing in liquid nitrogen and thawing at 37°C, which was repeated three times. The samples were centrifuged at 8000xg for 10 min at 4°C and supernatant was distributed in several microcentrifuge tubes. The tubes were frozen in liquid nitrogen and stored at –80°C.

2.2.9.2 Isolation of nuclear proteins
(Deryckere et al., 1994)

Lysis buffer A   10 mM HEPES, pH 7.9

                                    1.5 mM $MgCl_2$

                                    10 mM KCl

                                     0.5 mM dithiothreitol (DTT)

                                    0.5 mM phenylmethylsulphonyl fluoride (PMSF)

Lysis buffer B   Lysis buffer A + 0.05% Nonidet P-40

Lysis buffer C   5 mM HEPES, pH 7.9

                                        26% glycerol (v/v)

                                        1.5 mM MgCl$_2$

                                        0.2 mM EDTA

                                        0.5 mM DTT

                                        0.5 mM PMSF

5×10^6 cells/ml were harvested and washed with cold phosphate buffered saline and resuspended in 50 µl of lysis buffer A. The cells were allowed to swell on ice for 10 min, after which the cells were resuspended in 30 µl of lysis buffer B. Then the tube was vigorously mixed on a vortex machine 3 times for 3 sec, and centrifuged at 250xg for 10 min to pellet the nuclei. The nuclear pellet was resuspended in 40 µl of ice-cold lysis buffer C, and then incubated on ice for 30 min with intermittent mixing, and centrifuged at 24,000xg for 20 min at 4°C. The nuclear extract was either used immediately or stored at −80°C for later use.

2.2.9.3 Determination of protein concentration
(Bradford, 1976)

To determine the protein concentration, Bio-Rad protein assay was employed which is a dye-binding assay based on the differential colour change of a dye in response to various concentrations of protein. The assay is based on the observation that the absorbance maximum for an acidic solution of Coomasie Blue G-250 shifts from 494 to 595 nm when the binding to protein occurs. The BSA stock solution of 1 mg/ml was diluted in order to obtain standard dilutions in range of 10 µg/ml to 100 µg/ml. The Bio-Rad's color reagent was diluted 1:5 with H$_2$O, and filtered through 0.45 µm filters. In a 96-well microtiter plate, 20 µl of each standard dilution and the samples to be measured were pipetted with 280 µl of the color reagent. The absorption of the colour reaction was measured at 595 nm in a microplate reader (Microplate Reader 450, Bio-Rad).

2.2.10 Blotting techniques

2.2.10.1 Southern blotting of DNA to nitrocellulose filters
(Southern, 1975)

In Southern blotting, the transfer of denatured DNA from agarose gels to nitrocellulose membrane is achieved by capillary flow. 20x SSC buffer, in which nucleic acids are highly soluble, is drawn up through the gel into the nitrocellulose membrane, taking with it the single-stranded DNA that becomes immobilised in the membrane matrix.

After electrophoresis of DNA, the gel was treated with 0.25 M HCl for depurination. It was followed by denaturation solution for 30 min and 45 min in neutralization solution. The transfer of the DNA to the nitrocellulose membrane was done in a Turbo-Blot-apparatus (Schleicher & Schuell, Dassel). About 20 Whatman filter papers (GB 003) were layered on a Stack Tray followed by 4 Whatman filter papers (GB 002) and 1 Whatman filter paper GB 002 soaked with 2x SSC. The equilibrated nitrocellulose filter that was also soaked with 2x SSC was laid on the top. The agarose gel, which was treated as described above, was placed on the filter and was covered with 3 Whatman filter papers GB 002 soaked with 2x SSC. The buffer tray was placed and filled with 20x SSC. Finally a wick, which was soaked with 20x SSC, and the wick cover were put on the top of the blot. The transfer was carried out for overnight. Finally, after disassembling of the blot, the filter was washed briefly in 2x SSC and the DNA was fixed onto the filter by either baking it at 80°C for 2 hrs or by UV-crosslinking in UV Stratalinker 1800.

2.2.10.2 Northern blotting of RNA onto nitrocellulose filter

For the transfer of RNA onto a nitrocellulose filter, the same procedure as described above (2.2.10.1) was performed. In this case, however, the gel does not need to be denatured, but was transferred directly onto the filter.

2.2.10.3 Western blotting of protein onto PVDF membrane
(Gershoni and Palade, 1982)

Anode I buffer   0.3 M Tris/HCl, pH 10.4

                                         20 % Methanol

Anode II buffer	25 mM Tris/HCl, pH 10.4
	20 % Methanol
Cathode buffer	40 mM ε-Aminocaproic acid
	25 mM Tris/HCl, pH 9.4
	20 % Methanol

After the electrophoresis of proteins on a SDS-PAGE, the gel and the PVDF membrane, which was cut at the size of the gel, was first moistened with methanol and then equilibrated in anode II buffer. Six pieces of GB004 Whatman filter paper were also cut at the size of the gel. Two pieces of filter papers were soaked in anode buffer I and one paper in anode II buffer. First, the papers soaked with anode I buffer were placed on semi dry transfer machine's lower plate and than papers soaked with anode II buffer were placed over it. The equilibrated membrane was placed over them and then the gel was placed avoiding any air bubbles. Another three Whatman paper soaked with cathode buffer was placed over to complete the sandwich model. The upper plate was placed over this sandwich and the transfer was carried out at 3.5 mA/cm^2 for 1 hr.

2.2.11 "Random Prime" method for generation of ^{32}P labeled DNA
(Denhardt, 1966; Feinberg and Vogelstein, 1989)

Rediprime^{TM} II Random Prime Labeling System (Amersham Pharmacia) was used for labelling of DNA probes. The method depends on the random priming principle developed by Feinberg and Vogelstein (1989). The reaction mix contained dATP, dGTP, dTTP, Klenow fragment (4-8 U) and random oligodeoxyribonucleotides. Firstly, 25-50 ng of DNA were denatured in a total volume of 46 μl at boiling water for 10 min and quick chilled in ice for 5 min. After pipetting the denatured probe in Rediprime^{TM} II Random Prime Labeling System cup, 4 μl of [α-^{32}P] dCTP (3000 Ci/mmol) was added to the reaction mixture. The labelling reaction was carried out at 37°C for 1 hr. The labelled probe was purified from unincorporated [α-^{32}P] dCTP by using microspin columns (Amersham Pharmacia).

2.2.12 5'end radiolabeling of target DNA

For labeling of both 5'-ends of nucleotides, [γ-^{32}P]ATP and polynucleotide kinase were used. The following was mixed in a sterile microcentrifuge tube:

Dephosphorylated DNA, 5-ends	20 pmol
10X kinase buffer	5 µl
T4 polynucleotide kinase (5-10 units/µl)	1 µl
[γ-^{32}P]ATP (3000 Ci/mmol)	5 µl
Water	to 50 µl

Then, the labeling reaction was carried out at 37°C for 1 hr. The labelled probe was purified from unincorporated [γ-^{32}P]ATP by using microspin G-25 columns (Amersham Pharmacia).

2.2.13 Non-radioactive dye terminator cycle sequencing

Non-radioactive sequencing was performed with the Dye Terminator Cycle Sequencing-Kit (ABI PRISM). The reaction products were analysed with automatic sequencing equipment, namely 377 DNA Sequencer (ABI PRISM). For the sequencing reaction, four different dye labelled dideoxy nucleotides were used (Sanger et al., 1977), which, when exposed to an argon laser, emit fluorescent light which can be detected and interpreted. The reaction was carried out in a total volume of 10 µl containing 1 µg plasmid DNA or 100-200 ng purified PCR products, 10 pmol primer and 4 µl reaction mix (contains dNTPs, dideoxy dye terminators and *Taq* DNA polymerase). Elongation and chain termination take place during the following program in a thermocycler: 4 min denaturation followed by 25 cycles at 95°C, 30 sec; 55°C, 15 sec, annealing; 60°C, 4 min, elongation. After the sequencing reaction, the DNA was precipitated with 1/10 volume 3 M sodium acetate and 2.5 volume 100% ethanol and washed in 70% ethanol. The pellet was dissolved in 4 µl of loading buffer, denatured at 95°C for 3 min, and finally loaded into the sequence gel.

2.2.14 Hybridisation of nucleic acids
(Denhardt, 1966)

The membrane to be hybridised was equilibrated in 2x SSC and transferred to a hybridisation bottle. After adding 10 ml of hybridisation solution and sheared salmon DNA, the membrane was incubated for 2 hrs in the hybridization oven at an appropriate temperature, which was usually 65°C. Then, the labelled probe was denatured at 95°C for 10 min, quick chilled, and added to the hybridisation solution. The hybridisation was carried out overnight in the oven. Next day, the filter was washed for 10 min with 2x SSC at room temperature. Finally, it was washed with 0.2x SSC containing 0.1 % SDS at the hybridisation temperature. After drying the filter, it was sealed in Saran wrap and exposed to autoradiography overnight at -80°C or to Phosphoimager screen for 1-4 hrs. The film was developed in X-Ray Automatic Processor Curix 60 or screen was scanned in Phosphoimager. For quantification of detected bands, the program Quntity One (Bio-Rad) was used.

2.2.15 Generation of polyclonal antibody against peptide

2.2.15.1 Peptide analysis

Different computational tools were applied to select potential antigenic peptides. Before synthesis of the peptide, a hydrophilicity/hydrophobicity profile analysis was carried out and for further confirmation antigenicity prediction was performed. In next step, predictions of secondary structure such as β- turns and α-helices in combination with the surface probability of the protein region were the parameters, which enabled us to select the best peptides. In the last step, we compared the primary sequence of our protein with the international data bank (Genebank database http://www.ncbi.nlm.nih.gov) to select a unique sequence for antibody generation. One peptide was selected and synthesised with the following sequence.

Peptide : N_2H-CTF PQS DPR LQG ELR P– $CONH_2$ (16 aa)

2.2.15.2 Coupling of the synthetic peptide to BSA

20 mg of BSA (~ 0.3 μmol) were dissolved in 0.5 ml of 0.4 M PBS, pH 7.5. 10 μmol of synthetic peptide was dissolved separately in 1.5 ml of water and the pH was adjusted to 7.5. The solutions of BSA and peptide were mixed and added drop by drop during a course of 5 min time into a solution of 10 μM glutaraldehyde under continuous stirring. This composite mixture was stirred further for 30 min. The unincorporated glutaraldehyde was inactivated by adding 0.1 volume of 1 M glycine solution and the sample was stirred for 30 min and finally dialysed against PBS for overnight.

2.2.15.3 Immunisation of rabbit

Eurogentec Company did immunisation under the DOUBLE X program. Using modern algorithms for peptide selection, the success rate for peptide immunization can be as high as 75 %. This still means a 25 % chance of failure. Under the DOUBLE X program the success rate is increased to

$1-25\%^2 = 93.75\ \%$.

5 mg of peptide was conjugated with carrier protein molecules (KLH) as described in 2.2.9.4 and mixed together before immunisation. Two rabbits were immunised with 100 μg of antigen mixed with Freund's complete Adjuvant in a 1:1 ratio. Before injection, pre-immune serum was collected from the animals. After 14 days, a second booster immunisation was performed with a 1:1 ratio of antigen with Freund's incomplete Adjuvant. A third booster was given after 28 days and final bleeding was done after 36 days. The antiserum was aliquoted and stored at -80°C.

2.2.15.4 Determination of titre of polyclonal antibody

1x PBS II

4 mM	KH_2PO_4
16 mM	Na_2HPO_4
115 mM	NaCl

Blocking solution II

5%	Skimmed milk powder in

		washing stock 1x
	0.5%	Tween 20 in 1x PBS II
PBT II		
	0.1%	Tween 20 in 1x PBS II

10x washing stock:

	1.4 M	NaCl
	5 mM	$MgCl_2$
	100 mM	Tris/HCl, pH 7.5
	0.5%	Tween 20

Washing Buffer:

	2%	Skimmed milk powder
		in 1x Washing buffer

After SDS-PAGE and electrotransfer of the total mouse proteins to a PVDF membrane, the membrane was blocked with 20 ml of blocking solution II for 1 hr at RT. Then the filter was cut and each lane was incubated with different dilutions of antiserum (1:25, 1:100, 1:500, 1:1000, 1: 10000) in washing buffer for overnight at 4°C. Afterwards, the unbound antiserum was removed by washing the membrane 3 times for 20 min with washing buffer. The secondary antibody coupled with alkaline phosphatase was diluted 1:10000 in washing buffer and added to the blot and incubated for 1 hr. Again the unbound antibodies were removed by washing 4 times for 15 min with washing buffer. The chromogenic reaction was performed with 10 μl and 60 μl of BCIP solution in buffer D until chromogenic precipitate develops. The reaction was stopped by washing the membrane several times with water. The membrane was air-dried and stored in the dark.

2.2.15.5 Affinity purification of polyclonal antibody

For antibody purification, SulfoLink® Coupling Gel (PIERCE) was used. The gel consists of immobilized iodoacetyl on a crosslinked agarose support. SulfoLink® supports binds specifically to sulfhydryls. The 12-atom spacer arm deduces steric and makes binding more efficient. This longer arm is designed for conjugation small peptides to the support.

2.2.15.5.1 Immobilization

Sample preparation buffer:	0.1 M sodium phosphate
	5 mM EDTA-Na, pH6.0
Coupling buffer:	50 mM Tris
	5 mM EDTA-Na, pH 8.5

The peptide (10mg) was dissolved in 1 ml of sample preparation buffer. The solution was added to vial containing 6 mg of 2-mercaptoethylamine (2-MEA), and incubated at 37°C for 1.5 hrs. The mixture was cooled to room temperature and applied to the 5 ml desalting column which was equilibrated with 30 ml of coupling buffer to remove excess 2-MEA from the reduced sample. 1 ml fractions were collected and fractions 4, 5 and 6 were pooled for coupling to gel.

2.2.15.2 Coupling to gel

Reduced protein mixture (3 ml) was added to 2 ml SulfoLink® Coupling Gel column after equilibrating with 12 ml of coupling buffer. The column was mixed at room temperature for 15 min, and then incubated for 30 min without mixing. After that, the column was washed with 6 ml of coupling buffer.

2.2.15.5.3 Blocking nonspecific binding sites on gel

2 ml of 0.05 M cysteine in coupling buffer was applied to the column. The column was mixed for 15 min at room temperature, and then incubated for 30 min without mixing

2.2.15.5.4 Washing and deactivation

Washing buffer A:	1.0 M NaCl
Washing buffer B:	1.0 M NaCl
	0.05% sodium azide in PBS

A series of alternate washings with buffer A (injection 4x4 ml) and buffer B (injection 3x4 ml) was done. Finally, 4 ml of 0.05% degassed sodium azide in PBS was injected, and then the top porous disc was inserted to the column.

2.2.15.5.5 Purification

The column was equilibrated with 6 ml of PBS. The antiserum (8 ml) was applied onto the column. The column was incubated at room temperature for 1 hr. During pumping a constant flow rate of 0.5 ml/min was maintained. The column was washed with 16 ml of PBS. Elution was done with 8 ml of glycine buffer (100 mM, pH 2.5-3.0). 1 ml fractions were collected and monitored by A280. Fractions 3 and 4 were pooled and 0.05% sodium azide was added. Purified antiserum was stored -20°C and the column was re-equilibrated with 10 volumes of PBS.

2.2.16 Histological techniques

2.2.16.1 Tissue preparation for paraffin-embedding

The freshly prepared tissues were fixed in Bouin's solution or 4% (w/v) paraformaldehyde for 24 hrs to prevent alterations in the cellular structure. The tissue to be embedded in paraffin should be free of water. The dehydration process was accomplished by passing the tissue through a series of increasing alcohol concentrations. For this purpose, the tissue was let in 30%, 70%, 90%, and 100% (2x) ethanol for 1hr RT. Later, the alcohol was removed from the tissue by incubating it in methylbenzoat overnight. It was then incubated in 5 ml of histoclear (Xylol) for 10-30 min at RT. The second histoclear was not discarded but 5 ml of paraplast was added and the incubation was continued at 60°C for another 30 min. The histoclear and paraffin mixture was discarded and the tissue was further incubated in 5 ml of paraplast at 60°C overnight. Before embedding, the paraffin was changed at least three times. Finally, the tissue was placed in embedding mold and melted paraffin was poured into the mold to form a block. The block was allowed to cool and was then ready for sectioning.

2.2.16.2 Sections of the paraffin block

The paraffin blocks were pre-cut to the optimal size and clamped into the microtom (Hn 40 Ing., Nut hole, Germany). The cut-thickness of the section was for 6 μm. The sections were floated on 40°C water to allow actual spread and subsequently put onto pre-treated slides. In order to achieve a better adhesion of the sections, the slides were treated with a drop of serum-formalin. A fine brush was used to transfer the sections to the pre-treated slides. After complete evaporation at 37°C for 2-5 days, slides were stored at 4°C for further analysis.

Serum-Formalin:	15 ml	Fresh serum
	15 ml	Glycerin
	6 ml	Formalin 6%

2.2.16.3 Staining of the histological sections (Nissl staining)

The stored slides with the paraffin sections were stained by the following method:

1. Slides were incubated three times in histoclear (Xylol) for 3 min.
2. Incubation in 100%, 96%, 80%, 70% and 50% ethanol for 2 min in each.
3. 1 min in H_2O and then 7 min in Crystal Violet.
4. Running tap water (control) for 10 min, then 1 min in dH_2O.
5. Eosin 0.1% + 2 drops acetic acid for 5 min, then in dH_2O for 1 min.
6. Incubation in 50%, 70%, 80%, 90%, 96% and 100% ethanol for 2 min in each.
7. Slides were incubated two times in histoclear (Xylol) for 3 min.
8.

2.2.17 Transfection of Swiss3T3 cells with the cDNA construct

Approximately 4×10^5 fibroblast cells (Swiss3T3) were plated on a cell culture slide (Falcon) and cultured overnight in 1 ml DMEM medium containing 10% FCS and penicillin/streptomycin at 37°C and 5% CO_2. 2 μg of DNA was diluted with the cell growth medium containing no serum or antibiotics to a total volume of 100 μl, 10 μl of SuperFect Transfection Reagent (Qiagen) was added to DNA solution and mixed by vortexing for 10 sec. The mixture was incubated at RT for 10 min to allow complex formation. 1 ml of cell growth medium was added to the reaction tube, mixed and

immediately added into the cell chamber. Cells were incubated 3 hr at 37°C and 5% CO_2. Medium containing the DNA complex were removed from the cells by gentle aspiration and cells were washed 2 times with PBS. Fresh medium was added and incubated for 48 hrs to allow for gene expression. The glass slide of the culture chamber was rinsed with PBS and then fixed with methanol for 5 min.

2.2.18 Immunofluorescence staining of cells

Cells were fixed in 2% formaldehyde in PBS for 5 min at room temperature, followed by 100% methanol at -20°C for 5 min. The cells were rinsed in PBS. An initial blocking step was performed with the blocking solution (2% horse serum and 0.5% Triton X-100 in PBS) for 1 hr. A rabbit anti-mouse Sox15, mouse anti-mouse desmin and rabbit anti-mouse MF20 were applied for overnight at 4°C in a dilution of 1:100, 1:100, and 1:50 respectably. Cells were subsequently incubated with FIFC- or Cy3- conjugated goat anti-rabbit or goat anti-mouse IgG (Sigma) for 1 hr at room temperature. One drop of mounting medium with DAPI was dispensed onto the slides after washing with PBS. Fluorescent cells were visualised with Olympus BX60 microscope using 20X or 60X Neofluor lens, photographed using digital camera and analysed using analysis 3.0 soft imaging system.

2.2.19 Techniques for production of targeted mutant mice
(Joyner, 2000)

The discovery that cloned DNA introduced into cultured mouse embryonic stem cells can undergo homologous recombination at specific loci has revolutionized our ability to study gene function in vitro and in vivo. In theory, this technique will allow us to generate any type of mutation in any cloned gene. Over twenty years ago, pluripotent mouse embryonic stem cells (ES) derived from inner cell mass cells of mouse blastocysts were isolated and cultured (Martin, 1981; Evans and Kaufman, 1981). Using stringent culture conditions, these cells can maintain their pluripotent developmental potential even after many passages and following genetic manipulations. Genetic alterations introduced into ES cells in this way can be transmitted into the germline by producing mouse chimeras. Therefore, applying gene targeting technology to ES cells in culture gives the opportunity to alter and modify endogenous genes and study their functions in vivo.

2.2.19.1 Production of targeted embryonic stem cell clones

2.2.19.1.1 Preparation of MEFs feeder layers

A frozen vial of MEFs (mouse embryo fibroblasts) was quickly thawed at 37°C and transferred to 10 ml EMFI medium. After centrifugation at 270xg for 5 min, the cell pellet was gently resuspended in 10 ml MEFs medium and plated on a 50mm culture flask. Cells were incubated at 37°C in 5% CO_2. When the cells formed a confluent monolayer (three days), they were either trypsinized, transferred to five 150 mm dishes and grown until they formed confluent monolayer, or directly treated with mitomycin C. To treat the MEFs with mitomycin C, the medium was removed and 10 ml fresh medium containing 100 µl mitomycin C (1mg/ml) was added. After 2-3 hrs of incubation, the monolayer of cells was washed twice with 10 ml PBS. The cells were then resuspended with 10 ml medium and gentle pipetting dissolved any cell aggregates. The cells were centrifuged, resuspended in MEFs medium and plated onto dishes, which were treated with 0.1% gelatine for 30 min. The feeder cells were allowed to attach by incubation overnight at 37°C, 5% CO_2 or used after 2 hrs of incubation. Before adding ES cells on the feeder layer, the medium was changed to ES cell medium.

2.2.19.1.2 Growth of ES cells on feeder layer

One vial of frozen ES cells was quickly thawed at 37°C and cells were transferred to a 12 ml tube containing 6 ml ES cell medium. After centrifugation, the cell pellet was resuspended in 5 ml ES cell medium and plated on 60 mm dishes containing MEFs at 37°C, 5% CO_2. Next day the medium was changed. The second day, cells were washed with PBS, treated with 2 ml trypsin/EDTA at 37°C, 5% CO_2 for 5 min. The cells were gently pipetted up and down to dissolve cell clumps, resuspended with 5 ml ES medium and centrifuged. The cell pellet was resuspended in 10 ml ES cell medium and distributed either to 5 or 6 dishes (60 mm), containing feeder layers or to 2 dishes (100 mm) containing feeder layers. The cells were passaged every second day as described above.

2.2.19.1.3 Electroporation of ES cells

ES cells, which have grown for two days on 100 mm dishes, were trypsinized. The cell pellet was resuspended in 20 ml PBS and centrifuged .The cell pellet was then resuspended in 1 ml PBS. 0.8 ml of cell suspension was mixed with 40 µg of linearized DNA-construct and transferred into an electroporation cuvette. The electroporation was performed at 240 V, 500 µF with the BIO RAD gene pulser™. After electroporation, the cuvette was placed on ice for 20 min. The cell suspension was transferred from cuvette into 20 ml of ES cell medium and plated onto two 100 mm dishes containing feeder layers. The medium was changed every next day. Two days after the electroporation, the drugs for the selection were added (active G418 at 400µg/ml and gancyclovir at 2 µM). The medium was changed every day. After about eight days of selection, drug resistant colonies have appeared and were ready for screening by Southern blot analysis.

2.2.19.1.4 Growing ES cells for Southern blot analysis

The drug resistant colonies that were formed after about eight days of selection were picked with a drawn-out Pasteur pipette under a dissecting microscope. Each colony was transferred into a 24 well plate containing feeders and ES cell medium. After 2 days, the ES cells were trypsinized with 100 µl trypsin for 5 min and resuspended in 500 µl ES cell medium. Half of the cell suspension in each well was transferred to a well on two different 24 well plates, one gelatinised plate, and the other containing feeder cells (master plate). The gelatinised plate was used for preparing DNA and the master plate was kept frozen.

2.2.19.2 Production of chimeras by injection of ES cells into blastocyst.

The ability of mammalian embryos to incorporate foreign cells and develop as chimeras has been exploited for a variety of purposes including the perpetuation of mutations produced in embryonic stem (ES) cells by gene targeting, and the subsequent analysis of these mutations. The standard procedure is to inject 10-20 ES cells, which are recombinant for targeted locus, into the blastocoel cavity of recently cavitated blastocysts that have been recovered by flushing the uteri of day 4 pregnant mice (C57BL/6J). After injection, embryos are cultured for a short period (2-3 hrs) to allow re-expansion of the blastocoel

cavity and then transferred to the uterine horns of day 3 CD1 pseudopregnant mice. Pseudopregnant females are obtained by mating 6-8 weeks old oestrous females with vasectomized males.

2.2.19.3 Detection of chimerism and mice breeding.

The most convenient and readily apparent genetic marker of chimerism is coat colour. Chimeric males (and sometimes females) are bred to wild-type mice to ascertain contribution of the ES cells to germline. Once a germline chimera has been identified, the first priority will be to obtain and maintain the targeted allele in living animals. The chimeras were bred with C57BL/6J and with 129/Sv mice to compare the phenotype in two different genetic backgrounds.

2.2.20 Isolation of myoblast cells
(Rando and Blau, 1994)

2.2.20.1 Preparation of primary cultures

The hind limbs were removed from 2 month old mice and the dissected away. The remaining muscle was weighed. A few drops of PBS were added and the muscle was minced into coarse slurry using razor blades. Cells were enzymatically dissociated by the addition of 2 ml per g of tissue of a solution of dispase and collagenase, supplemented with $CaCl_2$ to a final concentration of 2.5 mM. The slurry maintained at 37°C for 30-45 min, was triturated every 15 min with 5-ml plastic pipette, and then passed through 80 μm nylon mesh. The filtrate was spun at 350xg to sediment the dissociated cells. The pellet was resuspended in growth medium, and the suspension was plated on gelatine coated dishes (35-mm). Medium was changed daily and cultured cells were routinely passed 1:3 as they reached 60-70% confluence. During the first several passages of the primary cultures, myoblasts were enriched by preplating

2.2.20.2 Culture conditions

Growth medium for primary myoblasts consisted of Ham's F-10 media supplemented with 20% FBS and 2.5 ng/ml bFGF. Differentiation medium consisted of DMEM supplemented 2% horse serum. All media contained penicillin G (200 U/ml) and streptomycin (200

µl/ml). Tissue culture plastic dishes were coated with 0.01% gelatine. Cells were grown in a humidified incubator at 37°C in 5% CO_2.

2.2.21 Injury test

2.2.21.1 Induced regeneration of skeletal muscle

12 week-old male mice were used in this experiment. Mice were anaesthetized through an intraperitoneal injection of Avertin (0.016 ml of 2.5% avertin/gram body weight) and received a slight cut injury across the middle of the tibialis anterior (TA) muscle of the right leg and an extensive crush injury to the TA of left leg. The skin of the right leg was opened and a pair of serrated forceps cooled in liquid nitrogen, were used to apply a crush injury to the TA. The incision was about 1 mm deep and 4 mm long: haemorrhage was minimal. A fine suture (10.0 Ethilon) was placed at either end of the cut for future identification of the lesion site. Although the crush was severe, longitudinal continuity of the muscle belly was maintained. Skin wounds overlying the lesion were closed and sutured.

2.2.21.2 Histological analysis

After 4 and 14 days of crush-injury, the damaged TA muscle and untreated TA from the control limb were prepared for electron microscope by fixation in 1.5% paraformaldhyde, 1.5% glutaraldehyde in 0.15 M HEPES buffer (pH 7.4), for 2 hr at 4°C. Samples were dehydrated through a graded alcohol series, and embedded in paraffin. Serial sections were taken at 6 µM and stained with hematoxylin-eosin. Randomly chosen fields for each section were viewed and assessed with a transmission electron microscope.

2.2.22 Gel retardation assay (Electronic mobility shift assay; EMSA)

2.2.22.1 Generation of double stranded oligonucleotides

The DNA probes used in this assay were complementary double-stranded DNA oligonucleotids. The sense and antisense oligonucleotieds for T-cell factor and Mut 3-4 were synthesized by Roth. To generate complementary double-stranded DNA, 10 pM of each strand was combined in a tube and boiled for 5 min. The tube was cooled down at room temperature to allow forming double stranded DNA.

2.2.22.3 Binding reactions and analysis

Binding reactions were performed by incubating 10 µl of nuclear extract for 20 min at room temperature with 2 pmol of ^{32}P-end labelled 25-mer double stranded T-cell factor in binding buffer (10 mM Tris-HCL, pH 7.9, 50 mM NaCl, 1 mM MgCl2, 0.5 mM DTT, 0.5 mM EDTA, 4% glycerol) containing 50 µg/ml of poly (dI-dC). The DNA-protein complex was separated from free oligonucleotides on 4% nondenaturing polyacrylamide gel. For supershift analysis, nuclear extracts were incubated on ice for 2 hrs with Sox15 antibody (1 µl) after the addition of radiolabeled oligonucleotide. Visualization of radioactive bands was carried out using the Molecular Imager (Bio-Rad).

2.2.23 Biochemical assay
(Done by Dr. Shwarz, Pflazenenbiologie Institut, TU-Braunschweig)

2.2.23.1 Determination of molybdopterin

Molybdopterin was detected using the very sensitive nit-1 reconstitution assay. Neurospora crassa nit-1 extract was prepared as described (Nason et al. 1971) and desalted by gelfiltration using Nick columns (Amersham/Pharmacia) prior use. Crude protein extracts from mouse liver were prepared using two volumes of nit-1 buffer (50 mM sodium phosphate, 200 mM NaCl, 5 mM EDTA, pH 7.2,), sonication and centrifugation. According to the linear range of the assay, 2 µl of different dilutions of liver extracts were co-incubated with 20 µl of nit-1 extract containing 5 mM sodium molybdate and 2 mM reduced gluthatione. Complementation was carried out overnight at 4°C under anaerobic conditions. After addition of 20 mM NADPH for 10 min, reconstituted NADPH-nitrate

reductase activity was determined. One unit molybdopterin activity is defined as reconstituted nit-1 nitrate reductase sufficient to produce an increase at 540 nm of 1.0 absorbance units per 20 min reaction time. Activity is expressed as units per mg protein in the crude extract.

2.2.23.2 Determination of sulfite oxidase activity

Sulfite oxidase activity was determined according to Johnson et al. (1991). Crude protein extracts from mouse liver were prepared using one volume of 0.1 M Tris/HCl, 0.1 mM EDTA, pH 8.5 by sonification. The reaction was performed in a reaction volume of 300 µl containing 0.5 M Tris/HCl, 0.16 mM sodium deoxycholic acid, 2 mM potassium cyanide, 0.25 mg cytochrome c and 1 mM sodium sulfite. One unit sulfite oxidase activity is defined as enzyme sufficient to produce an increase at 550 nm of 1.0 absorbance per min at 25°C. Activity is expressed as units per mg protein in the crude extract.

2.2.23.3 Determination of xanthine oxidase-related metabolites

Cryostat sections were fixed for 5min in 4% (w/v) paraformaldehyde and processed for immunofluorescence as previously described (Kneussel et al. 1999). In brief, cells were permeabilized in 0.5% (v/v) Triton-X-100, blocked in 5% (v/v) goat serum for 20min and processed for immunofluorescence. Gephyrin and glycine receptor were visualized using the monoclonal antibodies mAb7 and mAb4, respectively (Pfeiffer et al. 1984). As secondary antibodies Alexa 488/594 were used (Molecular Probes). Confocal microscopy was performed using a Leica TCS-SP confocal laser scanning microscope equipped with Leica TCS-NT image software.

Concentrations of the purines, uric acid, xanthine and hypoxanthine in urine were determined by reversed phase HPLC using a modification of a method described by Simmonds et al. (1991). In brief, separation of purines was achieved by gradient elution on a Spherisorb 5 µm ODS-2 analytical column (250*4.6mm inner diameter; Phenomenex, Aschaffenburg, Germany) at a flow rate of 1.3 ml/min. Eluent A consisted of 40 mM ammonium acetate in HPLC grade water adjusted to pH 5.00 with acetic acid and eluent B of 80% methanol:10% acetonitrile:10 % tetrahydrofuran (v/v/v). Urine was diluted with a nine-fold volume of eluent A. 50 µl of the diluted urine were directly injected into the HPLC system. Purines were quantitated based on peak area units obtained by UV detection

at 254 nm using calibration with authentic standard compounds. Peak identity was confirmed by comparison of both the retention times and of the spectra obtained with a diode array detector between 220 nm and 320 nm. The determination of the creatinine concentration was based on the Jaffé reaction (1886).

2.2.24 Proliferation assay of cells

2.2.24.1 Preparation of MEFs.
(Abbondanzo et al., 1993)

MEFs (Mouse embryo fibroblasts) were established from 14.5-day-old embryos. After removing of the limbs, head and internal organs, embryos were minced with a sterile razor blade until they were the consistency of sludge. The minced embryos were digested with trypsin/EDTA for 10 min at 37°C. After pipetting with Pasteur pipette for several times, the sludge was centrifuged at 1000 rpm. The pellet was resuspended with MEFs medium and seeded cells into culture dishes.

2.2.24.2 Counting of cells

Cells were maintained on a defined 3-day passage schedule by plating 9×10^5 (3T9) or 3×10^5 cells in 60 mm-diam. dishes. Plating after disaggregation of embryos was considered passage 1, and the first passage 3 days latter as passage 2. Cells were counted at each passage, and the total number was calculated prior to redilution.

2.2.25 Collecting of amniotic fluid and plasma

For collecting of amniotic fluids and plasma, 18.5-day-old embryos were isolated. Amniotic fluid was collected by puncture of amniotic sac. Blood plasma was collected by cutting of head, and immediately transferred to the heparin (1 µg for 5 µl blood) containing microcentrifuge tube. Heparin (Liquemin N 25000, Roche) was added to avoid coagulation of blood. After centrifuging at 10000 x g at 4°C, supernatant was transferred to the new tube. Both amniotic fluid and plasma were immediately frozen on dry ice and then stored at -80°C.

2.2.26 Computer Analysis

For the analysis of the nucleotide sequences, programs like BLAST, BLAST2, MEGABLAST and other programs from National Center for Biotechnology Information (NCBI) were used (www.ncbi.nlm.nih.gov). Information about mouse alleles, phenotypes and strains were used from Jackson Laboratory (www.informatics.jax.org). For protein studies ExPASy tools (www.expasy.ch) were used. Mouse genome sequence and other analysis on mouse genes, transcripts and putative proteins were downloaded from Celera discovery system (www.celera.com).

3. RESULTS

3.1 Homologous recombination of the mouse *MOCS1* gene

3.1.1 Isolation of a cosmid clone with mouse genomic DNA

The isolation of a cosmid clone with mouse genomic DNA was performed to clone suitable DNA fragments for a gene targeting vector. An RZPD mouse genomic DNA cosmid library (strain 129/Sv) consisting of 11 filters was hybridized with murine *MOCS1* exon 1 to exon 9 (5' region) and exon 10 (3' region) cDNA as radioactively labeled probe under high stringency conditions (60°C). The probes were cloned by PCR using the primers MocsF and Mocs8 from a *MOCS1* cDNA (Gray and Nicholls 2000); GenBank AF214016) for the 5' region and Mocs27 and Mocs28 from mouse genomic DNA for 3' region (Fig. 3.1 A). One clone was identified in this library (RZPD clone ID: MPMGc121C15173Q3)

3.1.2 Southern blot analysis of the isolated cosmid clone

The cosmid clone containing the murine *MOCS1* gene was restricted with the enzymes *Sal*I, *Xba*I, *Not*I, *Hind*III, *Kpn*I, *Sst*I, *Sst*II, *EcoR*I, *Xho*I, *Spe*I, and *Apa*I., blotted and radioactively hybridized with *MOCS1* exon fragments (Fig. 3.1 B). The size of fragments is calculated and compared to the known *MOCS1* genomic structure (http://www.ncbi.nlm.nih.gov, accession number NT_039655).

3.1.3 Construction of *MOCS1* targeting vector

To disrupt the *MOCS1* gene in the mouse, a replacement targeting vector was designed to delete exon 3 and replaced by the neomycin phosphotransferase (*NEO*) gene under the control of the phosphoglycerate kinase promoter. Exon 3 of *MOCS1* was chosen, since it encodes several amino acid residues which are highly conserved in homologus proteins of mammals, plants and a variety of prokaryotes (Reiss et al. 1998b). Substitution of this exon by the *NEO*-cassette should at least abolish the MOCS1A activity and, depending on the stability of the resulting mRNA, the MOCS1B activity could be affected as well (Reiss et al. 1998b; Gray and Nicholls 2000; Hanzelmann et al. 2002). Induction of negative

selection marker, the herpes simplex virus thymidine kinase (*TK*) gene, at the 3' end of the construct (Fig. 3.3) enabled us to use positive and negative selection (Mansour et al. 1988).
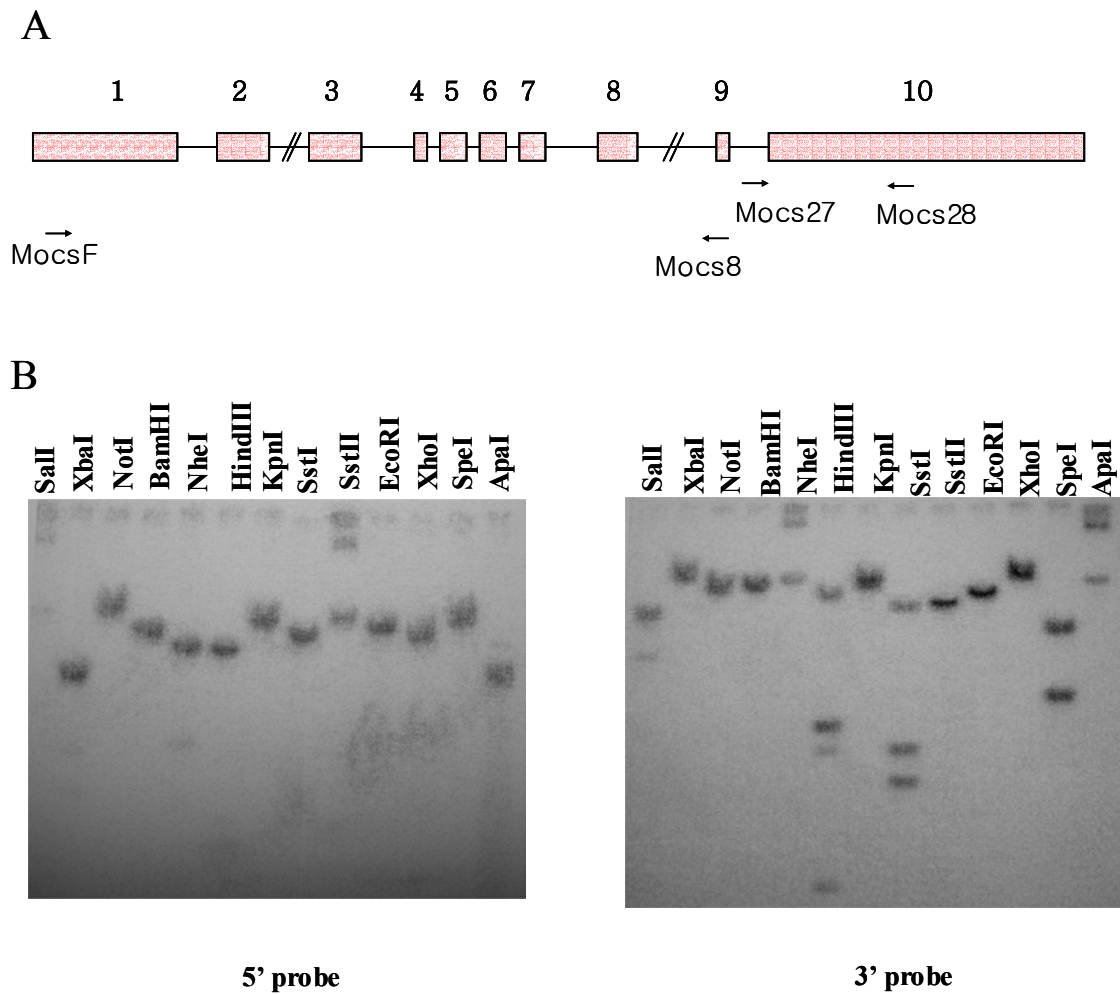

Figure 3.1: Enzymatic digestion of a cosmid clone and schematic representation of the *Mocs1* gene. (A) The schematic diagram shows *MOCS1* gene has 10 exons. The exons of *MOCS1* gene are shown as coloured boxes. Arrows indicate primer locations for probe cloning. (B) The clone of *MOCS1* was digested with various enzymes and hybridized with 5' probe (exon 1-9) and 3' probe (exon10).
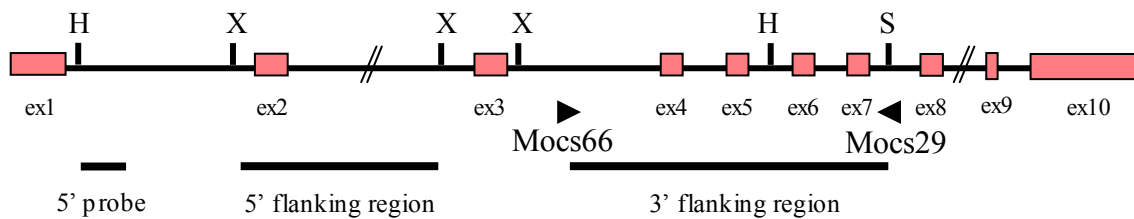
Figure 3.2: Restriction digestion map of *MOCS1* genomic DNA and fragments which were cloned. The cloning strategy for subcloning the 5' and 3' regions of the *MOCS1* gene and subcloning of the 5' external probe are designated. Site of primers for 3' flanking region cloning (arrows) are indicated. Abbreviations are: H, *Hind*III; X, *Xba*I; S, *Sac*I.

3.1.3.1 Subcloning of 5' flanking region of the murine *MOCS1* gene into the pPNT vector

A 4.6 kb *Xba*I fragment containing the 5'-flanking region of the *MOCS*1 gene (including exon 2, Fig. 3.2) was isolated from the cosmid clone and purified from the agarose gel. This fragment was ligated with *Xba*I digested pPNT vector (clone MOCS1/1).

3.1.3.2 Subcloning of 3' flanking region of the murine *MOCS1* gene into pPNT vector

A 4.4 kb fragment containing a 3'-flanking region of the *MOCS1* gene (including exons 4 through 7) was amplified by high fidelity PCR (Clontech) using the primers Mocs66 and Mocs29 (Fig. 3.2), subcloned into pGEM-Teasy and isolated again using the two *Not*I sites flanking the cloning site. This 3'-flanking region was inserted into the *Not*I digested clone MOCS1/1 resulting in the targeting construct (Fig. 3.3).

The replacement vector MOCS1-*Neo-Tk* was linearized at the unique *BamH*I site present in the polylinker site of the pPNT vector before transfection.

3.1.4 Subcloning of a 5' external probe

A 0.67 kb fragment of 5'region of the *MOCS1* (intron 1) was amplified by PCR using the primer MOCS12 and MOCS75. This PCR amplicon was subcloned into pGEM-Teasy and double digested with *EcoR*I and *Hind*III. The 0.67 kb fragment was extracted from the agarose gel and used as 5' external probe for hybridization in the Southern blot with DNA extracted from the recombinant ES-clones.
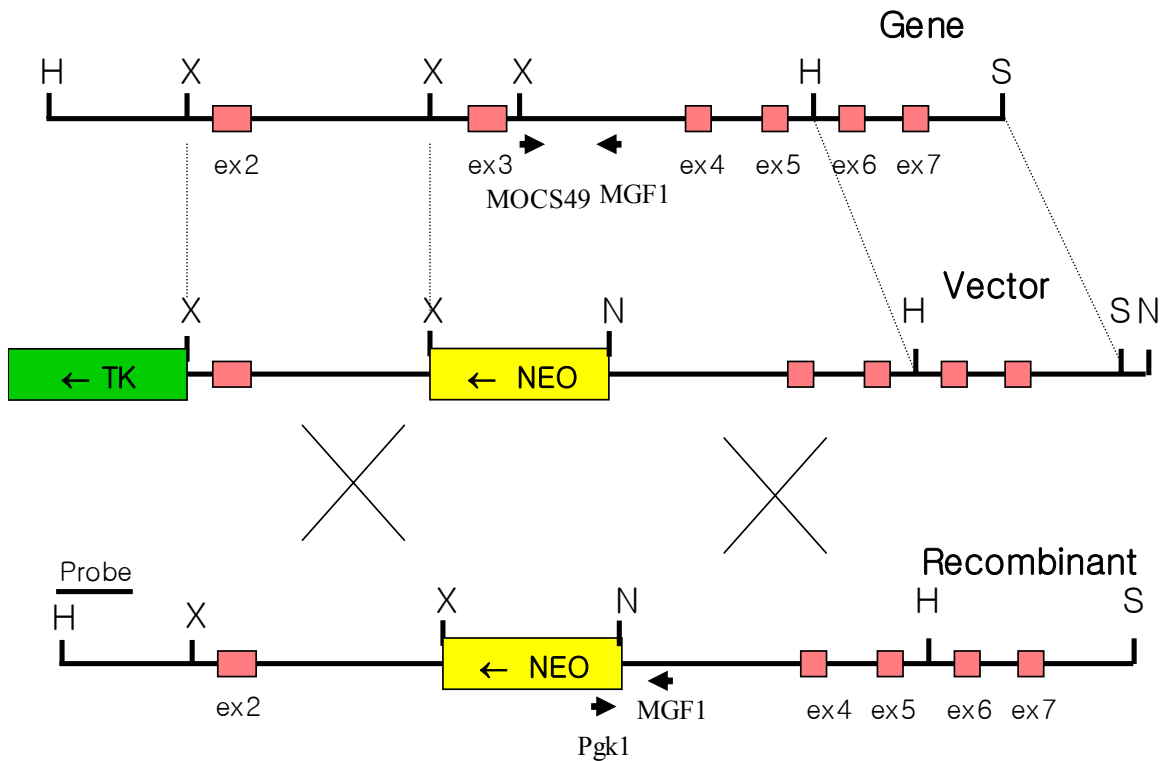
Figure 3.3: Targeted disruption of the *MOCS1* gene. Wild-type *MOCS1* gene (top), targeting vector (middle), and mutant locus (bottom) are shown. Site of external probe for Southern blot ("probe") is indicated. The pink boxes represent exons of *MOCS1* gene, green box stands for *Thymidine kinase* and yellow box stands for *Neomycin*. MGF1, MOCS49 and Pgk1 (arrows) were the primers used for genotyping. The restriction site abbreviations are: H, *Hind*III; X, *Xba*I; N, *Not*I; S, *Sac*I.

3.1.5 Electroporation of the RI ES-cells and screening of ES-clones for homologous recombination events.

The ES cell line RI was cultured as described (2.2.19). Confluent plates were washed in PBS buffer, trypsinized and the cells were suspended in the same buffer at 2×10^7 cells/ml. Aliquots of this cell suspension were mixed with 50 μg of linearized targeted vector MOCS1-*NEO-TK* and electroporated at 250V and 500 μF using a Bio-Rad Gene Pulser apparatus. The cells were plated onto nonselective medium in the presence of G418-resistant embryonic mouse fibroblasts. After 36 hours, selection was applied using medium containing G418 at 400 μg/ml and gancyclovir at 2 μM. After 10 days of selection, 200 individual drug-resistant clones were picked into 24-well trays for freezing and isolation of DNA.

To screen recombinant ES-clones for homologous recombination events, genomic DNA was extracted from the recombinant ES-clones, digested with *Hind*III, electrophoresed and blotted onto nitrocellulose filters. The blots were hybridized with ^{32}P-labeled 0.6 kb 5' probe (Fig. 3.3). In case of a homologous recombination event, the wild-type locus showed a 8.7 kb *Hind*III fragment and the targeted locus is 9.4 kb *Hind*III fragment (Fig. 3.4). Of the colonies screened, 3 of 68 clones had undergone correct homologous recombination.
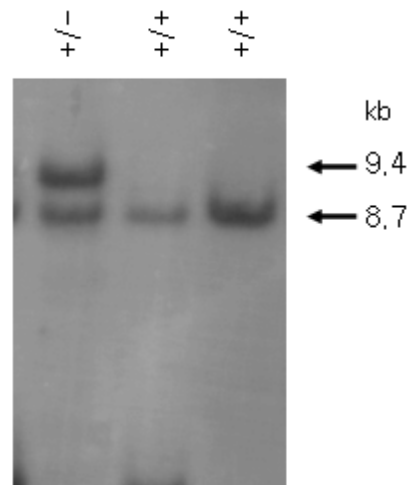

Figure 3.4: Genomic Southern analysis. The ES cell DNAs were digested with *Hind*III and hybridized with the 5' external probe shown in Fig. 3.3. Homologous recombination events yielded a 9.4 kb hybridizing band detected in heterozygous (+/-) cell line, while the wild type (+/+) cell line showed a 8.7 kb band

3.2 Generation of chimeric mice

ES cells from the recombinant clones were injected into 3.5 dpc blastocysts derived from C57BL/6J mice. The blastocysts were implanted into pseudopregnant CD1 mice to generate chimeric mice. 4 chimeras were obtained after 2 independent injections of one recombinant ES clone named MOCS37. The chimeras were scored according to coat color (in percentage). 4 male chimeras from MOCS37 line with 90-95 % of chimerism were bred with C57BL/6J and 129/Sv mice to obtain F1 animals in respective background namely C57BL/6J x 129/Sv and in 129/Sv. The germline transmission of a *MOCS1* deleted allele was checked by genomic PCR with MGF1, MOCS49, and Pgk1 primers (Fig. 3.3) with genomic DNA isolated from tail biopsies of the offspring (F1, Fig. 3.5)
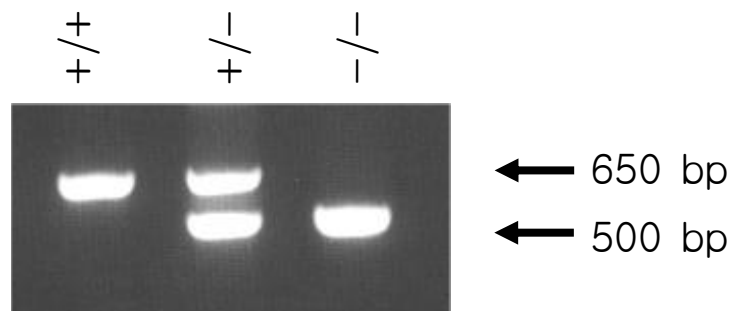
Figure 3.5: PCR genotyping of progeny. Wild-type (+/+), heterozygous (+/-), and homozygous (-/-) mice were identified by amplification of PCR products specific for either the *MOCS1* wild-type allele (650 bp) or the targeted allele (500 bp). The PCR products obtained using primers MGF1, MOCS49, and Pgk1 (Fig. 3.3) were electrophoresed on 1.5% agarose gel and stained with ethidium bromide.

3.3 Generation of the murine *MOCS1* deficient mice

F1 animals, which were heterozygous at the *MOCS1* locus, were intercrossed to obtain F2 animals. The breeding strategy was undertaken in such a way that the line MOCS37 line was established in both C57BL/6J x 129/Sv and in 129/Sv genetic background. Male and female mice heterozygous for the *MOCS1* mutation appeared normal and fertile. Heterozygous animals were mated and 25% of the offspring were homozygous for the mutant allele.

.

3.4 Analysis of *MOCS1* expression in knock-out mice

Total RNA (40 µg) was extracted from 3-day-old mouse liver. RNA samples were electrophoresed on 1% denaturing agarose gels containing formaldehyde (5%) and subsequently transferred onto nitrocellulose membrane (Hybond-C extra, Amersham). This filter was hybridized with ^{32}P-dCTP-labeled (3000 Ci/mmol) *MOCS1* exon 10 fragment (3' probe, Fig. 3.1). To check for integrity and equal amounts of RNA, the filter was rehybridized with a human elongation factor-2 (hEF) cDNA probe. Northern blot analysis showed absence of MOCS1 RNA in the -/- animals, indicating that, owing due to the integration of the neo cassette, the expression of both the MOCS1A and the MOCS1B proteins is hampered (Fig. 3.6).

3.5 Phenotypic analysis of murine *MOCS1* knock-out mice

3.5.1 Statistical analysis

In order to determine the mode of inheritance of *MOCS1* deleted allele in mice, F1 heterozygous mice from lines MOCS37 were intercrossed to obtain F2 generation. The mice were genotyped by genomic PCR on DNA isolated from tail biopsies. The results of this statistical analysis are summarized in Table 3.1. Genetic background C57BL/6J x 129/Sv and129/Sv of the line MOCS37 was in agreement with Mendelian inheritance.
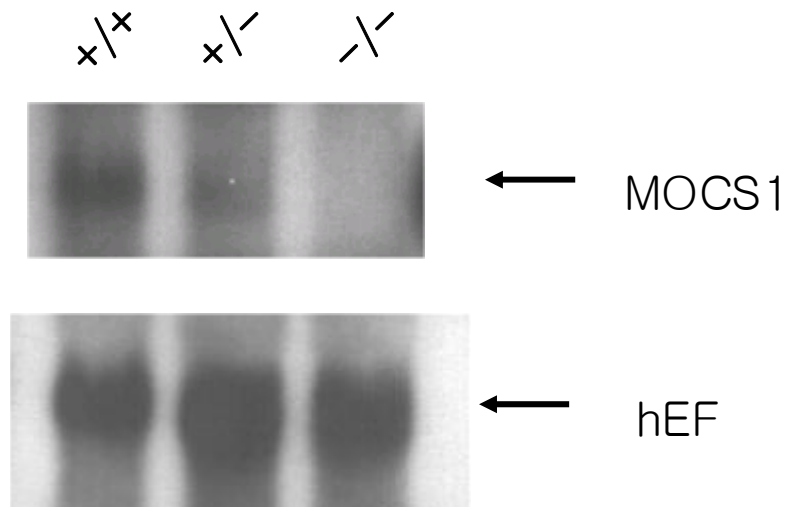
Figure 3.6: Northern blot analysis of liver RNA from the three genotypes. Hybridization with the mouse MOCS1 exon 10 probe (top) revealed a 3.6-kb mRNA prominent in *MOCS1*+/+, reduced in *MOCS1*+/-, and absent in *MOCS1*-/- mice. Rehybridizaion with human elongation factor (hEF, bottom) confirmed equal amount of mRNA.

A   **MOCS37/ C57BL/6J**

+/+		+/-		-/-	
M	F	M	F	M	F
17	19	28	33	16	17
36 (27.6%)		61 (47%)		33 (25.4%)	

B   **MOCS37/129/Sv**

+/+		+/-		-/-	
M	F	M	F	M	F
11	8	19	20	10	11
19 (24%)		39 (49.3%)		21 (26.5%)	

Table 3.1: Statistical analysis of genotype for *MOCS1* locus of mice from F2 generation. (A), (B) The results in both Lines, line MOCS37/C57BL/6J and Line MOCS37/129/Sv are in accordance with Mendelian segregation, here 130 animals for Line MOCS/ C57BL/6J and 79 animals for MOCS37/129/sv were genotyped. M, male; F, female.

3.5.2 *MOCS1* deficient mice and survival curve in days

Homozygous (-/-) animals appeared normal at birth and suckled. However, they failed to thrive and died between days 1 and 11 after birth (Fig. 3.7) with a mean life span of 7.5 days (C57BL/6J x 129/Sv) and 5.4days (129/Sv). However, homozygous animals displayed no morphological abnormalities except a smaller size in comparison to their littermates and curly whiskers (Fig. 3.8). *MOCS1*-deficient animals from the mixed background strain (129/Sv C57BL6J) showed no phenotypic differences as compared with those from the inbred line (129/Sv) and were used for all subsequent analyses.

3.5.3 Growth curve analysis

As *MOCS1-/-* mice showed apparent growth retardation, the growth curve of *MOCS1-/-* mice were investigated. *MOCS1* mice from different developmental stages and as control normal littermates were weighed. 11 wild-type, 18 heterozygous and 10 homozygous mice were weighed during the first 5 days post partum. The result of growth curve is summarized in figure 3.9 and it shows dramatic growth retardation of *MOCS1-/-* mice. The mean weight and standard deviation was taken for mice and plotted against days. 5 of 10 homozygous mice died between 4 days and 5 days post partum.
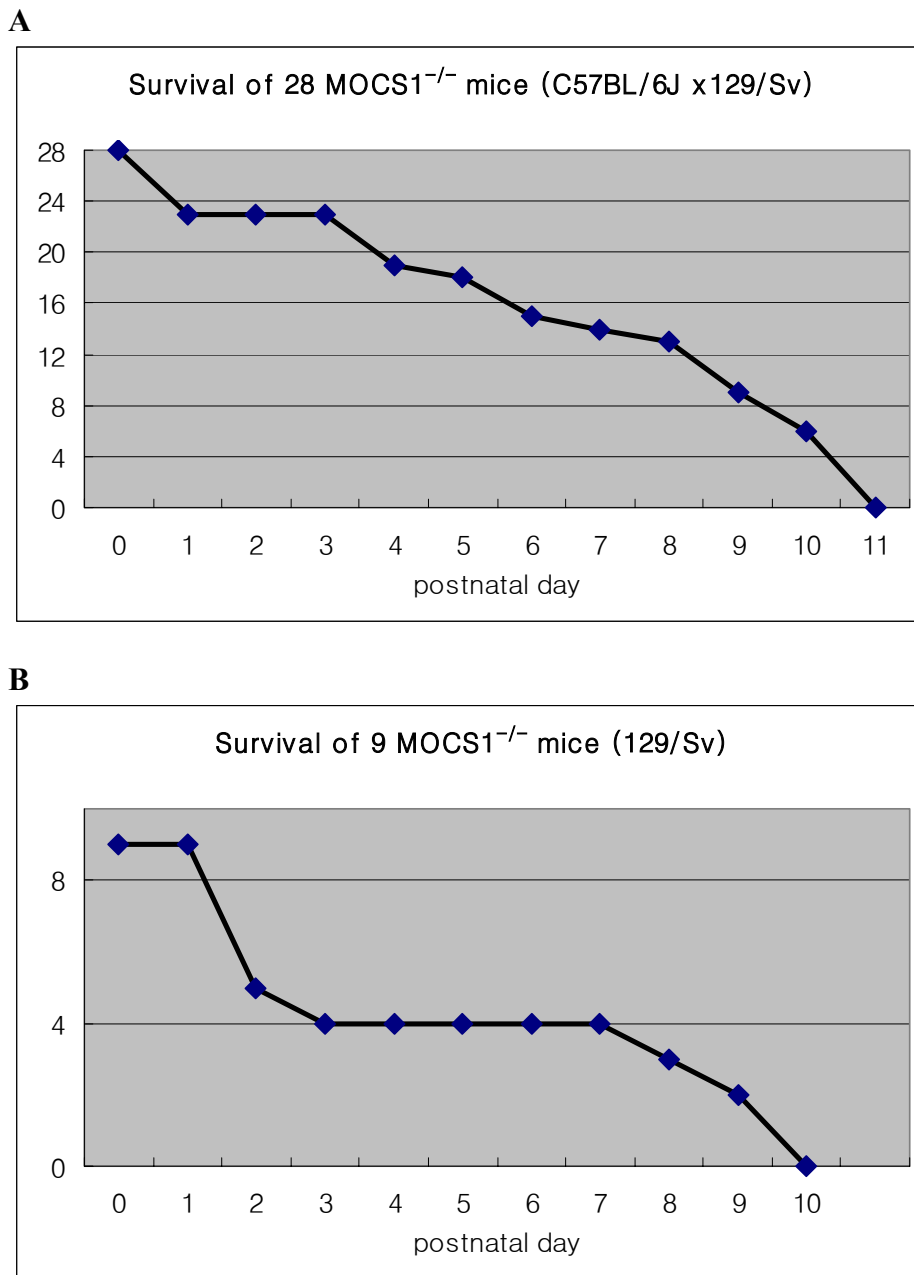
A

B

Figure 3.7: Survival of homozygous MoCo-deficient mice in days. No *MOCS1*-/- mouse so far survived beyond 11 postnatal day in both back ground C57BL/6J x 129/Sv (A), and 129/Sv (B).

Figure 3.8: MoCo-deficient mouse. *MOCS1*-/- mouse (left) and healthy littermate (right) on day 8 after birth. Homozygous animals displayed no morphological abnormalities except that smaller size in comparison to its littermate.
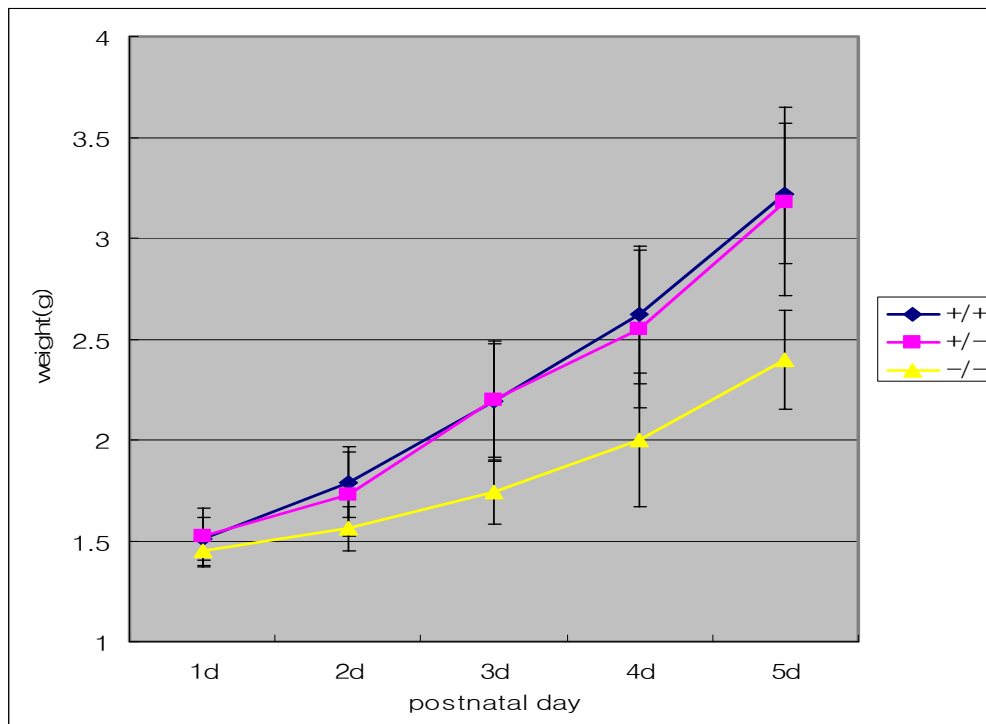

Figure 3.9: Weight development of +/+, +/-, and -/- mice during the first 5 days post partum. *MOCS1*-/- mice show a severe growth retardation.

3.5.4 Histological analysis of *MOCS1* mutant mice.

Since loss of white matter has repeatedly been reported for MoCo-deficient human patients (Graf et al. 1998; Johnson et al. 2001), nuclear staining of neuronal tissue was performed (Fig. 3.10). Hippocampus (Fig. 3.10 A), spinal cord (Fig. 3.10 B) and the cortex (Fig.3.10 C) of homozygous animals showed no macroscopic abnormalities in cell number or the development of cellular layers. For the MoCo-deficient gephyrin knock-out mouse, a disturbed postsynaptic clustering of inhibitory receptors has been reported (Kneussel et al. 1999). Immunostainings of *MOCS1*-deficient mice, in contrast, showed normal clusters for both gephyrin and glycine receptors (Fig. 3.11).
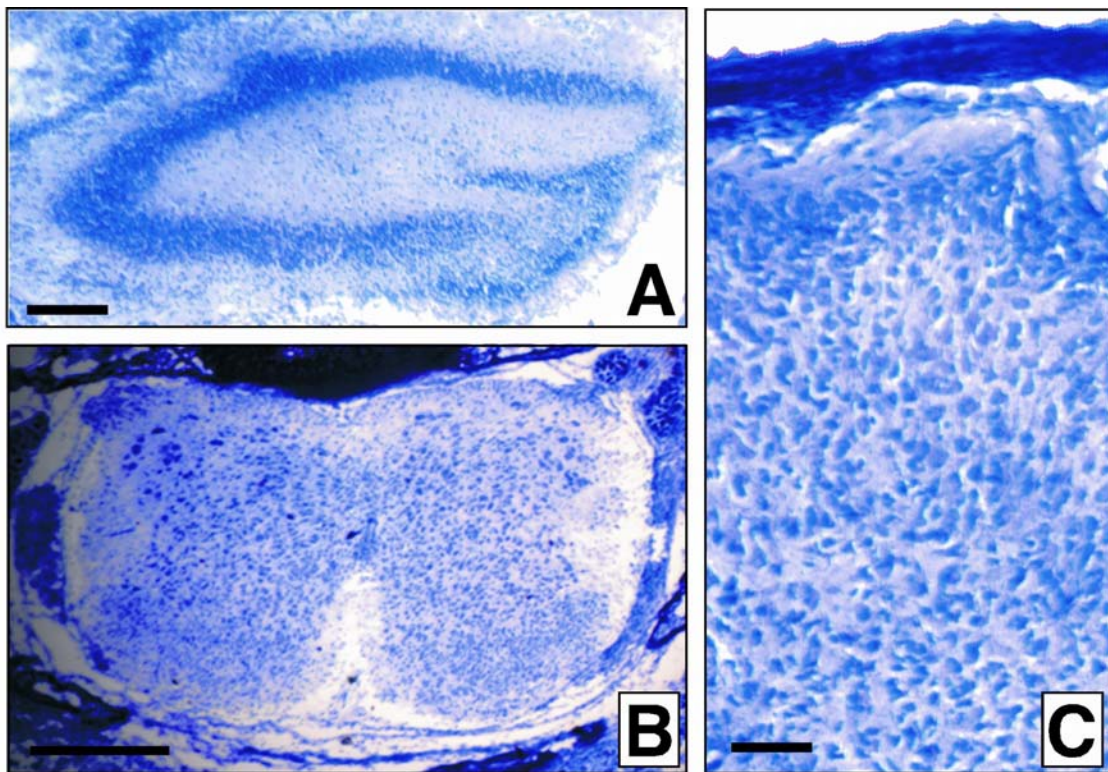
Figure 3.10: Nuclear staining of neuronal tissue derived from *MOCS1*-deficient mice. The hippocampus (A), the spinal cord (B), and a cortical detail (C) are shown. As compared to wild type tissue sections no macroscopic abnormalities in cell number or the development of cellular layers are detectable upon the loss of MOCS1 protein.
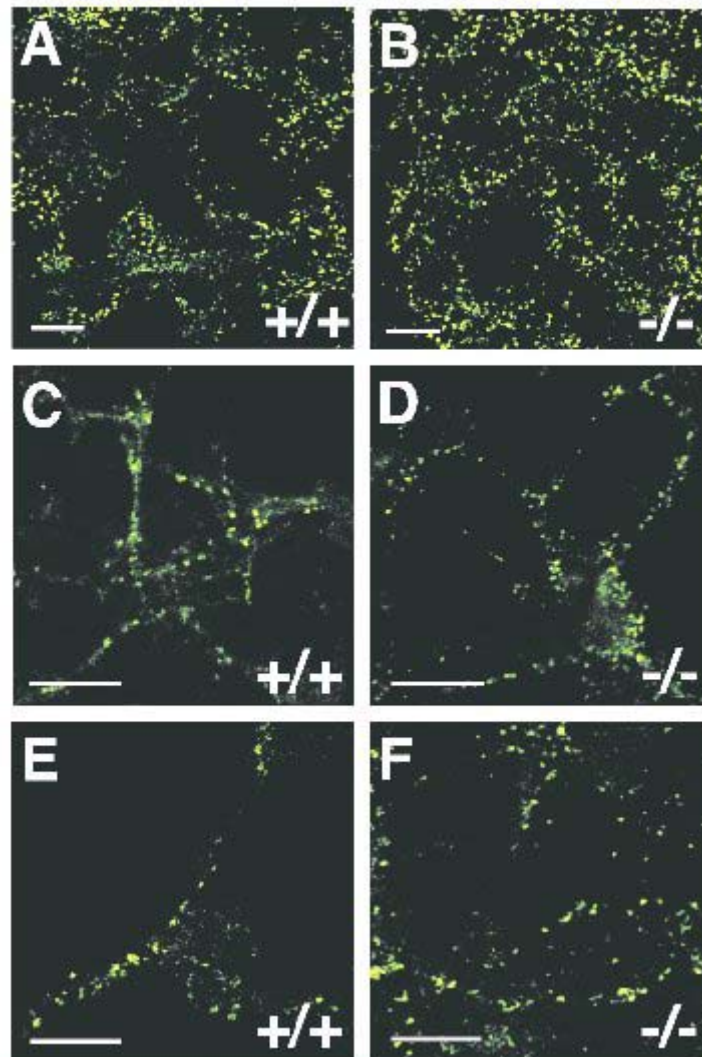
Figure 3.11: Postsynaptic immunoreactivities in spinal cord sections derived from wild-type (+/+) and *MOCS1* knock-out (-/-) mice. Immunostaining using antibodies specific for the postsynaptic clustering protein gephyrin (A–D) and the inhibitory glycine receptor (E and F) are shown. Sections derived from *MOCS1*-deficient mice display normal gephyrin clusters in number and size as compared to wild-type sections (A and B). At higher magnification gephyrin immunoreactivity is detectable in dendritic neuronal processes of both genotypes (C and D). Glycine receptor immunoreactive hotspots are concentrated along spinal dendrites of both genotypes as shown in representative projections (E and F).

3.5.5 Biochemical analysis of *MOCS1*-defecient mice

Molybdopterin was determined using the very sensitive nit-1 reconstitution assay. Figure 3.12 A shows that molybdopterin (free or in active cofactor form) in control animals is in the range 30–60 units/mg protein and virtually absent in the homozygous animals. Owe to the loss of MoCo all molybdenum-dependant enzymes are inactive, as demonstrated for sulfite oxidase and xanthine dehydrogenase by direct measurement of enzyme activity from liver extracts (Fig. 3.12 B and C). In control animals sulfite oxidase activity is increased in an age-dependent manner. Because of the total loss of molybdopterin, residual sulfite oxidase activities in homozygous mice are due to unspecific cytochrome c reductase activities in crude liver extracts (Johnson and Rajagopalan 1976). Semiquantitative determination of sulfite (Merckoquant) in fresh urine confirmed elevated sulfite levels in *MOCS1*-/- animals as compared to wild-type and heterozygotes (data not shown). Amino acid analysis showed elevated taurin levels as compared to other amino acid concentrations in -/- mice (data not shown). All urine samples revealed a signal coeluting with authentic sulfocystein reference compound, which was impaired by interfering components. This peak was higher in urine of -/- animals than in urine of wild-type or heterozygous animals. Cystin was clearly elevated in MoCo-deficient mice (Fig. 3.13 A). The loss of xanthine dehydrogenase activity results in an elevation of the substrate xanthine and undetectable levels of the product uric acid in the urine (Fig. 3.13 B and C). Wild-type as well as heterozygous mice show similar levels of xanthine oxidase educt and product. Hypoxanthine was undetectable in all samples.
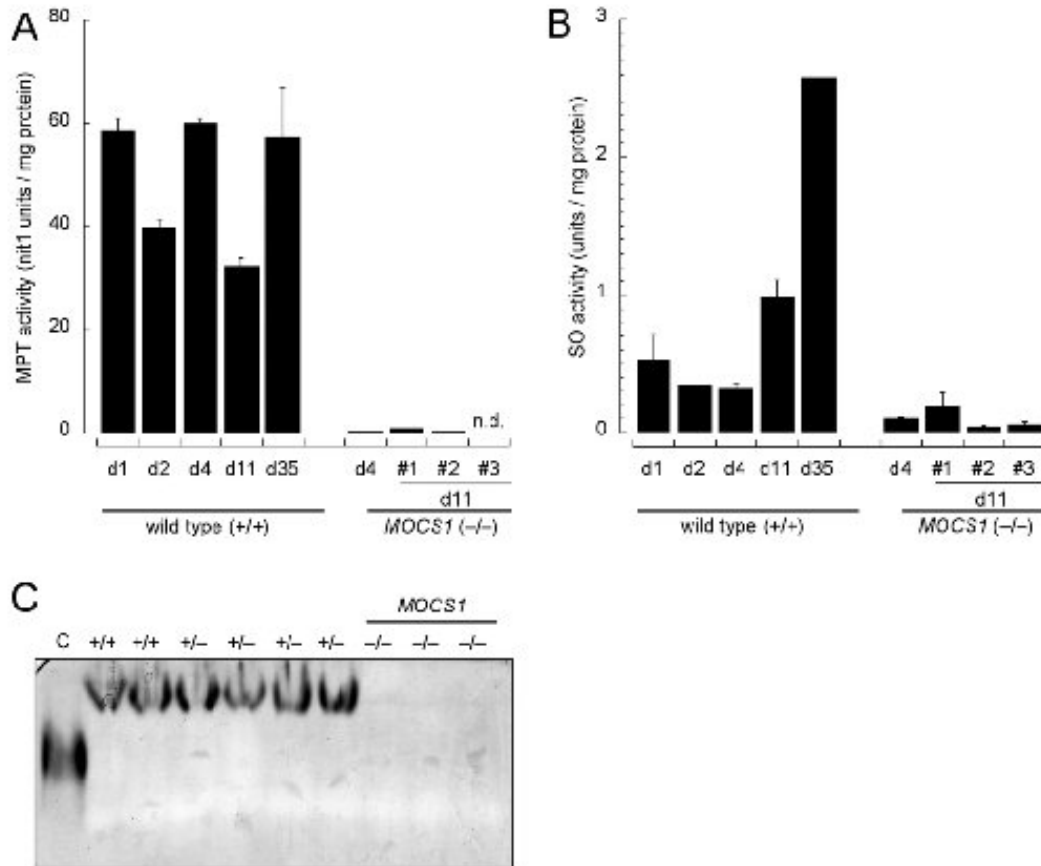
Figure 3.12: Biochemical analysis of *MOCS1*-deficient mice. (A) Molybdopterin content (including active molybdenum cofactor) of wild-type and *MOCS1*-deficient mice at various days after birth. (B) Sulfite oxidase activity of the same animals as investigated in (A). (C) In gel detection of xanthine dehydrogenase activity. As positive control (C) 0.75 mU of bovine xanthine oxidase were used.
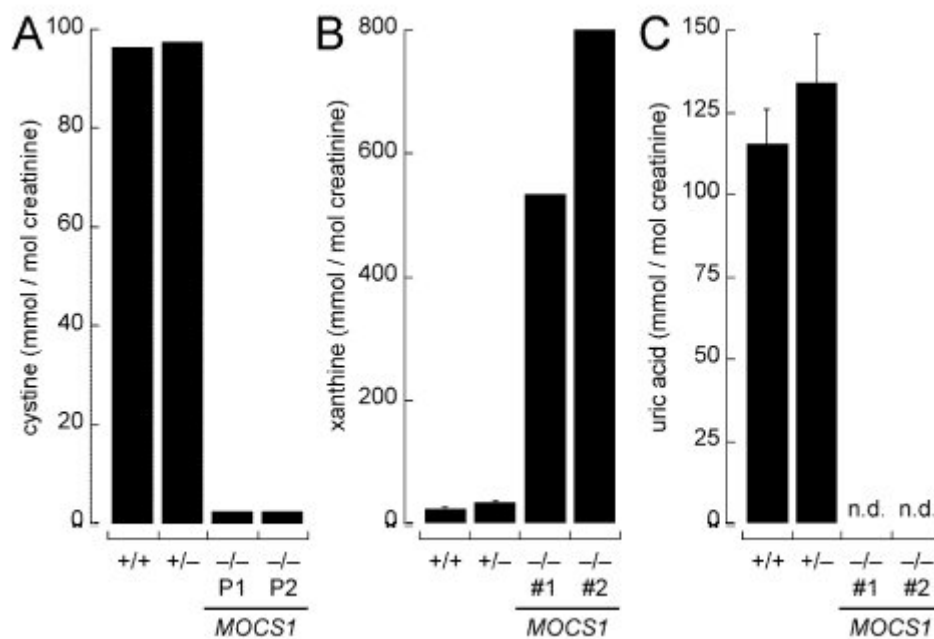
Figure 3.13: Metabolic analysis of *MOCS1*-deficient mice. (A) Cystine concentration of healthy (+/+), heterozygous (+/-), and homozygous (-/-) animals. Urine of at least three animals was collected on day 3 or 4 post partum and pooled. (B) Xanthine concentration in the urine of wild-type, heterozygous and -/- mice at day 5 post partum. (C) Uric acid levels in the urine of the same animals as investigated in (B).

3.6 Expression of *MOCS1* gene in the different developmental stages

To determine the expression of *MOCS1* gene in different tissues of the embryos and adult mouse, 30 µg of total RNA from liver, brain, placenta, kidney, and muscle was size fractionated in 1% agarose gel containing formaldehyde and transferred to nitrocellulose membranes. The Northern blot was hybridized with ^{32}P-labeled murine *MOCS1* exon 10 fragment. To check for integrity and equal amounts of RNA, the filter was rehybridized with a human elongation factor-2 (hEF) cDNA probe (Fig. 3.14). The bands were quantified using the program Quantity One (BIO-RAD) and the results are shown with graph (Fig. 3.15).
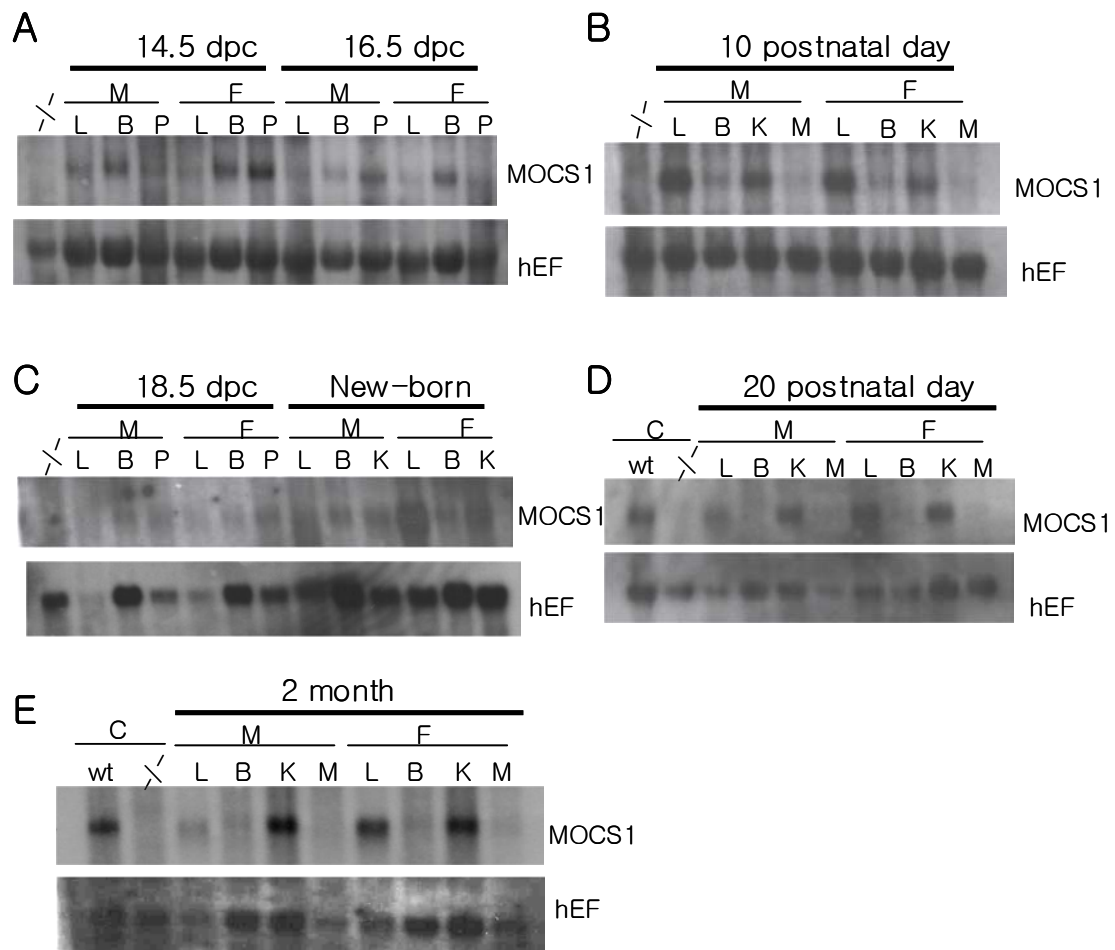
Figure 3.14: Northern blot analysis of *MOCS1* gene expression in mouse tissues from different developmental stages. Total RNA (30 µg) was extracted from various tissues (liver, brain, placenta, kidney, and muscle) and hybridized with *MOCS1* exon 10 probe (top). Rehybridization with human elongation factor (hEF, bottom) shows amount of RNA samples. Liver RNAs from wild-type and *MOCS1*-/- 3-day-old mice were used as positive and negative control, respectively. L, liver; B, brain; P, placenta; K, kidney; M, Muscle.
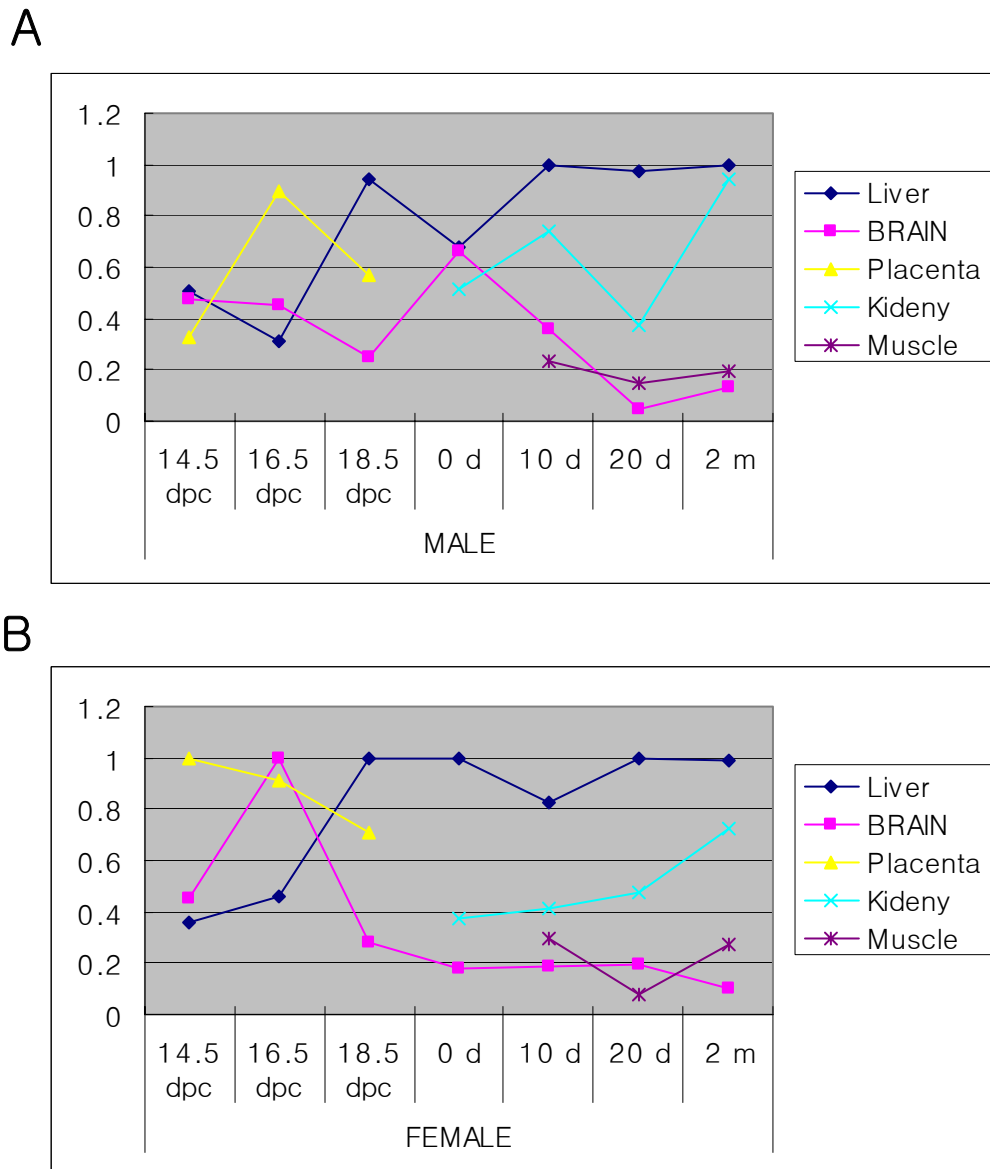
A

B

Figure 3.15: Relative expression of *MOCS1* gene in mouse tissues from different developmental stages. The density of each band from Northern blot (Fig. 3.14) was measured by the computer program Quantity One and calculated relative values of density by comparison to density of bands. The graph shows *MOCS1* expression of liver slowly grows up by time dependent manner in male (A) and female (B) mice.

Signal detection with *MOCS1* exon 10 probe required 4-5 days, whereas over-night for hEF cDNA probe. This indicates that expression level of *MOCS1* is quite low and small amount of *MOCS1* expression is sufficient for survival. However, the expression level in the liver slowly increased during development and reached to maximum expression level after birth. Low expression in the liver during the prenatal stage implies that MoCo activity can be supplemented from a healthy heterozygous mother via placenta.

3.7 Biochemical assay from the 18.5 dpc mouse embryos

In order to investigate maternal effect of MoCo for embryos, heterozygous animals were bred and amniotic fluid, liver, and blood plasma was isolated from 18.5 dpc embryos.

Elevation of xanthine and decline of uric acid were detected in amniotic fluid from homozygous embryos by resulting from the down-regulation of xnanthin dehydrogenase (Fig. 3.16). However, the level of xanthine was not as high as in urine of 5-day-old *MOCS1*-/- mice. Indeed, detectable uric acid level in amniotic fluid is far from the result of postnatal homozygous mice which has undetectable levels (Fig. 16 B and Fig. 3.13 C).

Amino acid analysis in blood showed small increased S-sulfo- L-cysteine (sulfocysteine) levels as compared to healthy mother, wild-type and heterozygous embryos (Fig. 3.17).

Sulfite oxidase activity was not detected in homozygous embryos (data not shown). However, the sensitive assay made it possible to determine the molybdopterin, which is absent in postnatal homozygous mice, from one of two homozygous embryos (Fig. 3.18). Although the result of molybdopterin assay is controversial, these data implies that MoCo activity is not completely removed in prenatal homozygous embryos and molecules for MoCo activity can be transferred from mother to embryos. The genotype of embryos was determined by PCR assay using tail and legs of embryos.
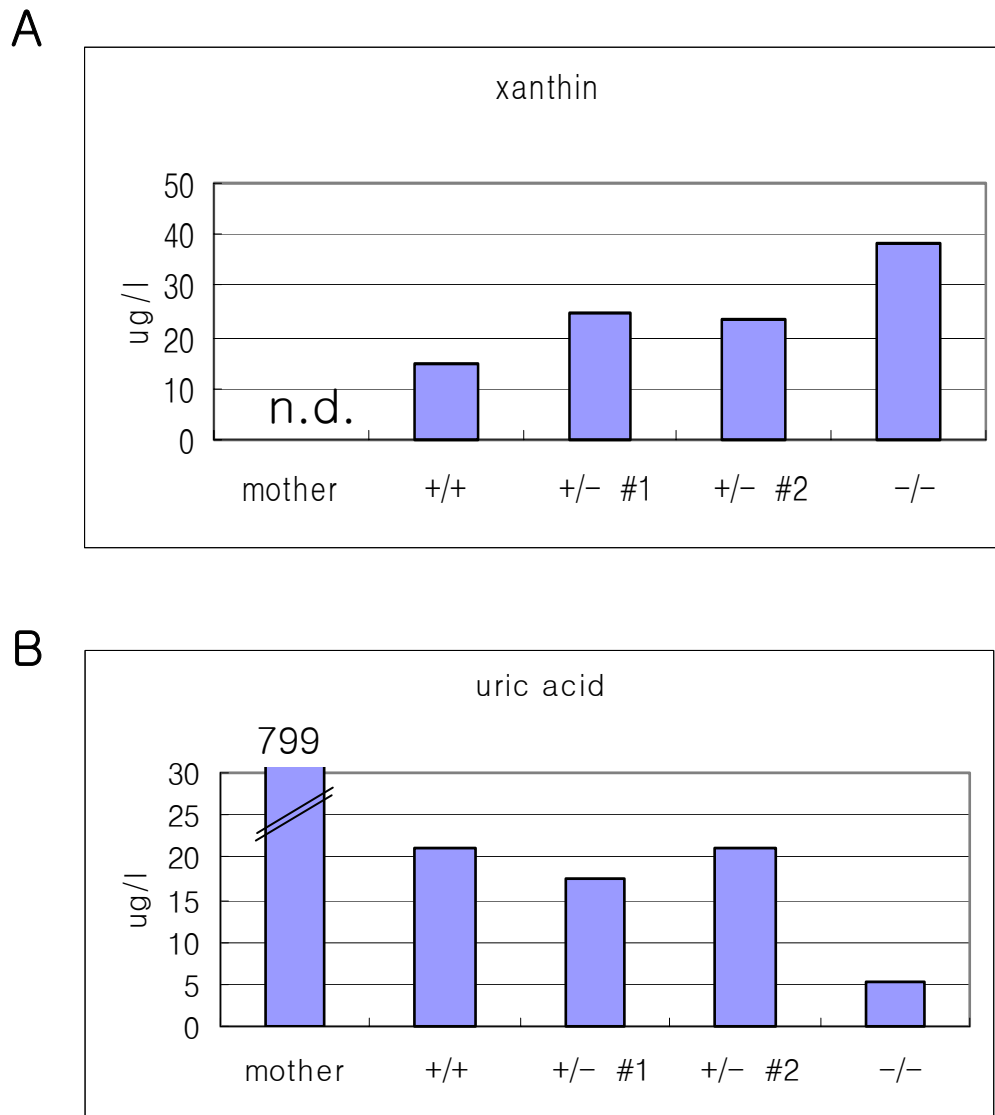
A

B

Figure 3.16: Metabolic analysis of *MOCS1*-deficient amniotic fluid. (A) Xantine concentration in the urine of heterozygous mother and in the amniotic fluid of wild type (+/+), heterozygous (+/-) and -/- embryos. Urine of mother was collected before being sacrificed. Amniotic fluid was collected from 18.5 dpc embryos and pooled. (B) Uric acid levels in the same samples as investigated in (A). n.d., non-detectable.
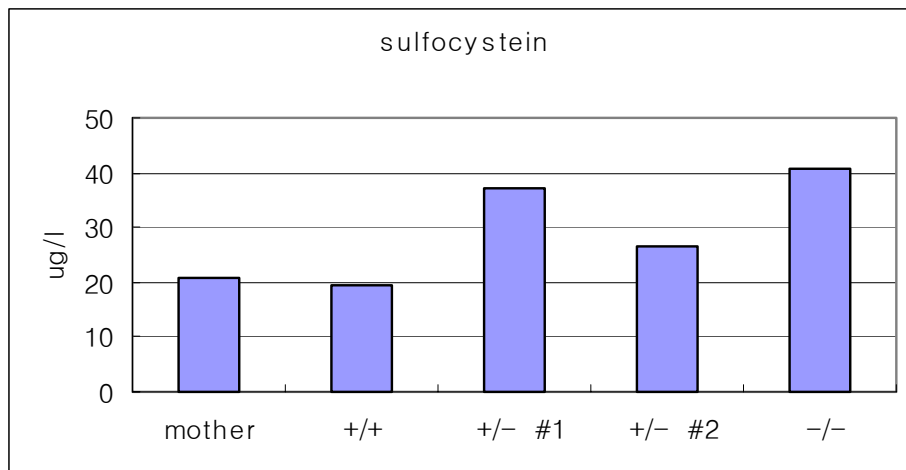
Figure 3.17: Metabolic analysis of *MOCS1*-deficient embryos. S-sulfo-L-cystein concentration of heterozygous mother and wild-type (+/+), heterozygous (+/-), and homozygous (-/-) embryos. Blood plasma of embryos was collected at 18.5 dpc and pooled.
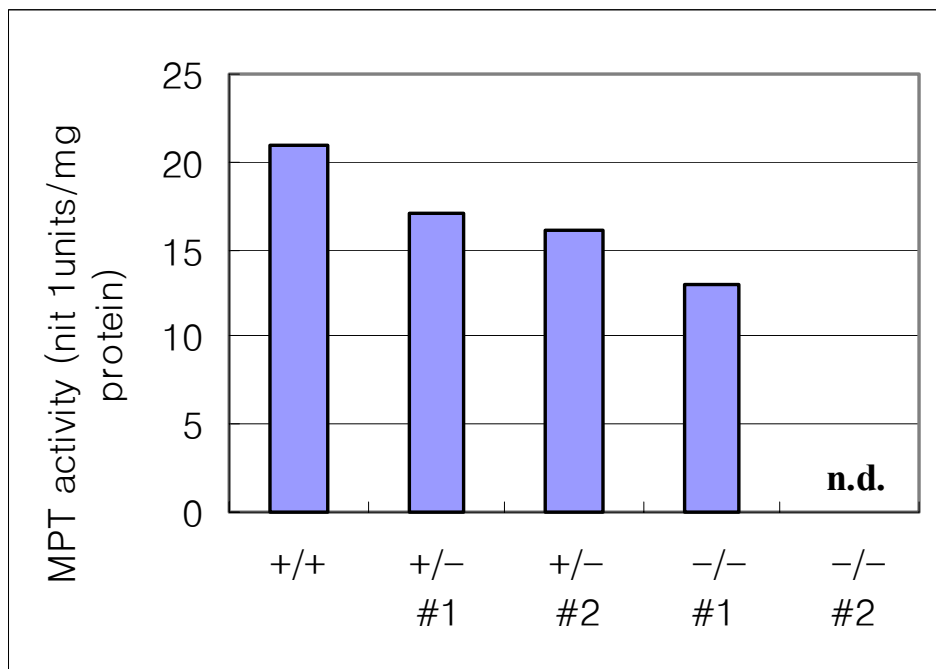

Figure 3.18: Biochemical analysis of *MOCS1*-deficient embryos. Molybdopterin content (including active molybdenum cofactor) of wild-type (+/+), heterozygous (+/-), and homozygous (-/-) embryos are shown. Liver of embryos at 18.5 dpc was isolated and analyzed. n.d., non-detectable.

3.8. Analysis of *Sox15* expression

3.8.1 Expression pattern of the *Sox15* gene in different tissues

To determine the expression of *Sox15* gene in ES cells and in different tissues of the adult mouse, 20 μg of total RNA from ES cells, brain, heart, kidney, liver, ovary, skeletal muscle, and testis was size fractionated in 1% agarose gel containing formaldehyde and transferred to nitrocellulose membrane. Equivalent loading and integrity of the RNA samples were confirmed by cross-hybridization of 18S ribosomal RNA. The Northern blot was hybridized with ^{32}P-labeled *Sox15* cDNA (GenBank AB014474, (Miyashita et al. 1999). A 1.4 kb transcript of the *Sox15* gene was detected only in ES cells (Fig. 3.19). To verify the results of Northern blot, the sensitive RT-PCR assay was carried out using the *Sox15* specific primers SoxF4 and SoxR3 and RNAs from different adult tissues and cell types, including heart, liver, lung, kidney, testis (Fig. 3.21 A), and testis of W/W^{v} mouse, Leydig cell line MA10 and Sertoli cell line 15P1 (Fig. 3.21 B). To avoid detection of contaminating DNA in mRNA samples, primers were designed from different exons (Fig.3.20). A 280 bp fragment was amplified in all samples (Fig.3.21). These results indicate that the *Sox15* is expressed at high level in embryonic stem cell and at lower level in other tissues.
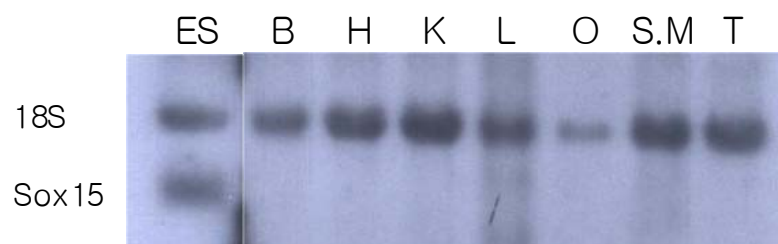

Figure 3.19: Northern blot analysis of Sox15 gene expression in ES cells and adult mouse tissues. Total RNA (20 μg) was extracted from ES cells and various tissues (B, brain; H, heart; K, kidney; L, liver; O, ovary; S.M, skeletal muscle; T, Testis) of adult mouse and subjected to Northern blot hybridization using the Sox15 cDNA as a probe. Cross-hybridization with 18S ribosomal RNA is also presented.
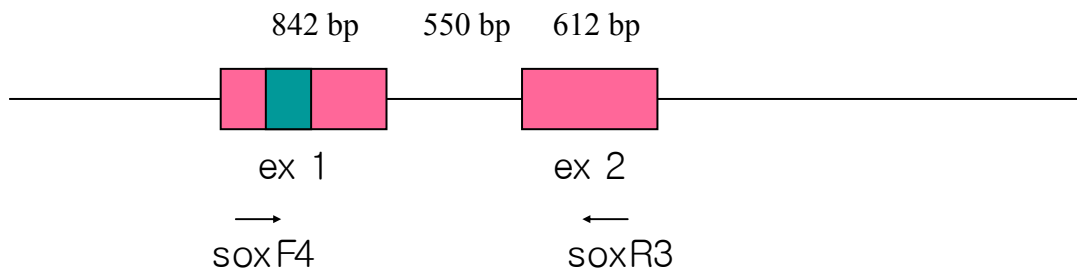
Figure 3.20: Schematic representation of exon-intron structure of *Sox15* gene. The exons of *Sox15* are shown as coloured boxes and HMG box is shown as green box in exon 1. Arrows indicate the primer locations used for RT-PCR.
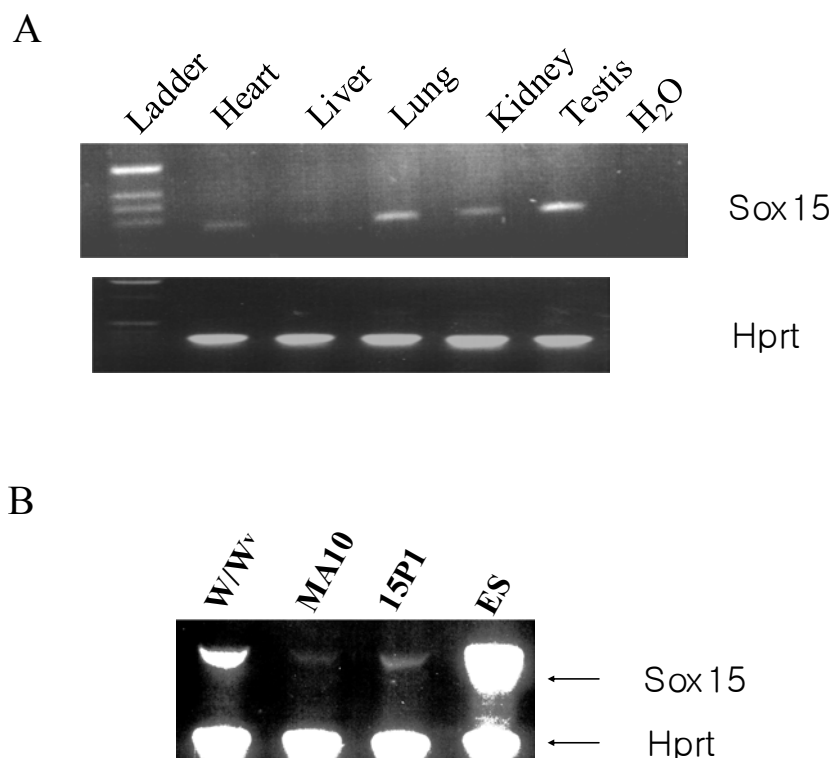

Figure 3.21: Expression analysis of *Sox15* gene by RT-PCR. Total RNA was isolated from different adult tissues (A) and testis of W/W^V mouse and various cell types (B). The RT-PCR was carried out using *Sox15* specific primers SoxF4 and SoxR3 (see Fig. 3.20). *Hprt* was used to standardize the quality of RNA amounts.

3.8.2 Sox15 protein analysis

3.8.2.1 Expression pattern of Sox15 protein

Polyclonal antibody against Sox15 peptide was generated as described in Methods (section 2.15). The position and sequence of the peptide used for immunization of the rabbits is shown in figure 3.22. In order to obtain high affinity antibody against Sox15 protein, purification of the antiserum was performed. An affinity column (SulfoLink®Coupling Gel) conjugated with Sox15 peptide was used to purify antibody against Sox15 peptide. Fractions were eluted after binding of antiserum to the column. In order to determine the specificity and affinity of antiserum, Western blot analysis was performed. Total protein extract from testis, muscle and ES cells were separated on SDS-PAGE and transferred onto a PVDF membrane. Western blot was performed with 1:100 dilution of anti-Sox15 antibody.

Western blot analysis showed that the anti-Sox15 antibody only recognizes a 25 kDa protein in extracts from ES cells and wild-type myobalsts (Fig. 3.23 B). This band, which was not detected by preimmune sera from the same rabbits (Fig. 3.23 A), corresponds to a protein of the size predicted from the *Sox15* cDNA. Indeed, the antibody strongly recognizes the 41 kDa of fusion protein, Sox15-GST.

To further verify the specificity of the affinity purified antibody, primary cultures of myoblasts, ES cells and Swiss3T3 cells were stained with the anti-Sox15 antibody. Figure 3.24 shows that ES cells and myoblasts are stained by Cy3-conjugated secondary antibody compared to differentiated myoblasts and Swiss3T3 cells (Fig. 3.24). In addition, anti-Sox15 staining was restricted to the nucleus. This result revealed *Sox15* gene is dominantly expressed in non-differentiated cell types and nuclear localization of *Sox15* corresponds to its predicted role as transcription factor.

```
   1 atggcgctgaccagctcctcacaagcagagacttggagcctgcat
     M   A   L   T   S   S   S   Q   A   E   T   W   S   L   H
  46 cctcgggcttccacggcctctttgcctttaggaccccaggagcag
     P   R   A   S   T   A   S   L   P   L   G   P   Q   E   Q
  91 gaggccggcgggagccctggagcgtctgggggacttccgctggag
     E   A   G   G   S   P   G   A   S   G   G   L   P   L   E
 136 aaggtgaagcggcccatgaacgccttcatggtgtggagctctgtt
     K   V   K   R   P   M   N   A   F   M   V   W   S   S   V
 181 cagcgccgccagatggcgcagcagaaccccaagatgcacaactct
     Q   R   R   Q   M   A   Q   Q   N   P   K   M   H   N   S
 226 gagatctccaagcgcttgggcgctcagtggaagctgctgggcgat
     E   I   S   K   R   L   G   A   Q   W   K   L   L   G   D
 271 gaagagaagcgacccttcgtggaggaggctaagcgtcttcgtgcc
     E   E   K   R   P   F   V   E   E   A   K   R   L   R   A
 316 cgccacctccgcgactatcccgactacaagtaccgacccggcgt
     R   H   L   R   D   Y   P   D   Y   K   Y   R   P   R   R
 361 aagagcaaaaactcgagcaccggggtctgtcccctttagccaagaa
     K   S   K   N   S   S   T   G   S   V   P   F   S   Q   E
 406 ggaggtggcctggcatgtggtggctcacactgggggccagggtac
     G   G   G   L   A   C   G   G   S   H   W   G   P   G   Y
 451 acaactacccaagggagcagaggctttgggtaccagcccccaac
     T   T   T   Q   G   S   R   G   F   G   Y   Q   P   P   N
 496 tattcgacagcctacctgcctggcagttacacctcttcccactgc
     Y   S   T   A   Y   L   P   G   S   Y   T   S   S   H   C
 541 agaccggaggccccttacca<span style="color:blue">tgcacttccctcagagtgatccc</span>
     R   P   E   A   P   L   P   <span style="color:blue">C   T   F   P   Q   S   D   P</span>
 586 <span style="color:blue">aggctccaggggggagctaagaccc</span>tctttctccccttacctatcc
     <span style="color:blue">R   L   Q   G   E   L   R   P</span>   S   F   S   P   Y   L   S
 631 ccagactcttccactccatataatacttcccttgctggagccccc
     P   D   S   S   T   P   Y   N   T   S   L   A   G   A   P
 676 atgccagtaacccacctttaa 696
     M   P   V   T   H   L   *
```

Figure 3.22: Nucleotide and deduced amino acid sequence of *Sox15* coding sequence. The sequence for peptide antibody is indicated by blue letters.
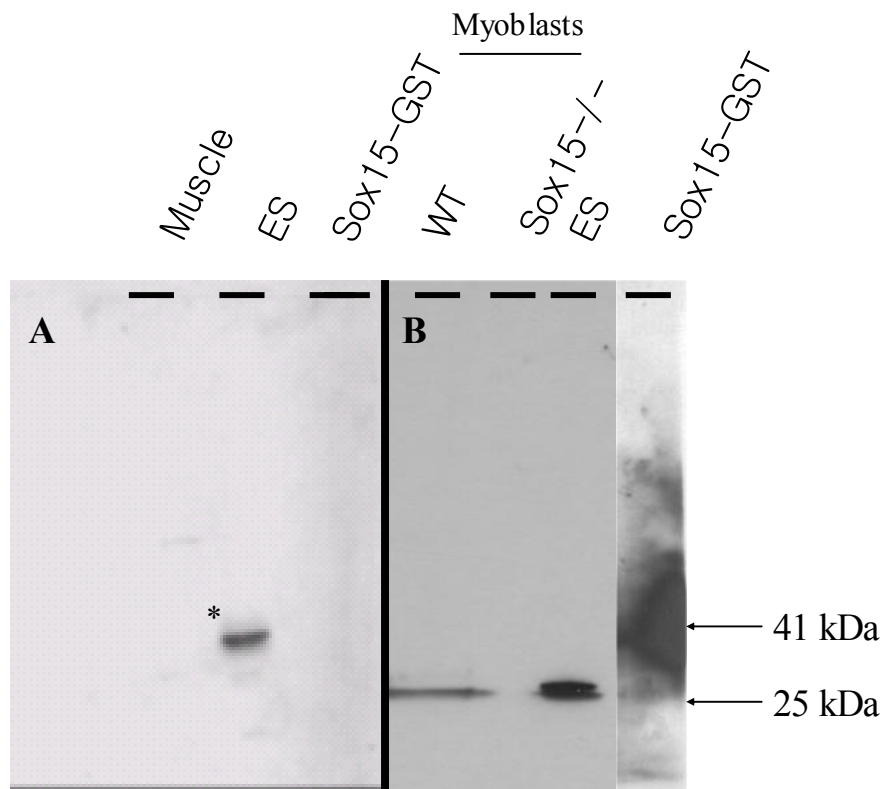
Figure 3.23: Western blot analysis with polyclonal antibody against Sox15 protein. In this analysis dilution of 1:100 was used. (A) Pre-immune serum showed cross-reactivity to ES cell extracts (*asterisk*) and no band from Sox15-GST fusion protein. (B) Affinity purified antibody detect a band corresponding to size 25 kDa in ES cell and myoblast protein extract and 41 kDa of Sox15-GST fusion protein. 20 µg of protein was loaded testicular and proteins.
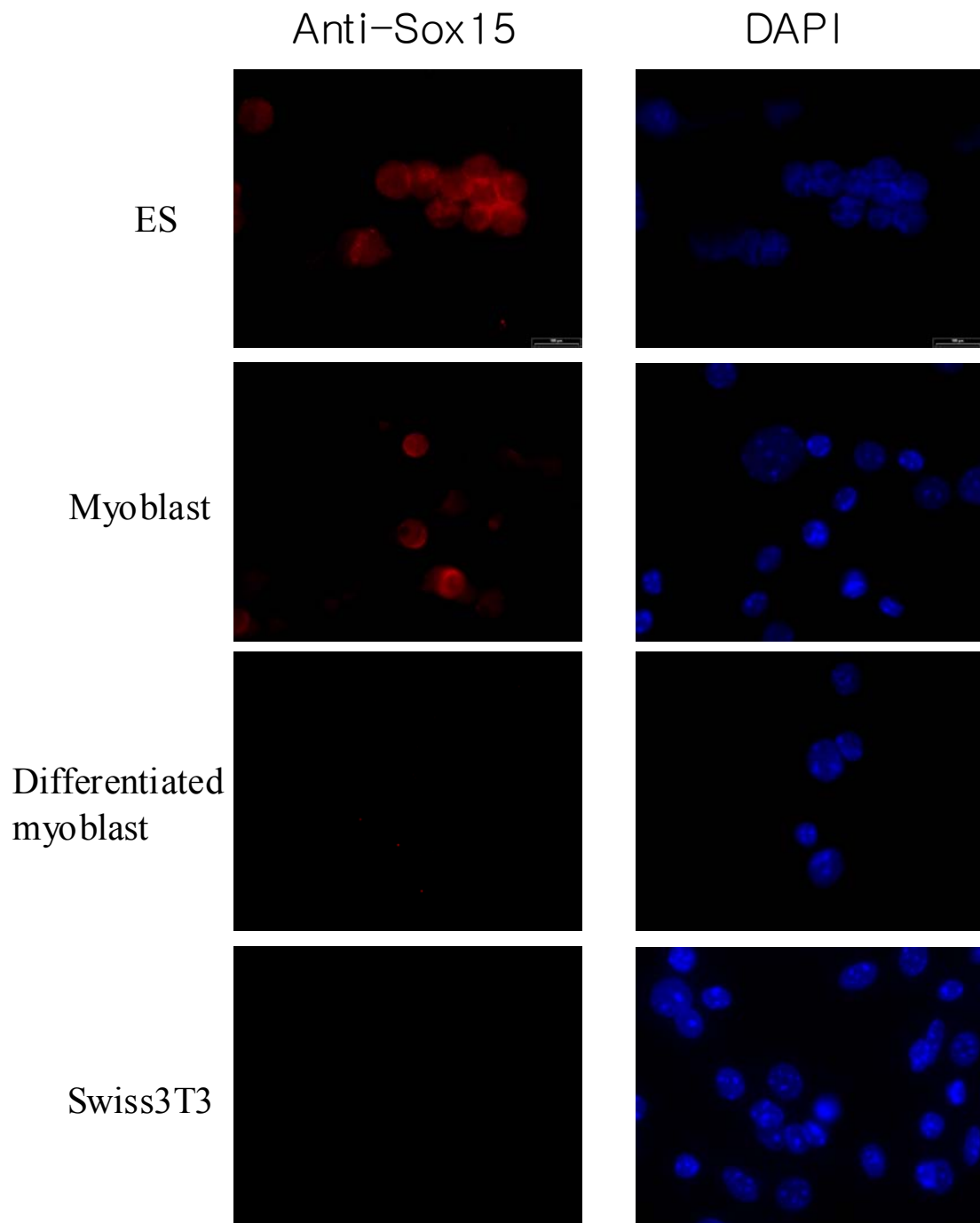
Figure 3.24: Affinity of the Sox15 antibody and subcellular localization of the Sox15. ES cells and myoblasts reacted with anti-Sox15 antibody. By contrast, differentiated myoblasts and 3T3 cells didn't react with the antibody. Localization of the Sox15 was only restricted to the nucleus. Reactivity with anti-Sox15 antibody was visualized with Cy3-conjugated secondary antibody (red). Cells were counterstained with DAPI (blue).

3.8.2.2 Nuclear localization of Sox15 protein

To verify nuclear localization of Sox15 protein, Sox15 protein was examined by transient transfection of Swiss3T3 cells with a pTri-EX-Neo1.1–Sox15 construct in which the *Sox15* cDNA under the control of the α-actin promoter. Figure 3.25 illustrates that Sox15 protein is mainly localized in the nucleus of the cell as can be seen by red Cy3 immunostaining of the cell. To confirm any effect of vector itself, pTri-EX-Neo1.1 vector was transfected as a control and showed no reaction against anti-Sox15 antibody. Cells were counterstained with DAPI to identify nuclei in these cells (Fig. 3.25).
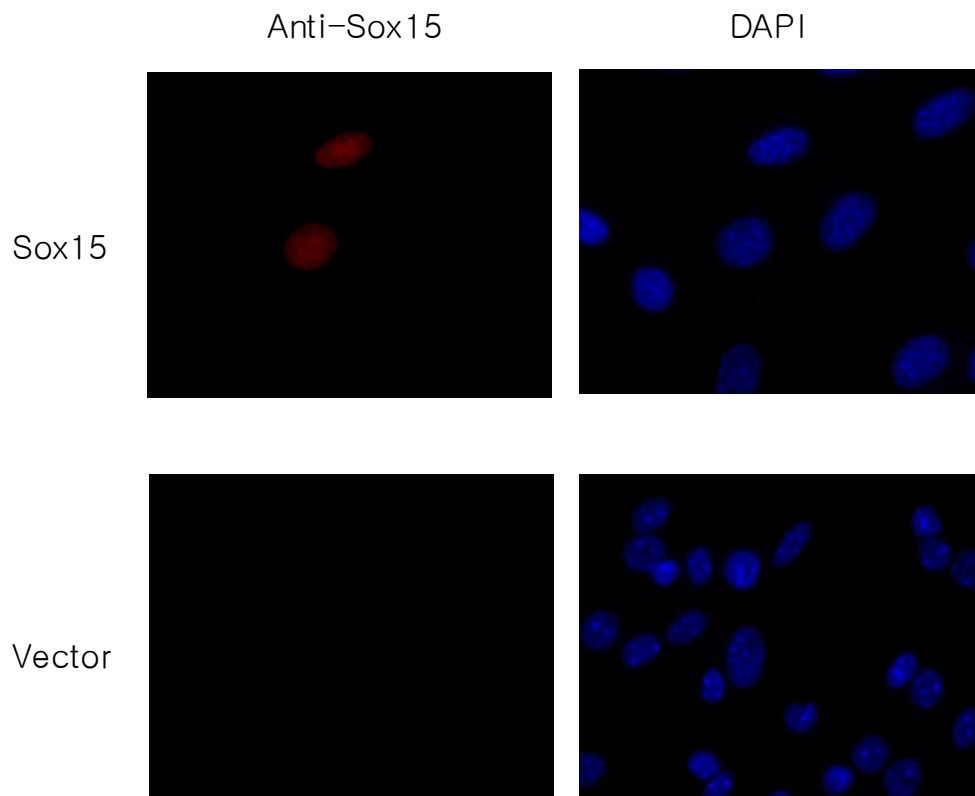

Figure 3.25: Cellular localization of *Sox15*. Swiss3T3 cells were transfected with pTri-EX – Neo1.1-Sox15 and vector only. 48 hrs after transfection, cells were fixed and analysed. *Sox15* transfected cells were visualized by staining with anti-Sox15 antibody (red) and counterstaining with DAPI (blue).

3.9 Homologous recombination of *Sox15*

3.9.1 Isolation of cosmid clone with mouse genomic DNA

A cosmid clone carrying the *Sox15* was isolated from a 129/Sv genomic mouse library (RZPD) by Dr. Adham (Institute of Human Genetics, Goettingen).

3.9.2 Construction of *Sox15* targeting vector

To disrupt the *Sox15* gene, a replacement targeting vector was designed to delete the 3-kb *Hind*III/*Kpn*I fragment containing 5'flanking region and exon 1, and replaced by the neomycin phosphotransferase (*NEO*) gene under the control of the phosphoglycerate kinase promoter. Introduction of a negative selection marker, the herpes simplex virus thymidine kinase (*TK*) gene, at the 3' end of the construct (Fig. 3.27) enabled us to perform positive selection (Mansour et al. 1988).

3.9.2.1 Subcloning of *Sox15* genomic fragment

For the determination of the restriction map of the *Sox15* locus and localization of the exonic sequences, the 4 and 10 kb *Xho*I genomic fragment was subcloned into the pZERO-TM-2 vector and examined by Southern blot analysis (Fig. 3.26 A).

3.9.2.2 Subcloning of the 5' flanking region of *Sox15* gene into the pPNT vector

The 5.5 kb *Hind*III fragment containing a 5´flanking region was isolated from the 10 kb *Xho*I subclone, inserted into *Spe*I/*Not*I restricted pBluscript vector and subsequently digested with *Xho*I and *Not*I (Fig. 3.26 B). The isolated 5.5 kb *Xho*I/*Not*I fragment was then inserted into *Xho*I/*Not*I –digested pPNT vector (clone Sox15/1).

3.9.2.3 Subcloning of the 3' flanking region in the pPNT vector

The 3.5 kb *Kpn*I/*Sal*I fragment containing a 3´sequence of the gene was isolated from the 4 kb *Xho*I subclone and ligated with *Eco*RI-digested clone Sox15/1 after filling the end with Klenow enzyme. The replacement vector *Sox15-Neo-Tk* was digested with different restriction enzymes to confirm the orientation of the cloned fragment in the pPNT vector.

The resulting 16 kb targeting vector (Fig. 3.26 D) was linearized with the unique *Not*I site present in the polylinker site of the pPNT vector before transfection.
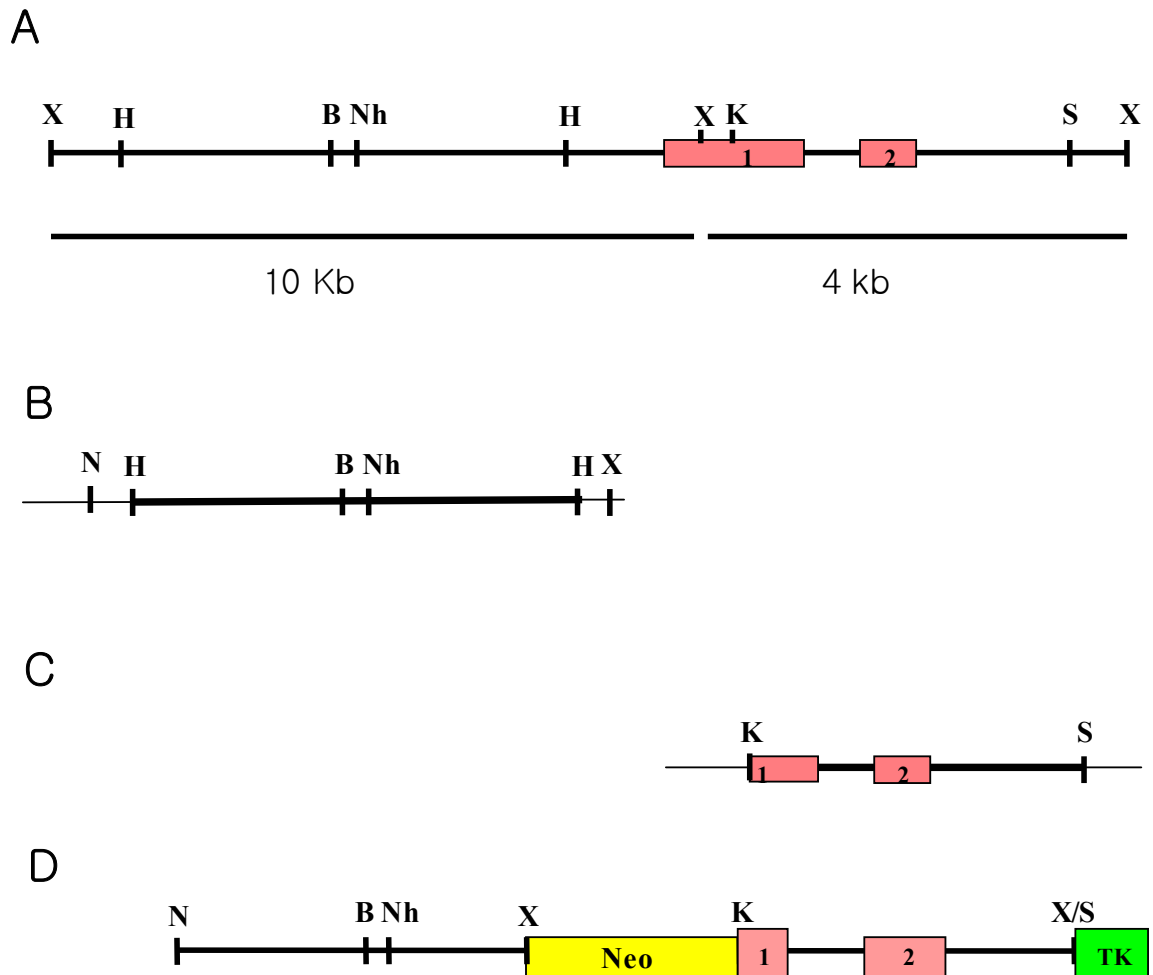

Figure 3.26: Restriction digestion map of *Sox15* genomic DNA and fragment which were cloned. (A) Schematic diagram of *Sox15* gene. (B) 5.5 kb *Hind*III fragment for 5' flanking region. (C) 3.5 kb fragment for 3' flanking region. (D) The replacement vector *Sox15-Neo-TK*. Abbreviations are: B, *Ba*mHI; H, *Hin*dIII; N, *Not*I; Nh, *Nhe*I; S, *Sal*I; X, *Xho*I.
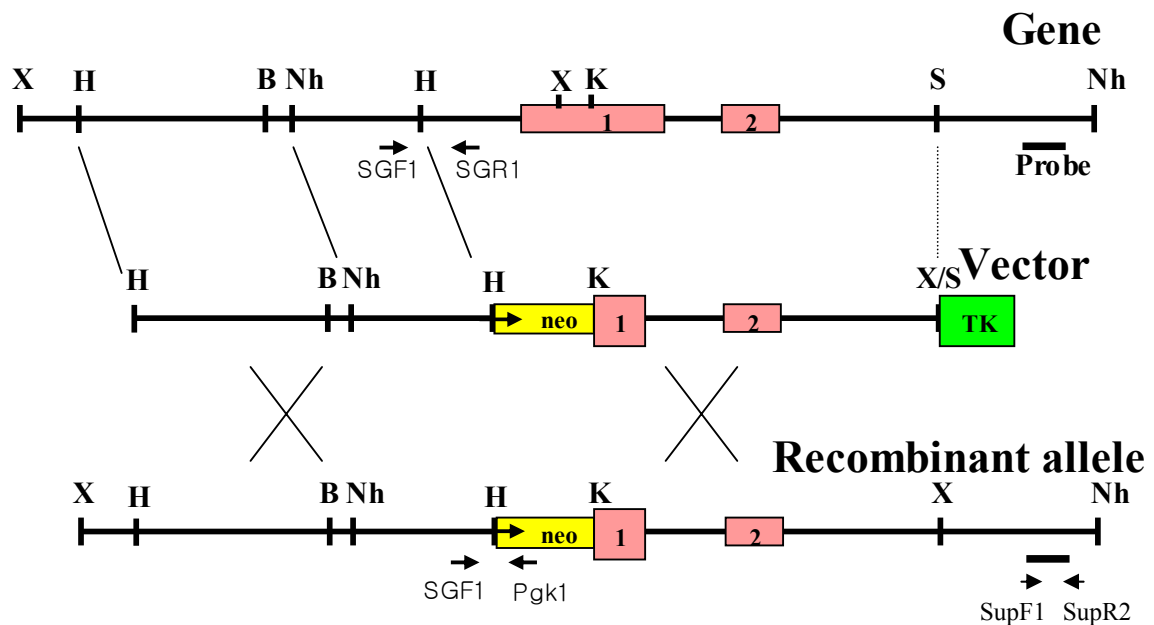
Figure 3.27: Targeted disruption of *Sox15* gene. Structure of the gene (top), targeting vector (middle), and targeted allele (bottom) are shown together with the relevant restriction sites. A 3 kb *Hind*III/*Kpn*I fragment containing 5' flanking region and part of exon 1 of the gene was replaced by Pgk-neo selection cassette (neo, yellow box). TK, Thymidine kinase cassette (green box); B, *Ba*mHI; H, *Hin*dIII; Nh, *NheI*; S, *SalI*; X, *XhoI*. The primers SGF1, SGR1 and Pgk1 were used to amplify wild-type and targeted allele in PCR assay is shown.

3.9.3 Subcloning of the 3' external probe

A 470 bp fragment at the 3' region of the *Sox15* was amplified by PCR using the primer SupF1 and SupR2 (Fig. 3.27). This PCR amplicon was subloned into pGEM-Teasy and digested with *EcoR*I for insert isolation. The 470 bp subcloned fragment was used as 3' external probe for hybridization in the Southern blot with DNA extracted from the recombinant ES-clones.

3.9.4 Electroporation of the RI ES-cells and screening of ES-clones for homologous recombination events

The ES cell line RI was cultured as described (2.2.19). Confluent plates were washed in PBS buffer, trypsinized and the cells were suspended in the same buffer at 2×10^7 cells/ml. Aliquots of this cell suspension were mixed with 50 µg of linearlized targeted vector *Sox15-NEO-TK* and electroporated at 250V and 500 µF using a Bio-Rad Gene Pulser apparatus. The cells were plated onto nonselective medium in the presence of G418-resistant embryonic mouse fibroblasts. After 36 hr, selection was applied using medium containing G418 at 400 µg/ml and gancyclovir at 2 µM. After 10 days of selection, 96 individual drug-resistant clones were picked into 24-well trays for freezing and isolation of DNA.

To screen recombinant ES-clones for homologous recombination events, genomic DNA was extracted from the recombinant ES-clones, digested with *Nhe*I, electrophoresed and blotted onto nitrocellulose filters. The blots were hybridized with ^{32}P-labeled 470 bp 3' probe (Fig. 3.25). In case of homologous recombination event, the wild-type locus showed a 12 kb *Nhe*I fragment and the targeted locus was 10.8 kb *Nhe*I fragment (Fig. 3.28). Of the colonies screened, 2 of 72 clones had undergone correct homologues recombination.
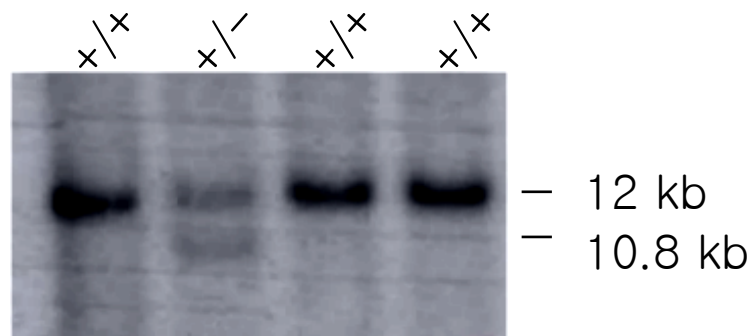

Figure 3.28: Analysis of transfected ES cells by Southern blot. The ES cell DNAs were digested with *Nhe*I and hybridized with the 3' external probe shown in Fig. 3.20. Homologous recombination events yielded a 10.8 kb hybridizing band detected in heterozygous (+/-) cell line, while the wild type (+/+) cell line showed only a 12 kb band

3.10 Generation of chimeric mice

ES cells from the recombinant clones were injected into 3.5 dpc blastocyst derived from C57BL/6J mice. The blastocysts were retransferred into pseudopregnant CD1 mice to generate chimeric mice. 7 chimeras were obtained after 2 independent injections of one recombinant ES clone named as Sox34. The chimeras were scored according to coat color (in percentage). 7 chimeras from Sox34 line with 90-95 % of chimerism were bred with C57BL/6J and 129/Sv mice to obtain F1 animals in respective genetic background namely C57BL/6J x 129/Sv and in 129/Sv. The germline transmission of Sox15 deleted allele was checked by genomic PCR using SGF1, SGR1, and Pgk1 primers (Fig. 3.27) with genomic DNA isolated from tail biopsies of the mice (Fig. 3.29)
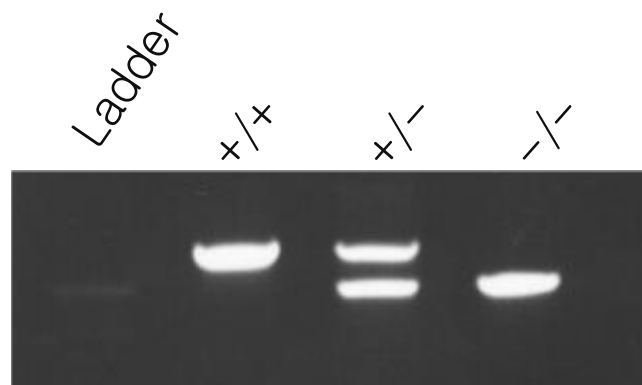

Figure 3.29: PCR genotyping of progeny. Wild-type (+/+), heterozygous (+/-), and homozygous (-/-) mice were identified by amplification of PCR products specific for either the *Sox15* wild-type allele (700 bp) or the targeted allele (490 bp). The PCR products obtained using primers SGF1, SGR1, and Pgk1 (Fig 3.20) were electrophoresed on 1.5% agarose gel and stained with ethidium bromide.

3.11 Generation of *Sox15* knock-out mice

F1 animals which were heterozygous at *Sox151* locus were intercrossed to obtain F2 animals. The breeding strategy was undertaken in such a way that the *Sox15* deleted allele was established in both C57BL/6J x 129/Sv and in 129/Sv genetic background. Male and female mice heterozygous for the *Sox15* mutation appeared normal and fertile. The tail PCR analysis of 201 offspring in C57BL/6J x 129/Sv and 193 offspring in the 129/Sv genetic background revealed no significant deviation from the predicted 1:2:1 Mendelian distribution (Table 3.2). The gross phenotypical appearance of homozygous *Sox15* mutant was normal.

A   Sox15/ C57BL/6J X 129/Sv

+/+		+/-		-/-	
M	F	M	F	M	F
21	23	60	42	23	32
44 (23%)		102 (50%)		55 (27%)	

B   Sox15/129/Sv

+/+		+/-		-/-	
M	F	M	F	M	F
29	25	40	51	26	22
54 (28%)		91 (47.2%)		48 (25%)	

Table 3.2: Statistical analysis of genotype for *Sox15* locus in F2 generation. (A), (B) Both Line Sox34/C57BL/6J and Line Sox34/129/Sv was in accordance with Mendelian segregation, here 204 animals for Line Sox15/ C57BL/6J and 193 animals for Sox15/129/sv were genotyped. M, male; F, female.

3.12 Fertility test of *Sox15*-/- mice

To study the reproductive functions of *Sox15*-/- mice, we systematically tested the reproductive capacity of homozygous mice of both sexes with wild type mates. Five homozygous *Sox15*-/- (129/Sv) males and 5 control males (129/Sv) were mated with wild-type NMR1 female mice. Each male was bred with 3 females and these females were changed every 3 month with young mice.

In addition, five homozygous *Sox15*-/- (129/Sv) females and 5 control females (129/Sv) were mated with wild-type 129 male mice. The fertility of *Sox15* deficient males and

females was determined by mean number of offspring. The result is summarized in figure 3. 30. Both male and female *Sox15*-/- mice showed no significant differences in comparison to wild-type mice, indicating *Sox15*-/- mice has normal reproductive capacity.
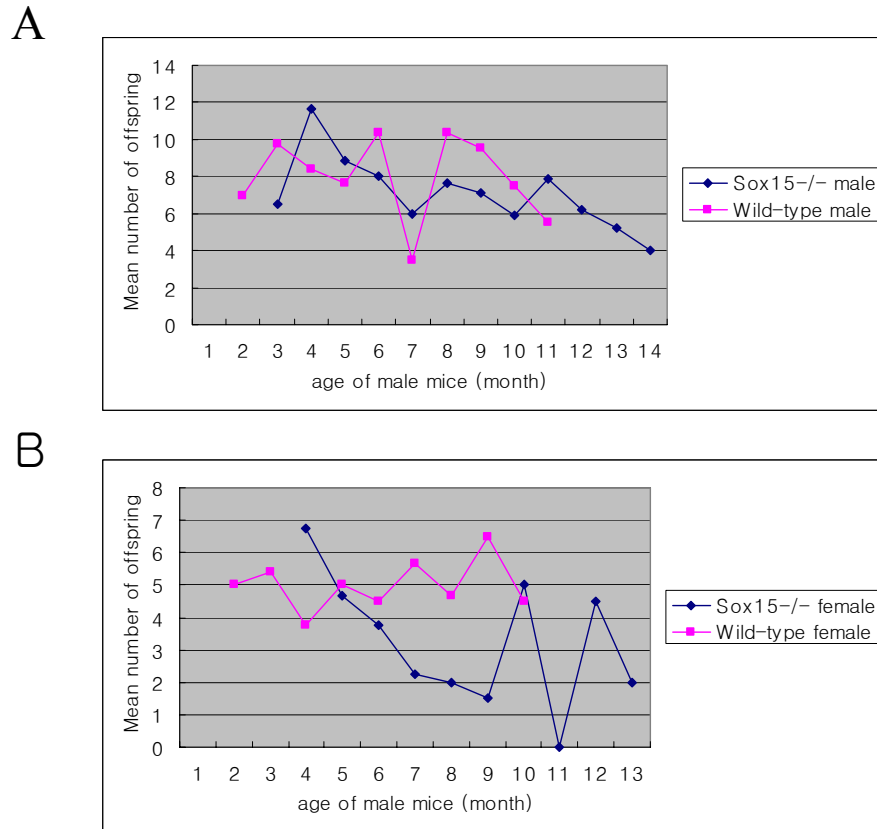
A

B

Figure 3.30: Fertility test of *Sox15*-/- mice. (A) The average litter size form *Sox15*-/- male (129/Sv) with wild-type (NMR1) showed no differences. (B) *Sox15*-/- female was mated with wild-type mice (129/Sv X 129/Sv) and their offspring has no significant differences. These data shows *Sox15*-/- mice have normal reproductive capacity**.**

3.12 Cellular and molecular analysis of *Sox15*-/- myoblasts

3.12.1 Altered cellular phenotype of *Sox15* -/- myogenic cells

Down-regulation of Sox15 in differentiated myogenic cells (Fig 3. 24) led to us to consider the hypothesis that Sox15 may have some important role in the proliferation and differentiation of myogenic cells.

To gain insight into the role of *Sox15* in proliferation and differentiation of myoblasts, low passage primary cultures were isolated from 2-month old wild-type and S*ox15*-/- mice to facilitate the generation of highly purified satellite cell-derived cultures and preclude the inclusion of neonatal myoblast. Cultures were grown with bFGF to allow the rapid recovery of high numbers of low passage primary myoblasts. In the early passage (3-passage), wild-type cells displayed the rounded morphology and small compact cytoplasm characteristic of primary myoblasts in the low passages. In contrast, *Sox15*-/- cells displayed flattened morphology with an enlarged cytoplasm and extended cytosolic processes (Fig. 3.31). In the seventh passage, wild-type myoblasts displayed the round morphology and small compact cytoplasm. In contrast, most of *Sox15*-/- myoblasts exhibit flattened morphology with enlarged cytoplasm (Fig. 3.32).

<div align="center">
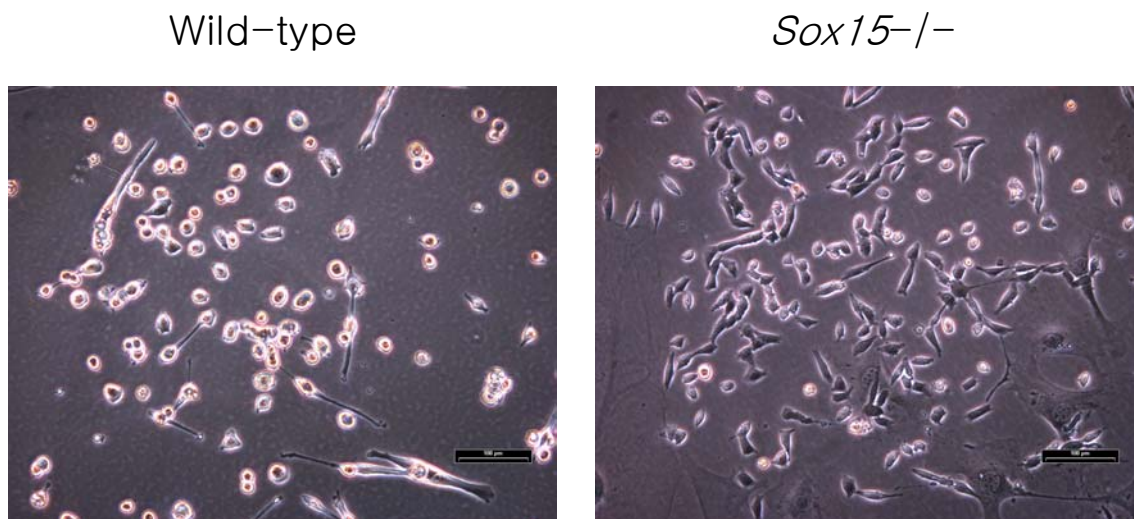Wild-type   Sox15-/-
</div>

Figure 3.31: Morphology of myoblasts (3rd passage). Primary cultures from muscle of wild-type and *Sox15*-/- were grown in medium with Ham's F10 medium containing of bFGF. Early passages (3rd passage) of wild-type cells revealed round and glossy cell morphology. In contrast, *Sox15*-/- cells displayed flattened morphology with enraged cytoplasm.
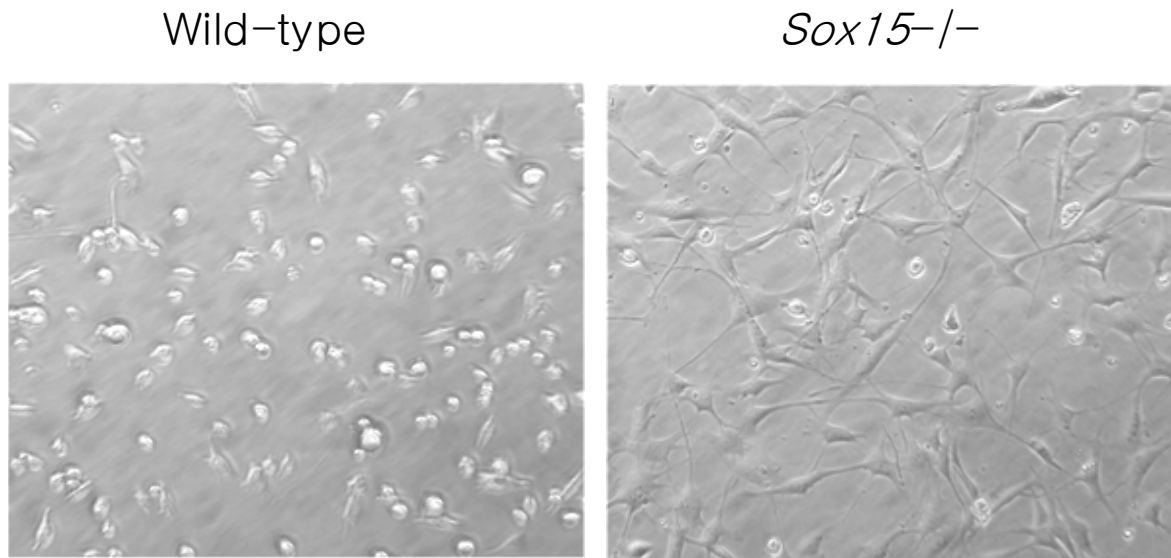
Figure 3.32: Morphology of myoblasts (7th passage). Primary cultures from muscle of wild-type and *Sox15*-/- were grown and maintained in medium with Ham's F10 medium containing of bFGF. Latter passages (7th passages) of *Sox15*-/- cells revealed flattened morphology and enlarged cytoplasm in comparison to round and glossy morphology of wild-type myoblasts.

Quiescent and activated satellite cell in vivo express the receptor tyrosin kinase c-met as do cultured myoblasts (Allen et al. 1995; Cornelison and Wold 1997). Proliferating myogenic precursor cells in vivo and myoblasts in vitro express the intermediate filament desmin. However, satellite cells do not express desmin (George-Weinstein et al. 1993). Therefore, primary cultures were immunostained with antibody reactive with c-met and desmin (DE-U-10) to assess their developmental status. Most of the primary cells derived from both wild-type and *Sox15*-/- animals expressed high levels of c-met as detected by immunofluorescence (Fig. 3. 33 A). Fibroblast cell lines do not express c-met(Sabourin et al. 1999). Therefore the isolation procedure generated highly purified cultures of myogenic cells. In contrast to the uniform expression of c-met, only 12% of *Sox15*-/- myogenic cells expressed the myoblast marker desmin, whereas 91% of wild-type cells expressed desmin (Fig. 3.33 B). These data indicate that *Sox15*-/- myogenic cells represent an intermediate development stage between a satellite cells and myogenic precursor cells.
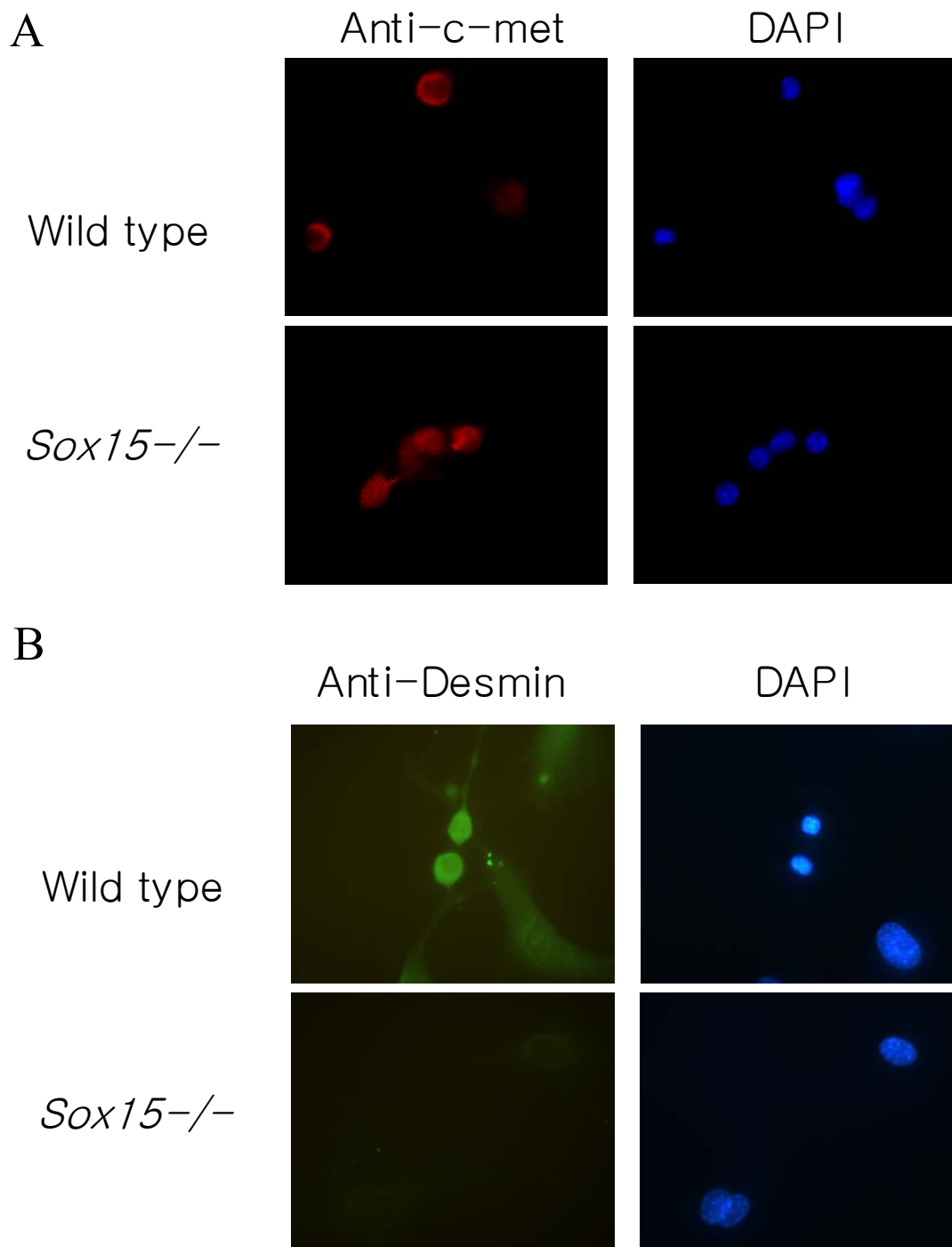
Figure 3.33: Expression of desmin and c-met in cultured myoblasts. Cultures were maintained in serum-rich growth medium and collected and stained at 3 passages with antibodies. (A) Immunostaining revealed that both wild-type and *Sox15-/-* myoblasts expressed the c-met receptor tyorosin kinase, a maker for proliferating myoblasts. (B) Immunohistochemical analysis for desmin expression revealed a marked reduction in the proportion of cells in *Sox15-/-* cultures expressed desmin relative to wild-type cultures. Cells were counterstained with DAPI.

3.12.2 Reduced differentiation potential of *Sox15*-/- myogenic cultures

To evaluate the differentiation potential of the Sox15 myogenic cultures the extent of myogenic differentiation was assessed at the cellular level by staining with antibody MF20 reactive with MHC (myosin heavy chain). MHC is a marker protein for myotubes after differentiation stage of myoblasts. 2 passages of cells were splitted onto culture slides with 4×10^5 cells in growth medium and cultured for additional 24 hr before addition of differentiation medium. Differentiation medium contained low serum (2% horse serum) without bFGF. Cell morphology was observed under the microscope each day. Under the light microscope, differentiated wild-type myoblasts displayed the typical elongated and multinucleated morphology, whereas differentiated *Sox15*-/- myoblasts retained a fibroblastic stellate cytomorphology and undifferentiated myoblasts form (Fig. 3.34). After 5 days, cells were fixed and stained. Green colour of the cells by FIFC conjugated secondary antibody represents reactive against MF20 antibody. Under growth conditions, few of both wild-type and *Sox15*-/- myoblasts exhibited green colour under high magnification (Fig. 3.35 A) by spontaneous differentiation. Under differentiation, *Sox15*-/- myoblasts exhibited strong reduction of differentiation potential compared to wild-type cells (Fig. 3.35 B). Taken together, these data indicate that differentiation potential of *Sox15*-/- myoblasts is reduced by loss of function of *Sox15*.
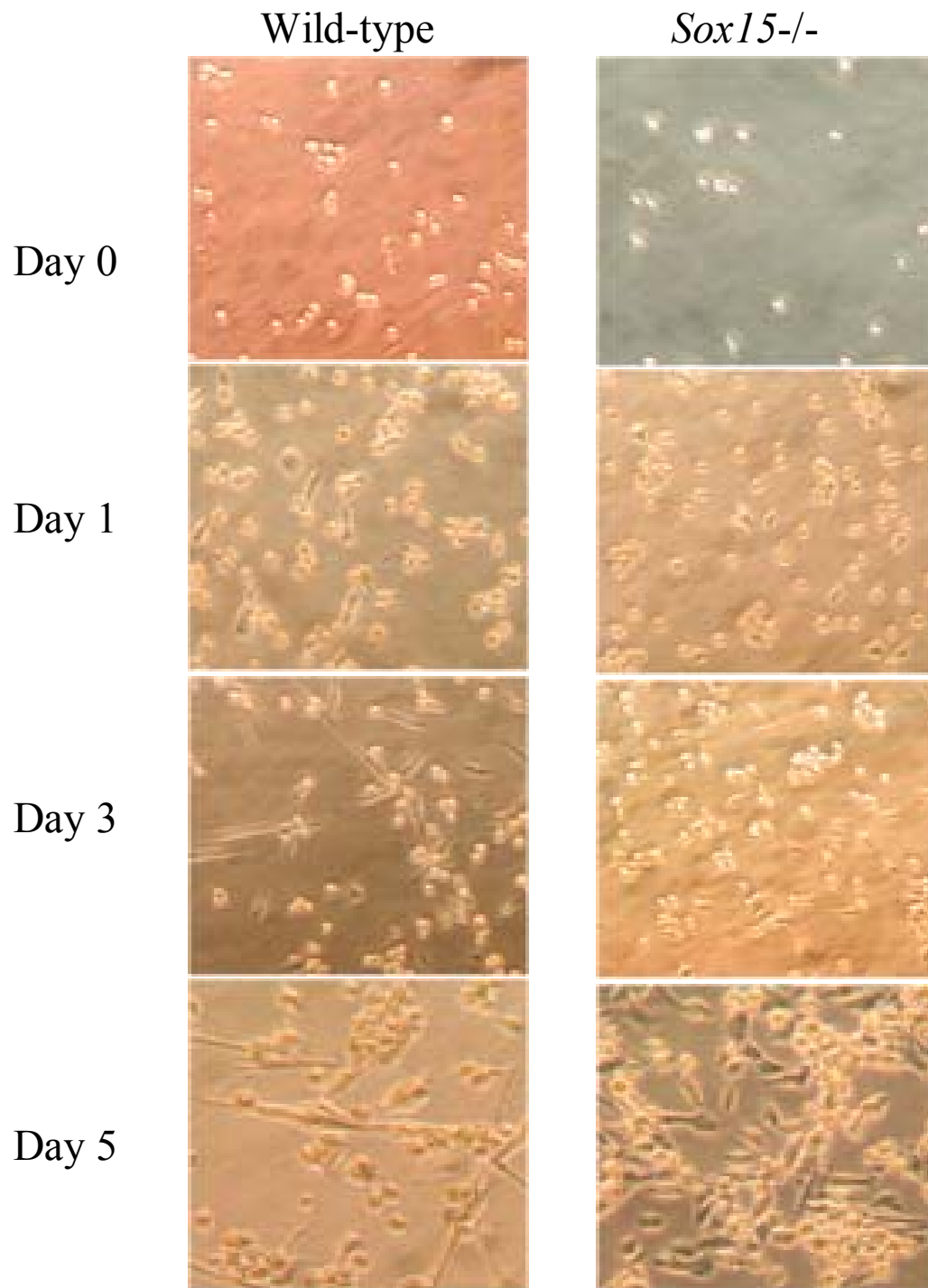
Figure 3.34: Cell morphology of cultured myoblasts after induction of differentiation. Myoblasts were incubated in differentiation medium and photos were taken under the inverted microscope (100x). Reduced differentiation potential of *Sox15*-/- myoblasts was observed in day 5. Days correspond to the time spent in differentiation medium, whereas day 0 represents cultures in growth medium.
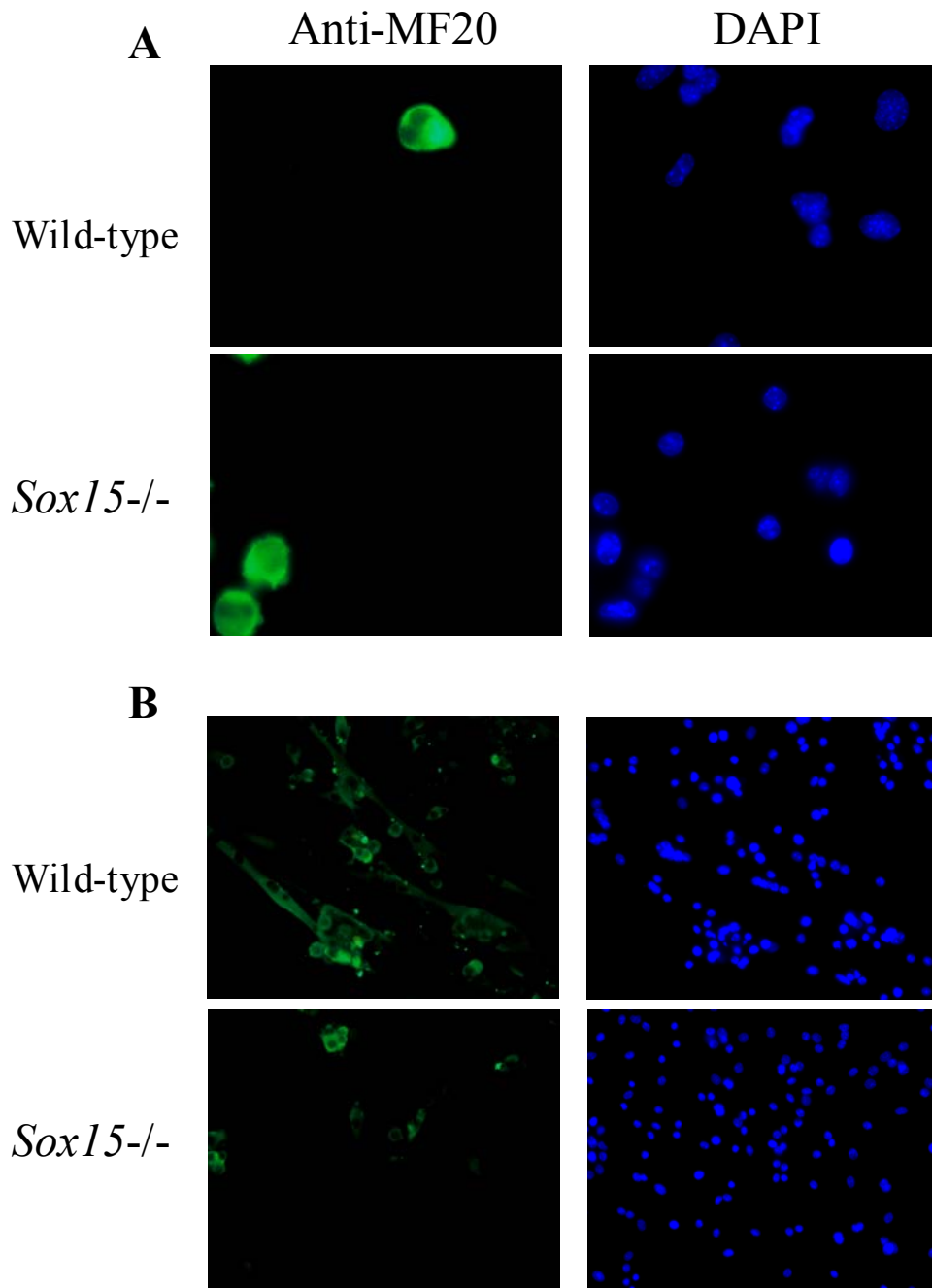
Figure 3.35: Differential expression of myosin heavy chain (MHC) in wild-type and *Sox15*-/-. Immunohistochemical analysis with the monoclonal antibody MF20 reactive with MHC was performed. (A) Under the growth condition, few of both wild-type and *Sox15*-/- myoblasts were stained by the antibody due to spontaneous differentiation (magnification 600x). (B) 5 days after inducing of differentiation, strong reduction of MF20-positive cells was observed in *Sox15*-/- cells (magnification 200x). Total nuclei were visualized using DAPI staining.

3.12.3 Expression pattern of myogenic regulatory factors (MRFs)

To examine the expression pattern of myogenic regulatory genes *MyoD* and *Myf5* known to be involved in muscle differentiation, RNA (20 μg) was isolated from primary myoblast cultures and hybridized with *MyoD* and *Myf5* cDNA fragments, which were generated by RT-PCR (MyoD-F and MyoD-R primers for MyoD and Myf5-F and Myf5-R primers for Myf5). Each PCR product is cloned into pGEMT-easy vector. The blot was re-hybridized with *Sox15* cDNA and hEF cDNA to avoid contamination and standardize the amount of RNA.

Northern blot analysis with *MyoD* cDNA probe showed high expression of *MyoD* in wild-type myoblasts but not in *Sox15*-/- myoblasts. In contrast, *Myf*5 was strongly expressed in *Sox15*-/- myoblasts as compared to wild-type cells (Fig. 3.37). RT-PCR using the *MyoD* specific primers (MyoD-F and MyoD-R) also revealed strong down-regulation of *MyoD* in *Sox15*-/- cells (Fig. 3.36)

It is known that the expression of the *Myf5* gene is up-regulated in the *MyoD*-/- myoblasts to compensate for *MyoD* (Kablar et al. 1997). These results suggest that the Sox15 protein can directly or indirectly regulate the expression of the *MyoD* in myogenic cells and the down-regulation of *Myo*D in *Sox15*-/- lead to up-regulation of the *Myf5* to compensate the lack of *MyoD* in *Sox15*-/- myoblasts.
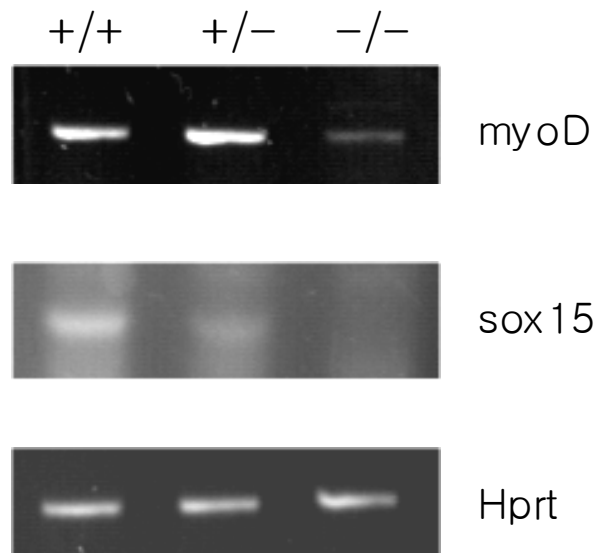
Figure 3.36: RT-PCR assay to determine the expression of MyoD and *Sox15* in myoblasts. RNA was isolated from myoblast of each genotype and used for RT-PCR with specific primers for MyoD, *Sox15* and *Hprt*. MyoD expression was strongly reduced in *Sox15*-/-. No RT-PCR fragment could be detected in *Sox15*-/- myoblasts, indicating that *Sox15* is inactivated in *Sox15*-/- cells. *Hprt* gene was amplified as a control to check the RNA amount and quality.
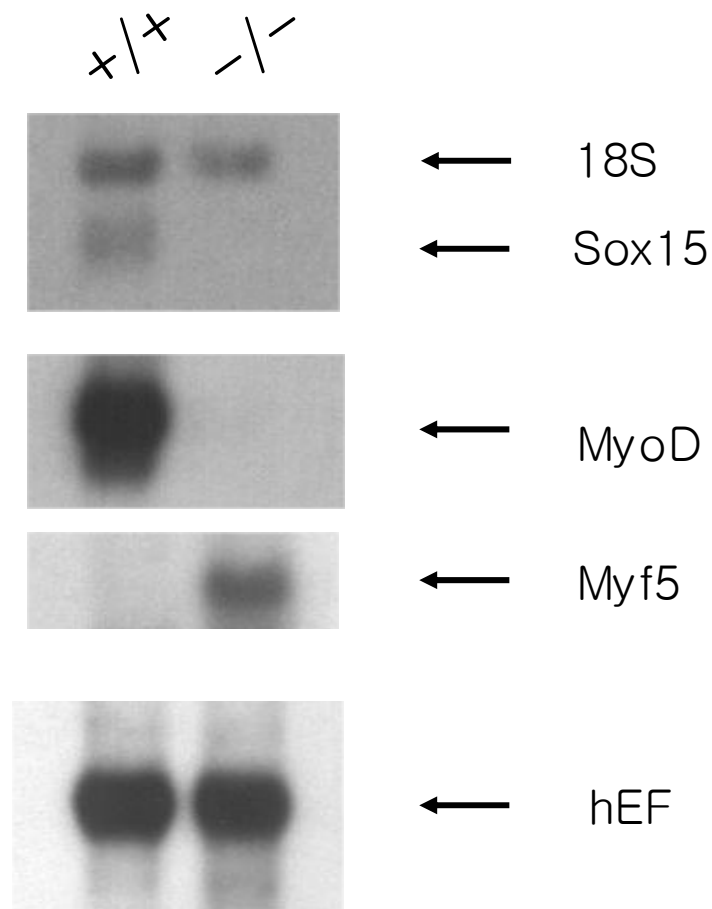
Figure 3.37: Expression of MyoD and Myf5 in *Sox15*-/- myoblasts. Total RNA (20μg) was extracted from wild-type and *Sox15*-/- myoblasts. *Sox15* expression was detected in wild-type myoblasts. MyoD was not expressed at detectable levels in *Sox15*-/- myoblasts. In contrast, Myf5 expression was elevated in *Sox15*-/- myoblasts. Rehybridization with human elongation factor (hEF) confirms equal amount of mRNA.

3.13 DNA binding activity of Sox15

Preparation of nuclear extracts from cultured myoblasts and electrophoretic mobility shift assay (EMSA) were done as described in 2.2.22. Sox proteins have the ability to recognize and bind to specific DNA sequences via their HMG domain. Analysis of the 5' flanking region of the MyoD gene revealed that the presence of consensus binding site of the Sox family protein in the distal regulatory region of MyoD gene. The consensus cis-acting element of Sox protein has been defined at the heptameric sequence 5'-(A/T)(A/T)CAA(A/T)G-3'. To examine whether the Sox15 is able to bind to the Sox binding site in the MyoD promoter, oligonucleotide containing the consensus sequence of Sox was designed from the MyoD promoter and used in electrophoretic mobility shift assay (EMSA) (Fig. 3.38). When the nuclear extract of wild-type myoblasts was incubated with the labeled oligonucleotide, one specific DNA-protein complex was observed (lane 1). In contrast, no corresponding complex was shown by incubation of the oligonucleotide with the protein extract of *Sox15*-/- cells (lane 2). To examine whether the Sox15 is a component in the observed shift band, a supershift assay with affinity purified anti-Sox15 antibody was performed. As shown in figure 3.38 lane 3, the Sox15 antibody (2 µg) interacted with the DNA-protein complex and formed a supershift. The DNA-protein complex and supershift were not detectable in the assay with nuclear extract of *Sox15*-/- myoblasts. The specificity of the interaction was determined with unlabeled competitor oligonucleotide (cold oligonucleotide). Strong reduction of DNA binding was observed in the presence of an excess of cold oligonucleotide (lane 6) and the binding was partially inhibited with mutant oligonucleotide (lane 5). These results implies that Sox15 protein can specifically bind to the Sox cis-acting element located in the distal promoter region of the MyoD gene and suggest that Sox15 directly transactivate the expression of the MyoD gene.
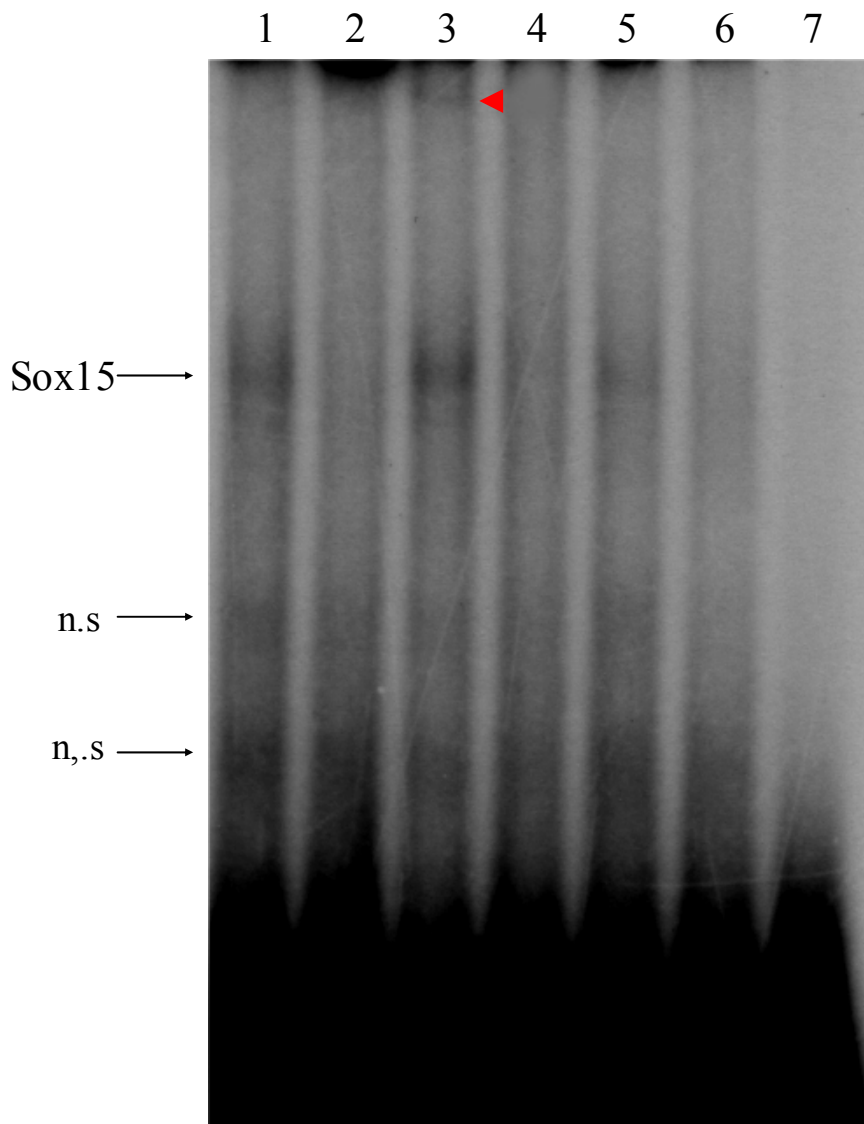
Figure 3.38: Binding of Sox15 to consensus Sox binding site of the MyoD promoter. Nuclear extracts were prepared from primary myoblast cultures. In an electrophoretic mobility shift assay reaction, ^{32}P-labeled Sox binding site probe which was designed from the *MyoD* promoter and 5 μg of nuclear extract from wild-type (lane 1) or *Sox15*-/- (lane 2) were incubated together. Supershift experiment was performed after incubation of 2 μl of Sox15 antibody with wild-type (lane 3) and *Sox15*-/- (lane 4). The specificity of retarded bands was controlled by the use of either an excess of cold binding site probe (10 pM, lane 6) or of mutated forms of oligonucleotide Mut3-5 (lane 5). As a negative control, labeled oligonucleotide was incubated without nuclear extracts (land 7). The arrows indicate the Sox15-DNA complex and non-specific binding, whereas the arrow head indicates the supershift (Sox15-DNA-antibody) complex.

3.14 Impaired muscle regeneration of the *Sox15*-/- mice after skeletal muscle injury

When skeletal muscle is injured, the damaged muscle fibers are usually replaced by newly-formed muscle cells (myotubes). Regeneration of new muscle results from an initial proliferation of mononuclear muscle precursors (myoblasts) and these precursors are derived from satellite cells of muscle which survive the injury.

To evaluate the importance of *Sox15* for skeletal muscle regeneration, crush injury-induced regeneration experiment was performed on *Sox15*-/- and wild-type mice. Briefly, the hindlimb muscle was exposed by an incision and a crush injury applied to the belly of the TA (tibialis anterior) muscle with forceps cooled in liquid nitrogen. Examination of HE-stained longitudinal sections of *Sox15*-/- TA muscle 4 days following injury revealed the presence of high number of mononuclear cells and few dispersed myotubes of small size (Fig. 3.39 D). In constant, wild-type TA muscle displayed well-advanced regeneration with myofibers crossing the entire wound site (Fig 3. 39 C). Two weeks after injury, virtually no signs of previous damage was detectable in wild-type mice, indicating a complete regeneration (Fig 3. 39 E). In *Sox15* mutant, however, high number of mononuclear cells and limited regeneration were visible, as evidenced by the presence of thin myofibers at the site of injury (Fig 3. 39 F). These results indicate that the skeletal muscle regeneration is impaired in the *Sox15*-/- muscle.

The limited regeneration of skeletal muscle in *Sox15*-/- mice following injury lead to suggest that *Sox15* deficient muscle contains reduced numbers of stem cells. To address this point, we estimated the number of satellite cells by electron microscopic examination of sectioned skeletal muscle. Quiescent satellite cells can be reliably identified by electron microscopy by their morphological appearance and location external to the muscle fiber and beneath the basal lamina encasing the fiber (Schultz 1976). Satellite cells comprise ~32% of sublaminal nuclei in newborn mice, and the proportion declines <5% by 9 weeks age. Electron microscopic experiments of TA skeletal muscle section clearly revealed the presence of morphological normal satellite cells in TA muscle of *Sox15*-/-. Examination of 400 nuclei in random fields identified 4 morphological normal satellite cells (1%), which located between the sarcolemma and basal lamina, in the *Sox15* deficient TA muscle. Examination of wild-type TA muscle displayed 6 satellite cells (1.2%). These results

indicate that quiescent satellite cells are present in normal proportions in *Sox15*-/- muscle (Fig. 3.40).
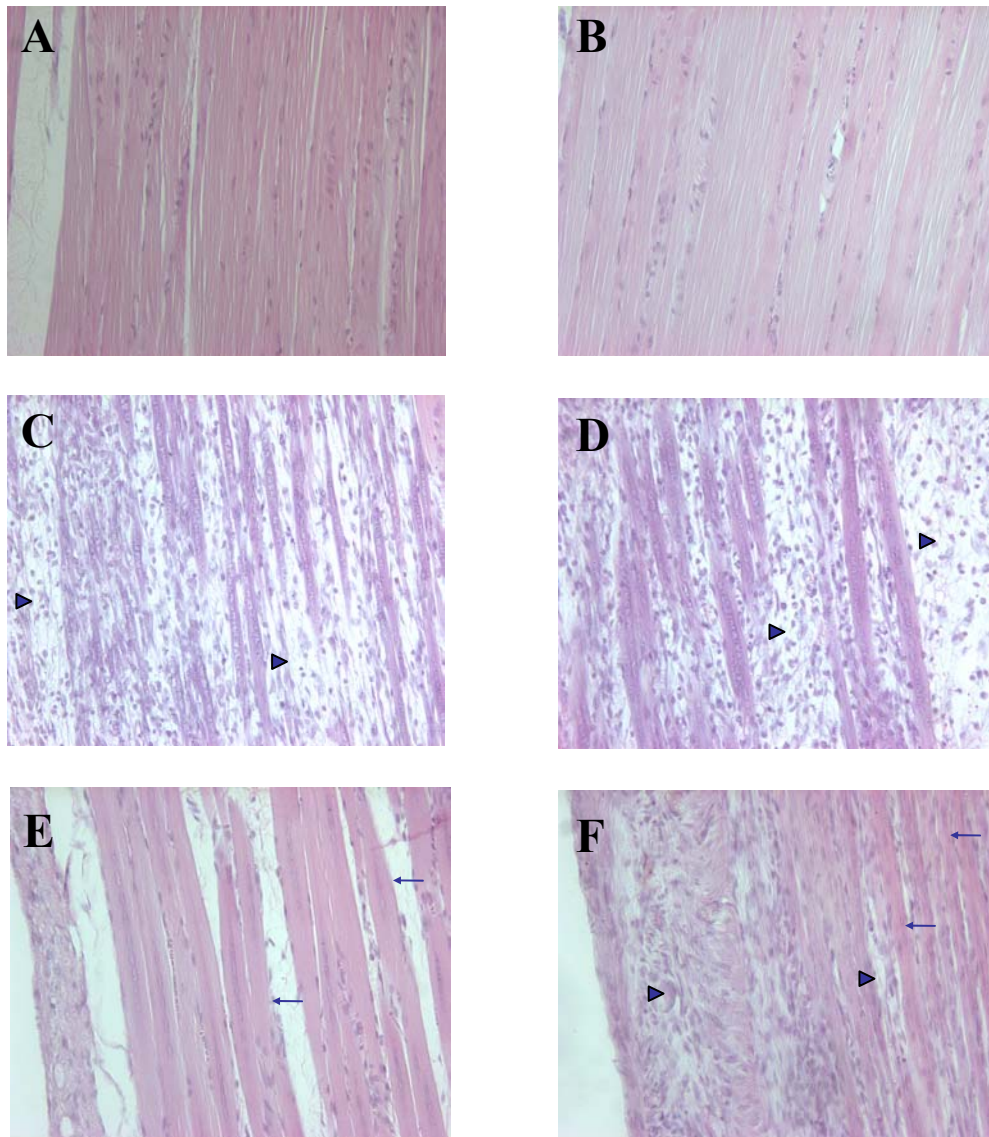
Figure 3. 39: Freeze-crush-induced injuries result in impaired skeletal muscle regeneration of *Sox15*-/- mice. Paraffin sections from wild-type (A, C, E) and mutant mice (B, D, F) were stained with HE. Sections sampled untreated muscle (A, B), 4 days (C, D), and 14 days (E, F) following injury. Wild-type muscle 4 days following injury displayed well-advanced regeneration with new myofibers that almost crossed the lesion (C). In mutants, the amount and size of newly formed myotubes (arrows) are reduced and the number of mononuclear cells (arrow heads) is much higher (D). Two weeks after injury, virtually no sign of muscle damage is observed in wild-type (E) indicating a complete regeneration. In mutants, high number of mononuclear cells is visible (F).
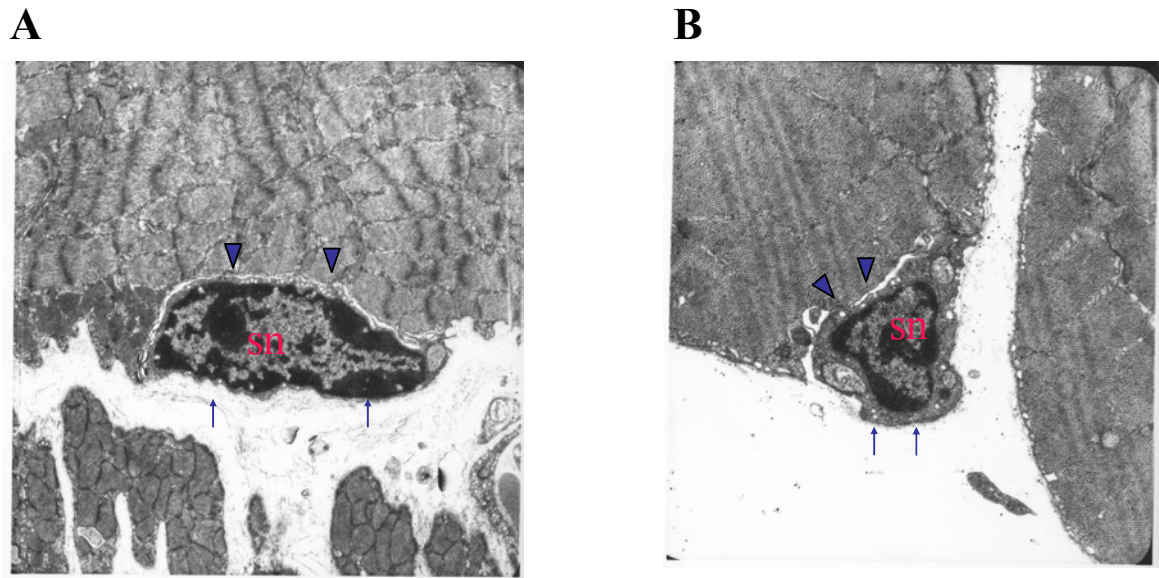
Fig. 3.40: Satellite cell in *Sox15*-/- skeletal muscle. Electron microscopic examination of sections revealed the presence of morphological normal satellite cells in *Sox15*-/- TA muscle located external to the sarcolemma (arrow heads) and the basal lamina (arrows), and ouside the myofiber membrane. sn, satellite cell nucleus.

3.15 Proliferation assay of MEFs and myoblasts

A normal morphology and number of the satellite cell in TA muscle of *Sox15*-/- mice lead us to address the question whether the impaired regeneration of the skeletal muscle in *Sox15* deficient mice after injury can be due to defect in proliferation potential of the *Sox15*-/- myoblasts. The 3T9 method was performed to determine the proliferation of myoblasts and embryonic fibroblast cells (MEFs) as described in 2.2.24.

MEFs and myoblasts were maintained on a defined 3-day passage schedule by plating 9 x 10^5 (3T9) or 3 x 10^5 (3T3) cells in 60 mm-diam-dishes. Cells were counted at each passage, and the total number was calculated prior to redilution. The result of cell number determination is summarized in figure 3.41. The figure shows that *Sox15*-/- MEFs slightly stop dividing earlier than wild-type MEFs (Fig. 3.41 A). This small reduction of

proliferation ability in MEFs is thought to due to the reduction of differentiation ability in *Sox15*-/- mice. Two embryos from each genotype were isolated and examined for proliferation assay of MEFs.

The reduction of proliferation potential was also observed in *Sox15*-/- myoblasts. As in the MEFs culture, cells were maintained in growth media. After 8 passages, *Sox15*-/- myoblasts showed 2-fold reduction rate of cell number (Fig. 3.41 B). Taken together, the observation that *Sox15*-/- cells exhibit a reduced proliferative potential under the growth condition supports that *Sox15* has an important role for cell differentiation and proliferation. Growth kinetic was determined by plating replicate cultures of each passage and the mean values and standard deviations were calculated.

A
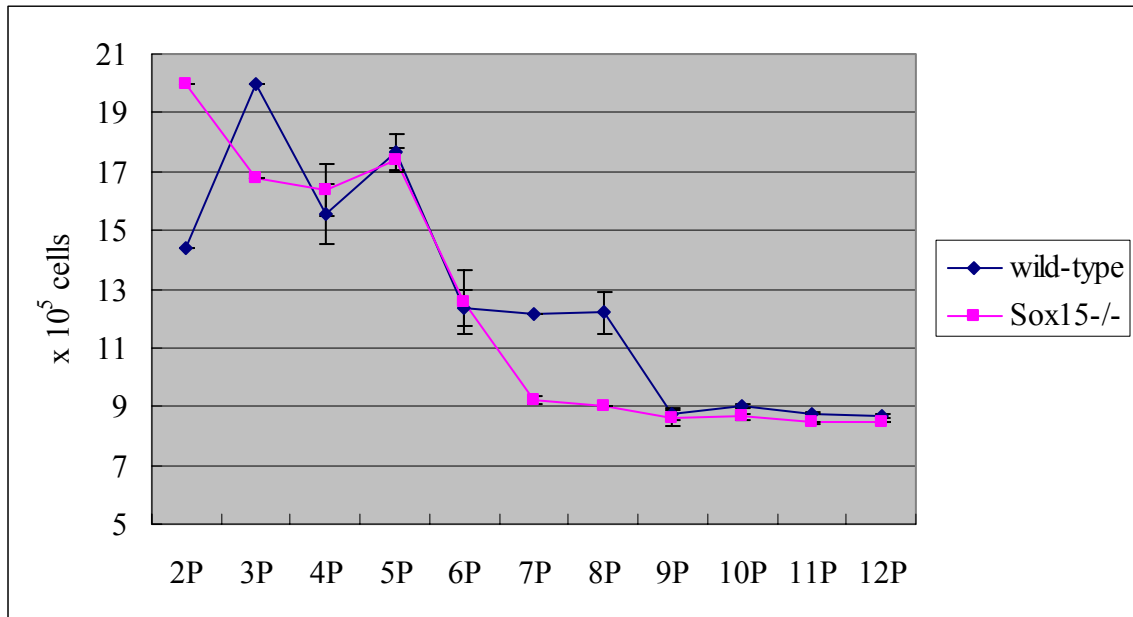
B
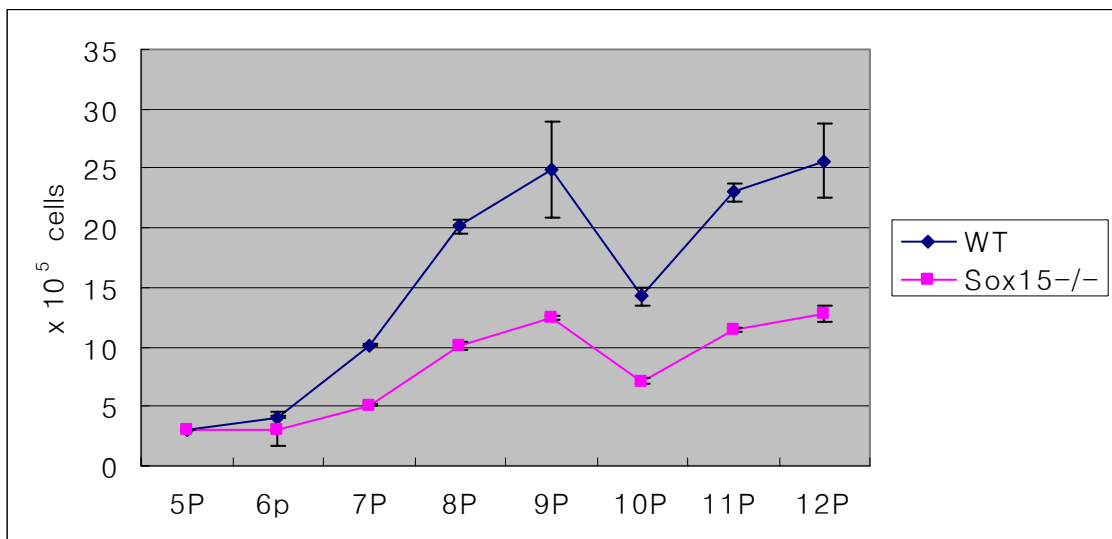
Figure 3.41: Growth kinetics of MEFs and myoblasts. (A) At 3-day intervals, the total number of MEFs per 60 mm-diam. culture dish was counted prior to redilution to 9 x 10^5 per dish for next passage. *Sox15*-/- MEFs entered senescence earlier than wild-type cells. Data were plotted from 2 embryos of each genotype (wild-type and *Sox15*-/-). (B) Myoblasts were counted prior to redilution to 3 x 10^5 per dish for next passage. Strong reduction of proliferation was found in *Sox15*-/- myoblasts. Two different cell lines were chosen for the assay.

3.16 Phenotypical analysis of *mdx:Sox15-/-* mice

3.16.1 Generation of double knock-out mice, *mdx:Sox15-/-*

To determine whether *Sox15* might have a role in skeletal muscle regeneration, *Sox15-/-* mice were interbred with the *mdx* mouse. The *mdx* mouse carries a loss-of-function point mutation in the X-linked dystrophin gene and is therefore an animal model for human Duchenne and Becker muscular dystrophy. The *mdx* mice display extensive necrosis of muscle fibers by 2 week of age, but unlike humans, maintain skeletal muscle integrity due to a high muscle regenerative capacity. This regeneration results in the formation of additional muscle fibers, which leads to a significant level of muscle hypertrophy.

In contrast, mice lacking both MyoD and dystrophin display a marked severe dorsal-ventral curvature of the spine and increased myopathy characterized by an abnormal waddling gait and weight-bearing on the hocks (Megeney et al. 1996).

Because the *mdx* mutant is an X-linked recessive null mutation, *mdx* male (X'Y) mice were bred with *Sox15-/-* female to generate the *Sox15+/-* female mice containing *mdx* allele (X'X) and *mdx:Sox15+/-* male mice. By second breeding of these mice, *mdx:Sox15-/-* male mice and *Sox15-/-* female mice carrying the *mdx* allele (X'X) were generated. Finally, *mdx:Sox15-/-* male and female mice were generated by breeding of S*ox15-/-* female mice carrying a *mdx* allele (X'X) with *mdx:Sox15-/-* male mice.

All offspring were genotyped by PCR from tail DNA. To genotype the *mdx* mice, two independent PCRs were performed using WT antisense and MDX-WT sense primers to detect WT allele and MDX antisense and MDX-WT primers to detect MDX allele of DNA. (Amalfitano and Chamberlain 1996; Fig. 3.42)
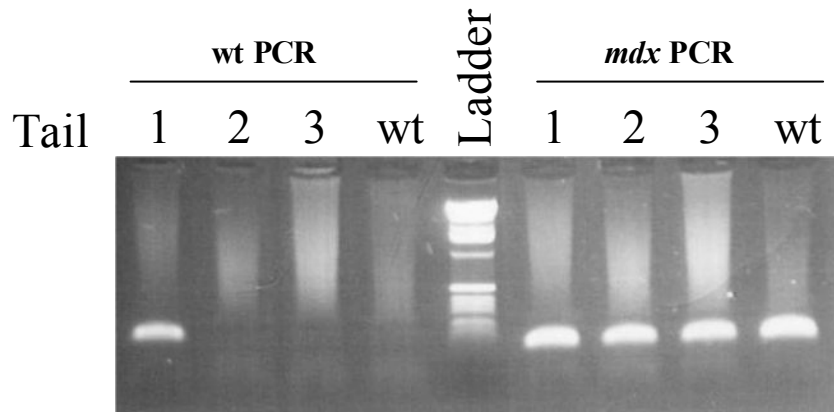
Figure 3.42: PCR genotyping of *mdx* mice. DNA of females (tail 1 and 3) and male (tail 2) tails was isolated and amplified using sense and anti-sense primers for both *mdx* and wt PCR. 105-bp products were electorophoresed on 1.5% agarose gel and stained with ethidium bromide. The bands indicate heterozygous female (tail 1) and mdx (tail 2 and 3) mice. wt, wild-type.

3.16.2 Phenotypical analysis of *mdx:Sox15-/-* by X-ray radiography

In order to take x-ray radiograph photos, mice were anaesthetized by injection of Avertin and exposed to X-ray.

X-Ray radiographic visualization (Fig.3.43) revealed increased phenotypic trait in the *mdx:Sox15-/-* mice. By 6 month of age, *mdx:Sox15-/-* mice developed marked increased in the penetrance of phenotype, such a profound dorsal-ventral curvature of the spine, similar to the old *Sox15-/-* mice (14- and 16-month-old). In contrast, *mdx* mice and its age matching *mdx:Sox15+/-* mice (6-month-old) displayed a normal phenotype. Taken together, the abnormal morphology of spinal cord of old *Sox15-/-* can be appeared earlier from *mdx:Sox15-/-* mice because of their severe phenotype. This data suggest that *Sox15* has a crucial role for regeneration of skeletal muscle, perhaps via the regulation of the MyoD expression.
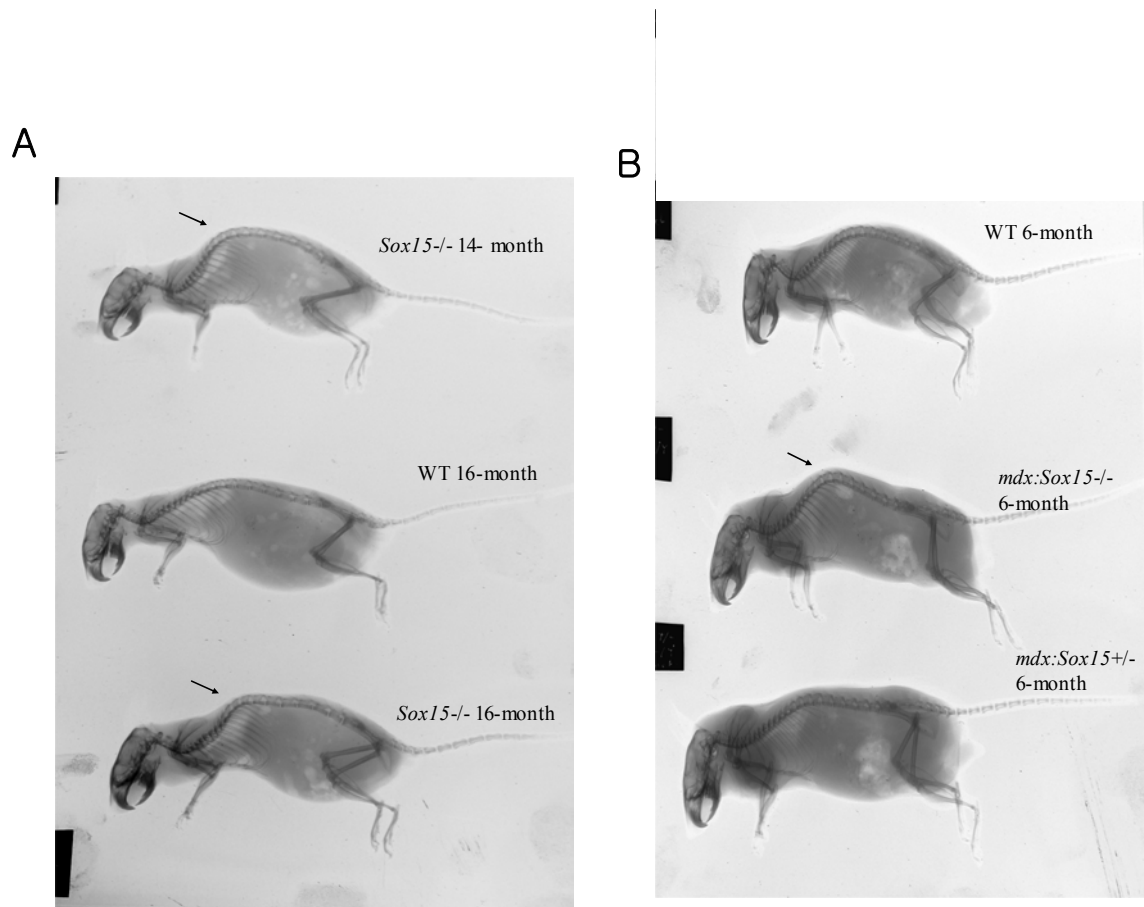
Figure 3.43: X-Ray radiographic examination of mice. (A) The old *Sox15*-/- mouse (up, 14-month-old; bottom 16-month-old) appears a severe dorsal –ventral curvature of the spine (arrows). Wild-type mouse (middle) displays morphologically normal compared to *Sox15*-/- mice. (b) 6-moth-old *mdx:Sox15*-/- mice appears the same dorsal-ventral curvature as old *Sox15*-/- mice. In contrast, wild-type (6 month old) and *mdx:Sox15*+/- mice appears normal morphology.

4. DISCUSSION

The present study can be divided into two parts:

In the first part, the function of the murine *MOCS1* gene is discussed. The murine *MOCS1* gene deficient mice by homologous recombination with a targeting vector resemble the phenotype of human patients. Therefore, as an animal model for molybdenum cofactor deficiency, the phenotype of *MOCS1* deficient mice is also discussed.

In the second part, functional characterization of the *Sox15*, which is a member of Sox family, is discussed. In this study, we suggest that the *Sox15* gene has a crucial role during the muscle development.

4.1 Characterization of the murine *MOCS1* gene and the mutant mice

4.1.1 Overview of molybdenum cofactor and the involved genes

The existence of a pleiotropic element affecting different molybdenum-containing enzymes was originally predicted by Pateman el al. (Pateman et al. 1964), who identified six groups of *Aspergillus* mutants with a simultaneous loss of two molybdoenzymes. They postulated a common cofactor for nitrate reductase and xanthine dehydrogenase. The derived acronym *cnx* (cofactor of nitrate reductase and xanthine oxidase) for mutant loci is still used in the botanical nomenclature. Ketchum et al. (Ketchum et al. 1970) identified the universal character of a molybdenum-containing moiety common to all molybdoenzymes, which led to the name molybdenum cofactor (Nason et al. 1971).

Molybdenum cofactor (MoCo) is an essential elememt in certain enzymes, but must first be complexed by molybdopterin (MPT), whose synthesis requires enzymatic activities. MPT is identical in all organisms, though some eubacteria form a dinucleotide from MoCo and either GTP or CTP (Rajagopalan and Johnson 1992), and some bacteria use tungsten instead of the molybdenum ion (Chan et al. 1995). Free MPT is not stable, and all organisms share a conserved pathway for its biosynthesis (Mendel 1997).

Several genes required for this pathway have been characterized from bacteria to man (Reiss 2000). In humans, the *MOCS1* gene encodes the enzymes necessary for precursor Z formation which is the precursor of molybdopterin, and the *MOCS2* gene encodes the enzymes necessary for the next step leading to molybdopterin.

The first step of human MoCo biosynthesis is catalyzed by the proteins MOCS1A and MOCS1B (Reiss et al. 1998b; Hanzelmann et al. 2002) and converts a guanosin derivative to the sulphur-free intermediate precursor Z that already contains the unique four carbon side-chain of molybdopterin (Wuebbens and Rajagopalan 1993). Mutations in the *MOCS1* gene, which abrogate this enzymatic activity, are found in two thirds of MoCo deficiency patients, who represent complementation group A and the MoCo deficiency type A, respectively (Reiss 2000). In a second step, this precursor Z is further converted to molybdopterin by enzymes encoded by the *MOCS2* gene, which before have to be activated by the *MOCS3* gene product (Stallmeyer et al. 1999a). The majority of type B patients carry *MOCS2* mutations (Reiss et al. 1999). Finally, molybdenum is inserted into molybdopterin by the multifunctional protein Gephyrin (Stallmeyer et al. 1999b). Only one family with Gephyrin mutations leading to MoCo deficiency (type C) has been described (Reiss et al. 2001)

In most MoCo-deficient patients, severe mutations such as frameshift mutations or substitutions of conserved positions are found in the genes *MOCS1*, *MOCS2* or Gephyrin (Reiss 2000). These mutations result in undetectable levels of molybdopterin, MoCo and sulfite oxidase activity with the consequence of considerable neurological damage and mental retardation. A few milder cases of isolated sulfite oxidase deficiency have been described (van der Klei-van Moorsel et al. 1991; Barbot et al. 1995), and (Johnson et al. 2001) have reported the first mutation in an unusually mild case of molybdenum cofactor deficiency. One of the two mutations identified in the *MOCS2* gene apparently results in residual MoCo activity, thus leading to a milder phenotype.

Structure of MoCo and related compounds are summarized in Figure 4.1
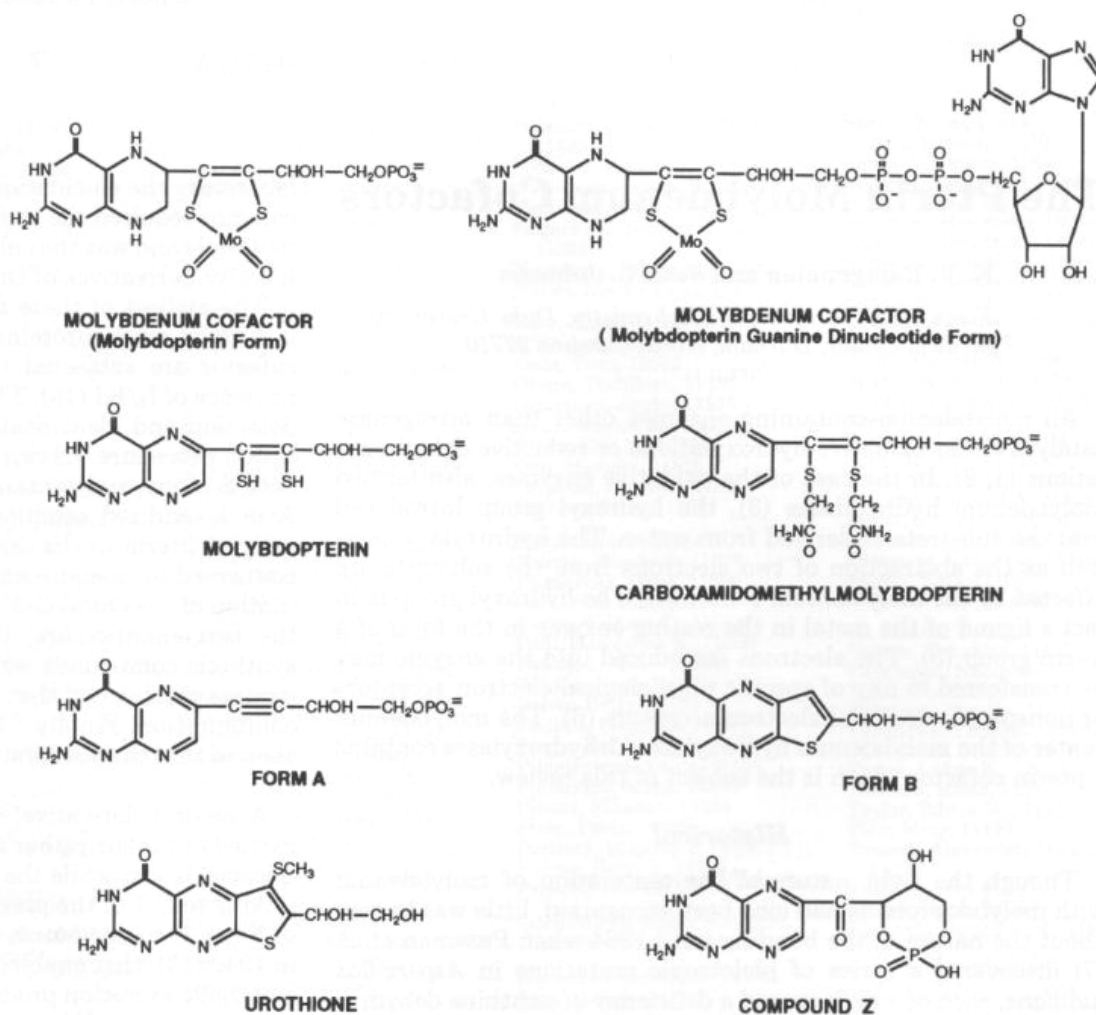
Figure 4.1: Structure of molybdenum cofactors and related compounds. The molybdenum cofactors are shown as tetrahydropterins. All others are drawn with fully oxidized pterin ring systems. The dioxo ligands to the molybdenum in the cofactor structures are features of the cofactor in sulfite oxidase and nitrate reductase. In xanthine oxidase and other molybdenum hydroxylases, the metal has one oxo and one sulfido ligand (adapted by Rajagopalan and Johnson 1992).

4.1.2 MoCo deficient patients and MoCo deficient mice

In mammals, MoCo is required for the activity of xanthine dehydrogenase, aldehyde oxidase and sulfite oxidase (Rajagopalan and Johnson 1992). MoCo deficiency (OMIM 252150 and 252160) is inherited autosomal-recessive and results in a fetal neurological disorder similar to the isolated form of sulfite oxidase deficiency (Johnson 2001).

Sulfite oxidase exists as a soluble protein compartmentalized in the intermembrane space of the mitochondrion. In this location it has ready access to its reducing substrate, sulfite, which can diffuse across the mitochondrial membranes, and to its physiological electron acceptor, cytochrome c (Rajagopalan 1980). At present the number of cases of cofactor-based sulfite oxidase deficiency is considerably larger than that of the specific single-enzyme deficiency, but the clinical picture is similar in the two diseases. These findings lead to the conclusion that most, if not all, of the devastating sequelae of molybdenum cofactor deficiency stem from the absence of sulfite oxidase. In sulfite oxidase deficiency, sulfite accumulates and sulfate production is decreased. Sulfite overflow is apparently moderated to some extent by an enhanced degradation of cystein sulfinate to taurine. The presence of elevated levels of sulfite leads to accumulation of S-sulfocysteine formed by direct reaction of sulfite with cysteine. Increased levels of thiosulfate are also characteristic of the sulfite oxidase deficiency as a consequence of elevated sulfite.

Sulfite oxidase (EC 1.8.2.1) represents as the terminal enzyme in the pathway of degradation of sulphur amino acids. Besides functioning to eliminate endogenously produced sulfite, the enzyme fulfils an important role in detoxifying exogenously supplied sulfite and sulfur dioxide (Cohen et al. 1973). Xanthine dehydrogenase deficiency is represented by markedly elevated urinary xanthine and moderately increased hypoxanthine. Uric acid is low, in both urine and blood plasma.

Xanthine dehydrogenase (EC 1.2.1.37) catalyzes the hydroxylation of hypoxanthine and xanthine to produce uric acid as the final product. The role of the enzyme in metabolism lies in the pathway of purine degradation for excretion. Because hypoxanthine and guanine can be reclaimed to a large extent by the action of hypoxanthine-guanine phosphoribosyl transferase and because hypoxanthine and xanthine are not highly toxic compounds, deficiencies of xanthine dehydrogenase in humans are largely benign (Johnson 1995). Xanthine dehydrogenase is a soluble enzyme present in liver and intestine and, at lower levels, in kidney, spleen, and skeletal and heart muscle (Johnson et al. 1974). It is also a normal constituent of milk; the enzyme from bovine milk is one of the most studied

enzymes to date. The function of the enzyme in milk is unknown, although the possibility that it may serve as a source of molybdenum or molybdenum cofactor for the suckling newborn must be considered.

Aldehyde oxidase (EC. 1.2.3.1) is present in the soluble cell fraction and exists as a constitutive and irreversible oxidase, reducing oxygen to hydrogen peroxide and superoxide. The enzyme shares many physicochemical properties with xanthine dehydrogenase (cofactor composition, molecular weight, and subunit structure) and shows some overlap in substrate specificity as well. Aldehyde oxidase may function as a part of the body's general detoxification (Johnson 1995). Aldehyde oxidase activity is difficult to assay directly in human tissues, in part because of its instability in frozen samples.

A combined deficiency of sulfite oxidase and xanthine dehydrogenase in humans was first described by Duran et al. (1978). The patient presented with feeding difficulties, severe neurological abnormalities, dislocated ocular lenses, and dysmorphic features of the head in the neonatal period. In a patient with a similar phenotype the molecular basis of the defect was identified as a deficiency of MoCo (Johnson et al. 1980). Since the organic moiety was absent in this patient, oral or parental supplementation with molybdenum salt did not result in clinical improvements. A metabolic consequence of MoCo deficiency which is not seen in isolated deficiencies of sulfite oxidase or xanthine dehydrogenase is an absence of urinary urothine, believed to be the excreted degradation product of molybdopterin (Johnson and Rajagopalan 1982).

All patients with MoCo deficiency display a similar metabolic profile characteristic of an absence of functional sulfite oxidase and xanthine dehydrogenase, although excretory levels of the various metabolites vary substantially due to differences in protein intake, catabolism, and creatinine production.

For the diagnosis of MoCo deficiency, urinary sulfite is easily detected with a semiquanitative dipstick test (Merckoquant) from fresh urine and quantitative determinations of sulfite, thiosulfate, and sulfate are best performed with anion column chromatography (Johnson et al. 1980; Cole and Scriver 1981).

HYPOXANTHINE   CYSTEINE

XDH   Hypotaurine   Cystein sulfinate   S-sulfo-L-cysteine

                  Taurine β-sulfinyl pyruvate   Mercapto pyruvate

XANTHINE

                                                                    thiosulphate

                                          Sulfite

XDH   MOLYBDENUM
               COFACTOR   SO

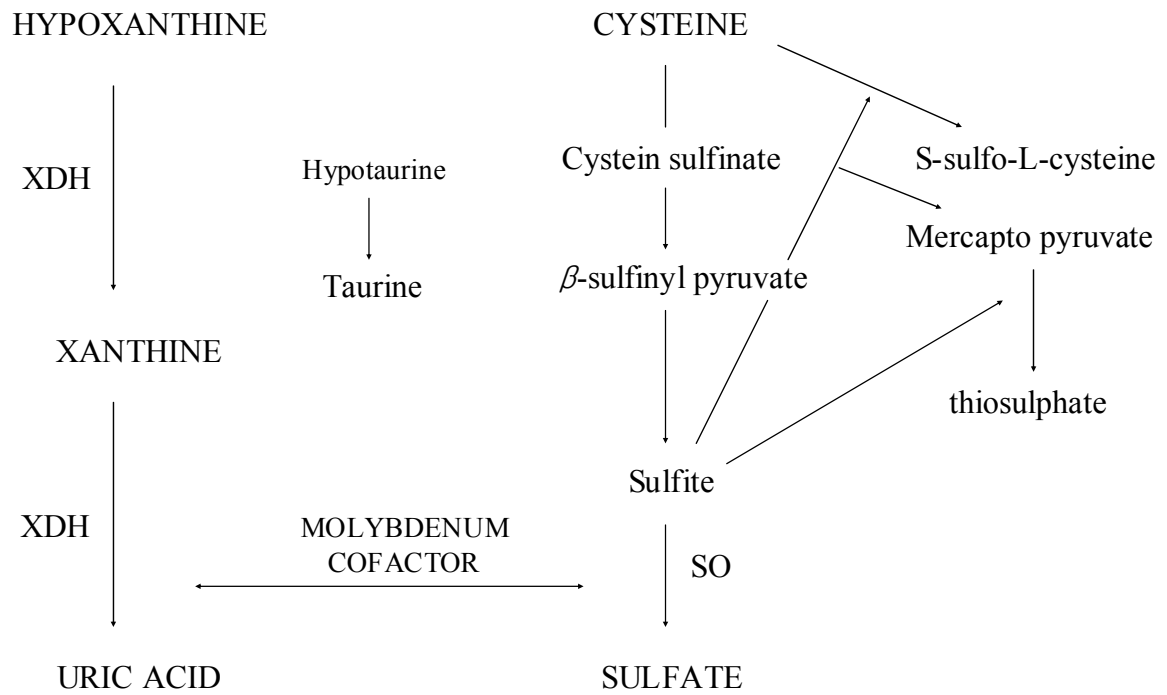URIC ACID   SULFATE

Figure 4.2: The role of the molybdenum cofactor in the hypoxanthine and cysteine biochemical pathway. XDH, xanthine dehydrogenase; SO, sulfite oxidase (adapted by Topcu et al. 2000).

In this study, we have set out to create an animal model for the more common form of the disease, which is devastating and untreatable by any known therapy. We therefore eliminated a complete exon of the *MOCS1* gene, removing a conserved domain of the MOCS1A ORF. Additionally, MOCS1B expression is hampered by the integration of the neo cassette. In the present study, we performed some biochemical analyses of *MOCS1-/-* mice including sulfite oxidase activity, xanthine dehydrogenase activity, MPT activity and level of amino acids. Every parameter of *MOCS1-/-* mice which we examined was exactly coincident with MoCo deficiency patient. However, the effects of these biochemical parameters seem to be different between human patients and mice. The presented data corroborate our assumption that thereby the synthesis of MoCo is completely abolished. As in humans, this results in a complete inactivation of the MoCo-dependent enzymes sulfite oxidase and xanthine dehydrogenase. It has been firmly established that sulfite oxidase deficiency alone is responsible for the severe neurological damages in MoCo deficiency (Johnson 2001).

The phenotypic variance of the MoCo-deficient mice, as expressed in a lifespan of 1–11 days (Fig. 3.7), is very similar to that observed in human patients, who show a survival of 1 week up to 10 years, but usually do not reach adolescence. The absence of any phenotypic differences between knock-out mice with either a genetic background from the inbred strain 129/Sv or the mixed background C57BL/6J 129/Sv excludes any additional genetic elements in the mouse with a potentially compensating or modifying effect. As in humans, murine MoCo (*MOCS1*) deficiency is inherited as a monogenetic autosomal recessive trait, for which our statistical data indicate complete penetrance.

4.1.3 Neuronal damage and sulfite toxicity in MoCo deficiency

Various brain dysmorphologies have been described in MoCo-deficient patients and explained by both sulfite toxicity to the CNS and sulfate deficiency leading to neuronal loss (Johnson 2001). Because the described MoCo-deficient animals die within their first days in life without any significant changes in CNS morphology, our observations put more emphasis on the critical role of sulfite toxicity.

The precise mechanisms of this toxicity are not completely understood. The reaction of sulfite with disulfide bonds or with sulfhydryl groups would be a general process without pronounced sensitivity of the brain. Graf et al. (Graf et al. 1998) already pointed out that one effect of elevated sulfite levels might be the depletion of glutathione, which itself is

necessary for cell membrane resistance to oxidative injury. Salman et al. (Salman et al. 2002) investigated a deceased MoCo-deficient patient in detail and concluded that the sulfite-induced toxic insult to the brain causes excitotoxic neuronal injury in the presence of excess magnesium

Another possible explanation for neurological damage of MoCo deficiency patients is diminished uric acid in patients. Uric acid is a potent natural antioxidant in man that accounts for two-thirds of radical scavenging activity of human extracellular fluids (Maxwell et al. 1997). Previous studies suggest that it may prevent excitotoxic neurological injury due to oxyradical formation in stroke, multiple sclerosis, and epilepsy (Stover et al. 1997). Oxidative stresses pose a major threat to the central nervous system where they may lead to lipid peroxidation and degrade protective neural protease inhibitors (Bolkenius and Monard 1995).

Consistently low uric acid concentration will allow accumulation of reactive oxyradicals, which may contribute to neurological damages, which is characteristic of molybdenum cofactor deficiency. Animal models of cerebral ischaemia and oxidative damage have shown limitation of neuronal loss in the presence of raised uric acid concentrations (Yu et al. 1998). However, because xanthine dehydrogenase deficient patients don't have severe neurological defect, although they present with low uric acid, the effect of low uric acid may affect to neurological damage combined with sulfite toxicity.

The connection of MoCo biosynthesis and postsynaptic receptor clustering, the two roles of the bifunctional protein Gephyrin, remains elusive for the time being. One might speculate that these two biological processes interact with each other and that a MoCo deficiency other than Gephyrin deficiency also disturbs the postsynaptic architecture. We therefore examined the distribution of Gephyrin itself as well as that of the inhibitory glycine receptor in *MOCS1*-deficient mice. However, we did not find any abnormalities at the molecular level (Fig. 3.11) and these findings are in accordance with the absence of motor defects as described for the Gephyrin knock-out mouse (Feng et al. 1998).

The phenotype of the MoCo-deficient mice described in this study corresponds to that found in the majority of human patients, a *MOCS1* mutation abolishing the formation of precursor Z. However, no morphological changes in brain tissue (Fig. 3.10) and no ectopic lenses were observed. These symptoms usually manifest after the neonatal period in human patients and a maximal life span of 11 days of the homozygous animals might be too short to develop such gross abnormalities. Although we did not observe any signs of convulsions or ataxia, it is difficult to exclude these symptoms in mice of such limited age.

In our knowledge, the sulfite toxicity and its oxidative stress are the major sources that can lead to the death of the MoCo deficient mice.

Clearly, further work is required here to determine the myelinization state of neurons.

Interestingly, we found the curly whiskers in 8-day-old *MOCS1-/-* mouse. This phenotype might be involved in defect of metabolic pathway due to the deficiency of molybdoenzymes. However, the mechanism for the curly whiskers in *MOCS1-/-* mice remains to be examined.

4.1.4 Possible therapies and approaches

The homozygous animals truly reflect the biochemical abnormalities typical and diagnostic of MoCo deficiency, which finally result in premature death. These animals therefore can now be used for testing therapeutical concepts for this hitherto incurable disease. Two options are available to this end. One is the purification of precursor Z, which is the product of the *MOCS1*-encoded proteins and more stable than molybdopterin or active MoCo, and its delivery in different therapeutical regimes. The second option is gene therapy, delivering one or two types of cDNAs to various organs by the use of viral or plasmid vectors. Although these protocols in attempts to cure other diseases often lack a sufficient expression level to reverse or at least improve the clinical phenotype, the apparently very low level of expression of all *MOCS* genes (Reiss et al. 1998b; Stallmeyer et al. 1999a) renders MoCo deficiency a promising candidate for this approach. A correction of the biochemical abnormalities of MoCo deficiency by these means will not necessarily translate into a reversal of neurological symptoms. The described murine model will therefore also be helpful to determine how early an effective treatment regime will have to start. Recently, the described MoCo deficient mice have been treated with purified precursor Z from *E. coli* by intrahepatic or intraperitoneal injections. If started shortly after birth, this treatment neutralizes the disease phenotype completely and results in healthy and fertile animals (*in progress for publication*).

4.1.5 Prenatal diagnosis and *MOCS1* expression

Since molybdenum cofactor deficiency is a devastating disease with no effective therapies, prenatal diagnosis is a valuable option for many families.

Sulfite oxidase is expressed in amniotic cells, and assay of this activity in cultured cells has

been used successfully many times for prenatal diagnosis of MoCo deficiency (Ogier et al. 1983). It has been shown that sulfite oxidase is present at high levels in chorionic villi obtained at 10 to 14 weeks gestation and can be assayed directly in the biopsy sample without cell culture (Johnson et al. 1991). Although sulfite oxidase activity was present at high levels in the control chorionic villus samples, no xanthine dehydrogenase activity was detected. Measurement of S-sulfocysteine in amniotic fluid is also of value in diagnosis and can be accomplished rapidly (Ogier et al. 1983).

One goal of prenatal diagnosis is treatment of the affected fetus. Although this is not currently possible for most conditions, some examples can be cited. The best-established form of *in utero* intervention is treatment for rare inborn errors of metabolism and treatment for hormone deficiencies. An important example of biochemical disorder for which treatment is available is biotine-responsive multiple carboxylase deficiency. This autosomal recessive enzyme deficiency can be diagnosed by amniocentesis. In one case report, oral administration of biotin to the mother was initiated at 23 weeks of pregnancy. This resulted in the birth of a normal baby (Jorde et al. 2000). Therefore our successful treatment of precursor Z to MoCo deficient mice can be applied to human patient from the prenatal stage, hopefully.

Our investigations from the liver of *MOCS1-/-* embryos and amniotic fluids show that *MOCS1-/-* embryos are able to uptake certain substances from their healthy mother which are essential for MoCo activity or the toxic substances can be neutralized in the embryos. However, the mechanism of the maternal effect is not clear. Although the MPT activity of embryonic liver is controversial, because from two independent experiments, at one time we could find more than 50% of MPT activity in *MOCS1-/-* embryos, and the second time we could not detect any MPT activity (Fig 3.16). Nevertheless, xanthine and uric acid level of amniotic fluids and sulfocystein level of plasma strongly supported the maternal effect for *MOCS1-/-* embryos (Fig 3.16, 3.17). This might be a explanation for the birth of normal *MOCS1-/-* mice.

However, the maternal effect could cause false-positive results of prenatal diagnosis in human patients, therefore this result must be considerable for prenatal diagnosis.

Although the overall expression of the murine *MOCS1* gene was very low, we could detect transcripts of approximately 3.6 kb by Northern blot from all prenatal and postnatal tissues we examined including liver, brain, placenta, kidney and muscle. Quantification of Northern blot (Fig 3. 15) shows high expression in liver and this increased expression in the liver coincides with high sulfite oxidase activity in this organ. Interestingly, prenatal

MOCS1 expression of the liver goes up during development and the expression shows a maximum peak after birth. These data imply that *MOCS1* gene expression is not strongly needed in the prenatal stage, perhaps due to the maternal effect i.e. supplementation of materials for MoCo activity from mother or clearance of toxic substances. There is no evidence that *MOCS1* is induced by any proteins, but it is possible that *MOCS1* gene can be regulated by the circumstance.

4.2 Functional characterization of the *Sox15* gene and its role in muscle differentiation

4.2.1 Introduction and expression of the *Sox15* gene

Sox genes encode a group of proteins that carry a DNA binding HMG domain implicated in transcriptional regulation (Pevny and Lovell-Badge 1997). Sox genes are expressed in various phases of embryonic development and cell differentiation in a manner linked to cell specification. Genes which belong to Sox family show a variety of functions concerning with development, including sex determination, early embryogenesis, neural development, chondrogenesis, etc. The functions of Sox family genes are summarized in table 4.1.

Sox proteins interact with DNA through the HMG domain, which is a 79-amino acid protein motif. Because Sox HMG domains share a number of conserved amino acid residues, HMG box sequences of the *Sox* genes have been identified by PCR-based cloning. Sox proteins were initially registered and classified by the deduced amino acid sequence of the HMG domain alone. To date, over 20 Sox proteins and their genes have been identified in vertebrates and they have been grouped into Groups A-I, Group G being assigned to Sox15. Our current data concurring Sox15 provide direct evidence for a specific role of Sox15 in regulation of myoblast proliferation, differentiation and regeneration.

The *Sox15* gene is specifically expressed in proliferating myoblasts. Detailed expression analysis of the distribution of *Sox15* mRNA was conducted using RT-PCR and Northern blot analysis. The RT-PCR analysis revealed that the *Sox15* is ubiquitously expressed in adult tissues. However, Northern blot analysis demonstrated that the *Sox15* was expressed exclusively in embryonic stem (ES) cells and proliferating primary myoblasts. No *Sox15* transcript was detectable in 20 μg of total RNA from several adult mouse tissue samples.

There are two explanations for the discrepancy between the results obtained by RT-PCR and Northern blot analysis. (1) The *Sox15* is expressed at high level in the ES cells and myoblast and at low level in the adult tissues. (2) The expression of the *Sox15* is restricted to the embryonic and adult stem cells. Based on the relatively low number of stem cells in the adult tissues, the *Sox15* transcript could be only detected using the RT-PCR assay. Immunostaining using the monospecific anti-Sox15 antibody revealed that the Sox15 was down-regulated after myogenic differentiation. Furthermore, Sox15 was detected in nucleus of proliferating C2C12 mouse myoblast, which is a continuous cell line originally derived from myogenic stem cells. In contrast, no Sox15 was detected in non-muscle cell line as primary fibroblasts and Swiss3T3 cell line. These results clearly demonstrate that Sox15 is highly expressed in proliferated myogenic stem cells and down-regulated after the fusion and differentiation of the myogenic cells. It remains to be addressed, whether the Sox15 is expressed at high level in other adult stem cells such as spermatogonia, hematopoietic and neural stem cells.

An alternative method to determine the specific expression of the Sox15 in different precursor cells is the induction of ES cells to differentiation and immunostaining the resulted precursor cells with anti-Sox15 antibody and different antibodies, which recognize specific protein in different stem cells.

(Hiraoka et al. 1998) reported that *SOX20* is highly expressed in fetal testis and down-regulated in adult testis. These results led to suggest that its murine homolog *Sox15* has a potential role in the sex determination or testis development. However, the genotyping PCR, combining with the *Sry* gene PCR, of 10 *Sox15-/-* mice showed that there was no sex reversal like in *Sox9* knock-out mice. Indeed, immunohistological section of *Sox15-/-* testis revealed normal structure of testis (data not shown).

Based on the increased expression of Sox15 in proliferating primary myoblasts and down regulation of the gene after myogenic differentiation lead us to consider the hypothesis that Sox15 may have some roles in proliferation and differentiation of myogenic cells and regeneration of skeletal muscle. To confirm this hypothesis we have investigated the following points:

1. The proliferation and differentiation potential of primary *Sox15-/-* myogenic cells
2. The expression pattern of myogenic factors that regulate the proliferation and differentiation of myogenic cells in the primary *Sox15-/-* myoblasts

3. Role of the *Sox15* in skeletal muscle regeneration and determine whether the impaired skeletal muscle regeneration shown in *Sox15*-/- mice is due to decreased number of the satellite cells in the skeletal muscle.

4. Effect of the *dystrophin* (*mdx*) and *Sox15* deficiency in the double mutant mice on the skeletal muscle development.

Group	Gene	Functional data
A	Sry	Mammalian testis-determining gene.
B1	Soxb1	Expressed in early developing CNS in *Drosophila* (also called *SoxNeuro*). Neuroectoderm expression may be controlled by the zygotic dorsoventral patterning genes *(dpp, sog, brk, twi)*.
	Sox1	Expressed in mouse embryonic CNS, lens; putative neural differentiation gene. Knockout mice show microphthalmia, cataracts, seizures.
	Sox2	Expressed in pluripotent lineages of preimplantation mouse embryo, developing CNS, lens.
	Sox3	Expressed in mouse embryonic CNS, lens. No direct functional data. May act
	Sox19	Expressed in early CNS and lens in zebrafish. No direct functional data.
B2	SoxB2.1	Also called *dichaete*. Involved in early embryo segmentation and brain development and is required for the correct differentiation of the hindgut.
	Sox14	May specify a subset of ventral interneurons in the spinal cord and neuronal subtypes in the brain. Transcriptional repressor. Expressed in developing CNS. Transcriptional repressor.
	Sox21	Roles in cardiac outflow tract development and B-cell development revealed by phenotype of knockout mice.
C	Sox4	Expressed in maturing neurons in CNS, also in PNS and sites of epithelial–mesenchymal interaction.
	Sox11	Involved in oligodendrocyte differentiation.
	Sox12	Not known.
	Sox22	Expressed in CNS and many other tissues. No direct functional data.
	Sox24	Expressed in oocytes. Not studied in detail. No direct functional data.
D	SoxD	Also called *COG-2* (connection of gonad); regulates late-stage uterine seam cell differentiation and fusion.
	Sox5	Expressed during spermatogenesis and chondrogenesis. Involvement in chondrogenesis supported by interaction with SOX9. Homo- and heterodimerization with SOX6.
	Sox6	Expressed during spermatogenesis and chondrogenesis, and in CNS. Involvement in chondrogenesis supported by interaction with SOX9. May act redundantly with SOX5.
	Sox13	Expressed in developing arteries and thymus, and widely in adult human tissues.
	Sox23	Expressed in embryonic ovary and brain. Homodimerization.
E	SoxE	Also called *Sox100B*. Expressed in large intestinal cells, in basophilic cells in the midgut, in the Malpighian tubules, and at the posterior cap of gonadal mesoderm.
	Sox8	Expressed in fetal CNS, brain, branchial arches, limb, heart, dorsal root ganglia, and testes. Deleted in ATR-16 patient. No direct functional data.
	Sox9	Key regulator of chondrogenesis and sex determination, roles also in heart, kidney, and brain development, as revealed by phenotype of campomelic dysplasia patients. Cells lacking SOX9 cannot form chondrocytes.
	Sox10	Regulator of neural crest cell differentiation. Mutation leads to neurocristopathy in humans and mice.
F	Sox7	Not known.
	Sox17	Regulator of endoderm development and spermatogenesis. Role in endoderm induction shown by protein function interference in *Xenopus*.
	Sox18	Blood vessel and hair follicle development, as demonstrated by mutations in *ragged* mice.
G	Sox20	Expressed in fetal testes but expression and function not studied in detail.
	Sox15	Inhibitor of myoblast differentiation, as revealed by experiments involving ultured myoblasts.
	Sox16	Not known.
H	Sox30	Expressed in germ cells of embryonic testes.
I	Sox31	Expressed in late blastula, gastrula, and neural tissues. Dominant negative xperiments in *Xenopus* demonstrate role in neural induction.

Table 4.1: Functions of *Sox* genes in development (adapted by Bowles et al. 2000).

4.2.2 Generation of *Sox15* deficient mice

To elucidate the function of *Sox15* gene in mice, a targeted mutation of the gene was generated by deleting of 5' flanking region of the gene. We deleted a genomic locus of Sox15 that include 5' UTR and HMG box of the gene. The homozygous mice for *Sox15* deleted allele were generated in two different genetic backgrounds namely, inbred strain 129/Sv and in hybrid strain C57BL/6J X 129/Sv. The homozygous animals appeared phenotypically normal and were fertile. Indeed, they showed normal reproductive capacity (Fig. 3.30).

4.2.3 Role of *Sox15* in skeletal muscle differentiation and regeneration

4.2.3.1 Overview about myogenic satellite cells and myogenic factors in skeletal muscle development

Skeletal muscle of adult mammalian species exhibits a remarkable capacity to adapt to physiologic demands such as growth, training and injury. The processes by which these adaptations occur are largely attributed to a small population of satellite cells. Skeletal muscle stem cells, also known as muscle satellite cells, are located adjacent to the plasma membrane of myofibers beneath the basement membrane. Satellite cells make up 2% − 7% of sublaminar muscle nuclei in mice, and the proportion varies with age and muscle group (Bischoff and Heintz 1994). They are normally mitotically quiescent, however, in response to stimuli such as injury, satellite cell becomes activated, proliferate, and express myogenic factors. The descendants of the activated satellite cells, called myogenic precursor cells (mpc), undergo multiple rounds of division before fusing to existing myofibers or forming new myofibers, leading to repair and/or hypertrophy of the damaged or stressed muscle fibers, respectively (Bischoff and Heintz 1994).

Histopathological analysis has shown that muscle satellite cells differentiate into myotubes and myofibers exclusively (Saito and Nonaka 1994), and there is no evidence that these cells are able to differentiate into non-muscle cells *in vivo*. However, both primary cultured mouse myoblasts and the immortalized mouse myoblastic cell line C2C12 differentiate into osteoblasts and adipocytes as well as myotubes under appropriate culture conditions (Katagiri et al. 1994; Teboul et al. 1995; Yamamoto et al. 1997; Chalaux et al. 1998; Nishimura et al. 1998; Fujii et al. 1999). Although these observations suggest that muscle satellite cells preserve multipotentiality, the source of the muscle-derived cells (so-called myoblasts) analyzed in these studies is unknown. Recently, multipotentiality of muscle

satellite cells was also suggested by the analysis of multiclonal myoblasts derived from multiple satellite cells (Asakura et al. 2001). However, it is unclear whether different fates are generated form a single satellite cell.

The myogenic regulatory factors (MRFs) form a group of basic helix-loop-helix (bHLH) transcription factors consisting of MyoD, Myf5, myogenin and MRF4. The MRFs are expressed exclusively in skeletal muscle. Quiescent satellite cells express no detectable MRFs but express c-met receptor tyrosine kinase. Activated satellite cells (satellite cells entering the cell cycle) first express either Myf5 or MyD and subsequently both proliferating Myf5 and MyoD positive precursors coexpress Myf5 and MyoD (Cornelison and Wold 1997). After proliferation, myogenin and MRF4 are expressed in cells beginning their differentiation program (Fig. 4.3). MRFs, MyoD and Myf5 appear to be required for myogenic determination, whereas the secondary MRFs myogenin and MRF4 are required later in the developmental program as differentiation factors (Megeney et al. 1996).

Gene knock-out experiments have shown that MyoD and Myf5 play redundant roles in establishing myoblast identity, development, whereas deletion of both gene results in the complete absence of skeletal myoblasts (Braun et al. 1992; Rudnicki et al. 1992; Rudnicki et al. 1993). In mice lacking myogenin, myoblasts are specified and primary muscle fibers are formed, but secondary myogenesis fails to occur, resulting in a severe deficiency of skeletal muscle at birth (Hasty et al. 1993; Nabeshima et al. 1993; Venuti et al. 1995). Mice lacking MRF4 develop normal skeletal muscle and show about a four-fold increase in expression of myogenin (Patapoutian et al. 1995; Zhang et al. 1995a), which raises the possibility that myogenin may compensate for the function of MRF4.

4.2.3.2 Reduced differentiation potential of *Sox15*-/- myogenic cells

To characterize the phenotype of *Sox15*-/- myoblasts and to gain insight into the role of the *Sox15* gene in the activation and differentiation of satellite cells, satellite cells were isolated from 3-month old wild-type and *Sox15*-/- mice and primary myoblasts cultures were established. Primary *Sox15* deficient myogenic cells exhibited a flattened morphology with an enlarged cytoplasm and extended cytosolic processes and small compact cytoplasm characteristic of primary myoblasts. Indirect immunofluorescence analysis revealed that all cultured myogenic wild-type and *Sox15*-/- cells expressed high levels of c-met, which is expressed in quiescent and activated satellite cells but not in fibroblasts. In contrast, reduced numbers of *Sox15*-/- myogenic cells express the

intermediate filament desmin, which is expressed in myoblasts but not in satellite cells (Fig. 3.33). These results demonstrate that most *Sox15*-/- cells represent an intermediate developmental stage between a quiescent satellite cell and a proliferating myogenic cell. Transfer of primary *Sox15*-/- cells into differentiation medium resulted in formation of reduced numbers of mononuclear myocytes and delayed differentiation of multinuclear myotubes. The reduced rate of *Sox15*-/- myogenic cells that express the myosin heavy chain (MHC) of the serum withdrawal demonstrates a marked delay in differentiation of the *Sox15*-/- myogenic cells.

4.2.3.3 Down-regulation of *MyoD* expression in myogenic cells lacking *Sox15*

Northern blot analysis revealed that the *MyoD* is not expressed in the *Sox15*-/- myogenic cells. In contrast, the *Sox15*-/- cells showed significant increase of *Myf5* mRNA. RT-PCR analysis revealed that the inactivation of the *Sox15* has a significant influence on the expression of the myogenin in the *Sox15*-/- myogenic cells. These results indicate that the *Sox15* gene regulate directly or indirectly the expression of the *MyoD* gene.

Similar results have been obtained by analysing the cell morphology and differentiation capacity of the cultured myogenic cells of *MyoD* deficient mice. The *MyoD*-/- myogenic cells do not exhibit a reflective and compact morphology, typical for wild-type primary myoblasts. *MyoD*-/- myogenic cells exposed to differentiation medium for 5 days displayed decreased number of differentiation myocytes. Furthermore, Northern blot analysis revealed approximately a four-fold up-regulation of the *Myf5* mRNA in *MyoD*-/- cells. The results indicate that lack of *MyoD* results in a deficiency in the satellite cell differentiation program; *Myf5* and *MyoD* cannot fully substitute for each other during myogenesis and suggests that *Myf5* and *MyoD* activate discrete subsets of target gene that differentially define myogenic cell identity (Sabourin et al. 1999). The expression pattern of *Myf5* and *MyoD* in *Sox15*-/- myogenic cells indicate that the reduced differentiation is due to the down-regulation of the *MyoD*. Activated satellite cells first express either Myf5 alone or MyoD and subsequently progress through the myogenic program (Fig. 4.3).
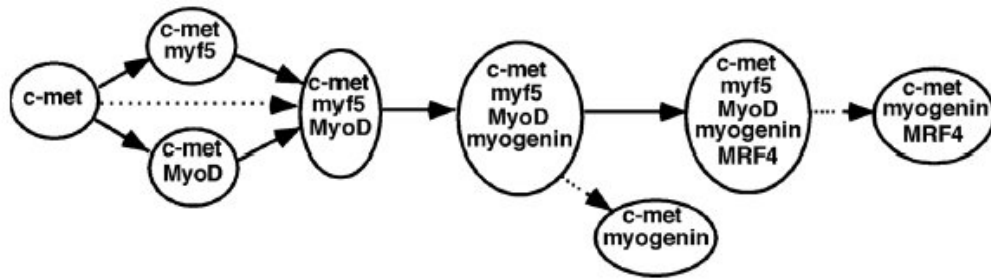
Figure 4.3: Model of MRF coexpression status in satellite cells during the course of a regeneration respose in fiber culture (adapted by Cornelison and Wold 1997).

Therefore, it can be suggested that the observed expression pattern of *MyoD* and *Myf5* in the *Sox15-/-* myogenic cells is due either to the lack of the Sox15 activated satellite cells to *Myf5* positive cell lineage or to the down-regulation of *MyoD*, which up-regulates the expression of the *Myf5* in the proliferating *Sox15-/-* myogenic cells.

Results of RT-PCR analysis showed that the *MyoD* is expressed at very low levels in cultured *Sox15*-deficient cells. Therefore, it is important to address the question, whether the *Sox15-/-* myogenic cells contain a small population of the MyoD-positive cell lineage. This can be performed by immunostaining the *Sox15-/-* myogenic cells by anti-MyoD antibody.

In transient transfection experiment, (Beranger et al. 2000) showed that the overexpression of *Sox15* in the myogenic cell line C2C12 down-regulates the expression of the *MyoD* and the *Sox15* overexpressed cells do not undergo differentiation after 2-3 days of culture in differentiation medium. These results suggest that the *Sox15* repress the expression of *MyoD* and they are different from our results suggesting that the *Sox15* activates directly or indirectly the *MyoD* expression.

At least three transcription factors Pax3, Myf5 (Kucharczuk et al. 1999), and serum response factor SRF (Carnac et al. 1998) have been postulated as upstream regulators of *MyoD*. However, it is not known whether these factors or Sox15 act directly by binding to the *MyoD* regulatory regions. This may be due to the complexity of the *MyoD* gene, which

is regulated by at least three different enhancers located up to 20 kb upstream from the transcription start site. One of these regions, the distal regulatory region is unusual because it requires stable chromosomal integration for muscle-specific activity (Tapscott et al. 1992). Nevertheless, the distal regulatory region contains several putative Sox binding sites, one of which is identical to the Sox binding site used in this study (Fig. 3.38). Although the signal of shifted bands was very low because the endogenous expression of Sox15 is not so high, binding of Sox15 to the Sox binding site in Sox15 transfectd COS7 cells showed strong binding activity with this site (Beranger et al. 2000). Taken together, we can propose the model Sox15 is able to regulate *MyoD* gene by binding to MyoD promoter region.

4.2.3.4 Mice lacking *Sox15* exhibit impaired regulation of skeletal muscle

Wild-type skeletal muscle typically undergoes several stages following injury leading to complete repair of the lesion. Within 24 hours, damaged fibers become necrotic and begin to degenerate, and large numbers of infiltrating eosinophils, neutrophils and macrophages accumulate and remove debris from the area of damages. Satellite cells invade the site, proliferate, and fuse to each other as they differentiate to form new muscle fibers within pre-existing basal lamina. By two weeks, every fiber is continuous and fiber calibres are comparable with undamaged muscle (Grounds and Yablonka-Reuveni 1993).

To investigate the capacity of *Sox15*-/- skeletal muscle to repair damage, injury-induced regeneration experiments on *Sox15* deficient mice were performed. Two weeks after injury, virtually no sign of previous damage was detectable in wild-type mice, indicating a complete regeneration (Fig 3.39 E). In contrast, high number of mononuclear cells were visible in injured muscle of *Sox15*-/- and limited regeneration, as evidence by the presence of thin myofibers at the site of injury (Fig. 3.39 E). These results indicate that the skeletal muscle regeneration is impaired in the *Sox15*-/- muscle.

Electron microscopic experiment of TA skeletal muscle sections clearly revealed the presence of morphologically normal satellite cells in TA muscle of *Sox15*-/- mice. The rate of satellite cell in *Sox15*-/- TA muscle does not significantly differ from that in wild-type TA muscle. These results together with the observed delay of the differentiation of the *Sox15*-/- myogenic cell *in vitro* suggest that the limitation of skeletal muscle repair is due to deficit in the satellite cell differentiation program.

Interestingly the knock-out mice lacking *MyoD* exhibit normal muscle development but display impaired skeletal muscle regeneration after injury. The regeneration deficit of *MyoD*-/- mice is not due to the reduced rate of satellite cells in the skeletal muscle but due to impaired differentiation of the satellite cells (Megeney et al. 1996). Phenotypic similarity of the skeletal muscle repair in *MyoD*-/- and *Sox15*-/- strongly suggests that the impaired regeneration of the skeletal muscle in the *Sox15*-/-mice is due to the lack of MyoD.

4.2.4 Muscular dystrophy

Muscular dystrophies are a diverse group of inherited disorders characterized by progressive muscle weakness and wasting (Bushby 2000; Cohn and Campbell 2000). Current hypotheses suggest two main biological cascades involved in the dystrophic disease process. First, the dystrophin-glycoprotein complex plays an essential role in protecting the sarcolemma against muscle contraction-induced injury. Second, factors regulate the proliferation of satellite cells and differentiation of the myogenic precursors. Failure of the myogenic satellite cells to maintain muscle regeneration results in muscular dystrophy.

Dystrophin-glycoprotein complex (DGC) is a multisubunit complex comprised of peripheral and integral proteins, which links the cytoskeleton to the extracellular matrix. The proteins that comprise the DGC are the intracellular proteins (dystrophin and utrophin) and the sarcolemmal proteins (dystroglycans, sacoglycans and sarcospan). Disruption of this linkage, due to mutation of dystrophin or sarcoglycans, causes sarcolemmal instability. Subsequent to the sarcolemmal damage, increased calcium influx has been observed, which in turn may render the muscle fibers susceptible to necrosis. Duchenne muscular dystrophy (DMD) is a common, X-linked disease that results in progressive muscle wasting (Gussoni et al. 1997). DMD is caused by mutation in the gene encoding *dystrophin*. The *mdx* mice carry a point mutation in the *dystrophin* gene and are therefore an animal model for human DMD. Unlike humans, *mdx* maintain skeletal muscle integrity due to a high muscle regenerative capacity. This regeneration results in the formation of additional muscle fibers, which lead to a significant level of muscular hypertrophy. The *mdx* mice display normal external appearance and normal life spans of 1.5 – 2 years (Coulton et al. 1988).

If *Sox15* is required for efficient regeneration of skeletal muscle, mice lacking *Sox15* and *dystrophin* (*mdx:Sox15*-/-) should display more extensive dystrophic change in skeletal muscle. The *mdx:Sox15*-/- mice were outwardly similar to wild-type. Two of 10 double mutants, which live over one year in our mouse colony, died at 3- and 5-month-old. The cause of death of these two animals is unknown. Radiographs of 6-month-old animals of three genotypes revealed a severe dorsal-ventral curvature of the spine (Fig. 3.43) in the *mdx:Sox15*-/-mice, which is a common feature in DMD thought to result from asymmetric weakening of the muscle that support the spinal column (Oda et al. 1993). Kyphosis was also observed in older *Sox15*-/- mice. Comparison of the phenotypes of the *mdx:Sox15*-/- with those of *mdx:MyoD*-/- showed partial overlap. Both double mutant mice display a profound kyphosis, whereas the *mdx:MyoD*-/- mice show an abnormal wadding gait by 3 – 5 month of age. We have not observed a similar phenotype in the *mdx:Sox15*-/- mice. The *mdx:MyoD*-/- mice display an increased myopathy of skeletal muscle. According to current small number of the *mdx:Sox15*-/- in our mouse colony, we could not analyse the skeletal muscle degeneration in double mutant mice. In this context, further histological analysis of skeletal muscle in double mutant mice will be informative to determine the skeletal muscle regeneration.

Severe dorsal-ventral curvature were also observed in double mutant mice lacking the *dystrophin* and *FGF-6* gene (Floss et al. 1997), which code for growth factor that is believed to activate the satellite cells, and dystrophin and utrophin, a homolog of dystrophin (Grady et al. 1997).
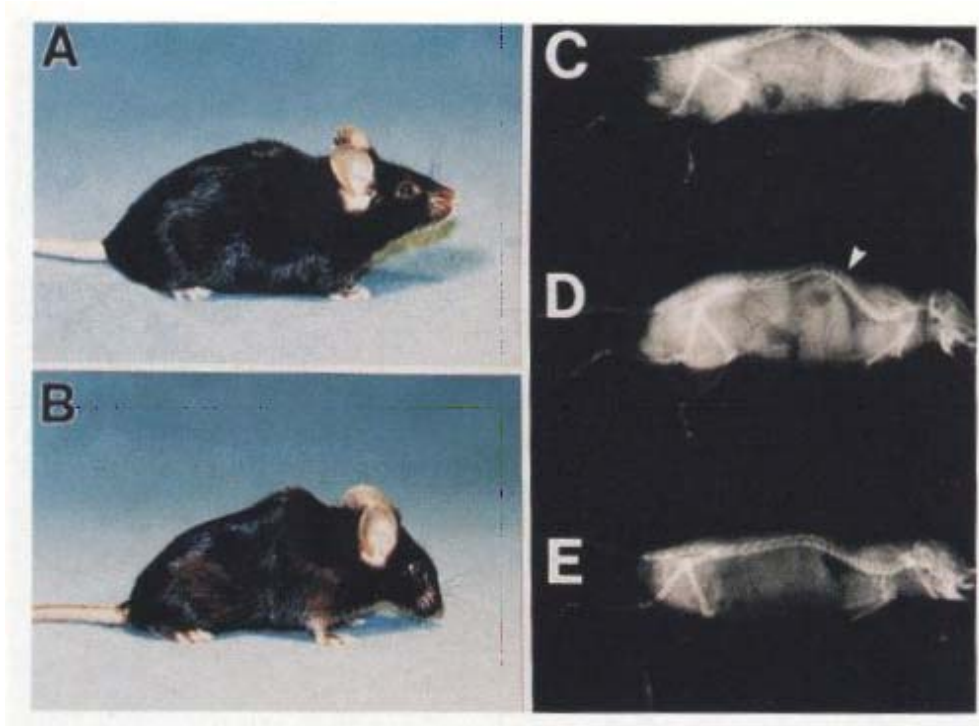
Figure 4.4: Increased penetrance of the *mdx* pheonotype in *mdx:MyoD*-/- mice. (A) The *mdx* mouse appears morphologically normal compared with wild-type mouse. (B) In contrast, the *mdx:MyoD*-/- mouse displays a severe dorsal-ventral curvature of the spine and increased myopathy characterized by an abnormal wadding gait and weight-bearing on the hocks. X-Ray radiographic visualization revealed abnormal curvature of the spine (arrow head) of *mdx:MyoD*-/- mice (D), compared with *mdx* mice (C), and *MyoD*-/- mice (E). All animals shown are 5 month of age (adapted by Megeney et al. 1996)

4.2.5 Role of the *Sox15* gene in specification of the myogenic cell lineage

Satellite cells clearly represent the progenitors of the myogenic cells that give rise to the majority of the nuclei within adult skeletal muscle. However, recent studies have identified a population of pluripotent stem cells also called side-population (SP) cells. Purified SP cells derived from muscle exhibit the capacity to give rise to myogenic satellite cells (Gussoni et al. 1999). This result led to suggest that SP cells are the muscle derived stem cells (MSC) and are progenitors for satellite cells. Cell culture and electron microscopic analysis revealed a complete absence of satellite cells in knock-out mice lacking transcription factor *Pax7*. However, muscle derived stem cells were unaffected in *Pax7*-/-.

These results indicate that the *Pax7* is responsible for specification the MSC to satellite cells. After activation of the quiescent satellite cells, two proliferating myogenic cell lineages are developed. One expressed *MyoD* alone and the other expressed *Myf5* alone. Later, these two cell lineages express both *MyoD* and *Myf5*. Based on the down-regulation of the *MyoD* in the *Sox15*-/- myogenic cells, it can be suggested the *MyoD*-positive cell are not developed and the *Myf5* positive cells proliferate and give rise the terminal differentiated myotubes. To confirm that the *Sox15* determines the fate of *MyoD*-positive myogenic cells, immunostaining of the wild-type myoblasts with either anti-MyoD and anti-Sox15 antibodies or anti-Myf5 and anti-Sox15 antibodies can exhibit, whether the Sox15 colocalize only with the *MyoD* positive myoblasts but absent in the *Myf5*–positive cells
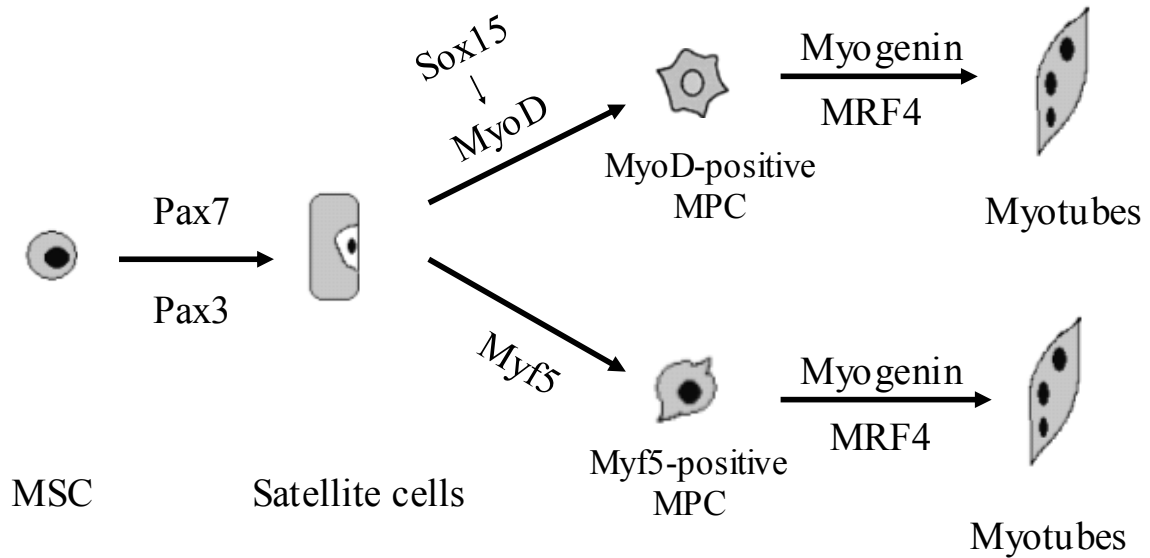
Figure 4.5: Possible role for Sox15 during the myogenesis. Muscle-derived pluripotent stem cells (MSC) primary give rise to myoblasts when cultured in growth medium. Satellite cells are activated in response to physiological stimuli to generate two different daughter myogenic precursors (MPC) before terminal differentiation into new or previously existing fibers. One of MPC (MyoD-positive MPC) is stimulated by MyoD, which is activated by Sox15.

4.2.6 Differentiation into neuronal cell of *Sox15*-/- satellite cells.

Interestingly, from the late passages (>7th passage) of S*ox15*-/- satellite cells, we could observe astrocyte like morphology cells by induction of differentiation. They were positively stained by astrocytic marker, anti-GFAP antibody. Recently it was reported that muscle stem cells could be differentiated into neuronal cells *in vitro* (Romero-Ramos et al. 2002). However, whether this population of muscle stem cells can be induced to primarily express a neural phenotype is unclear. If muscle stem cells could differentiate into neurons and glia, the capacity for neuronal differentiation might be increased in *Sox15*-/- satellite cells. The mechanism for neuronal differentiation of *Sox15*-/- satellite cells must be further elucidated.

4.2.7 Combined deletion of 3' UTR of the *Fxr2* in *Sox15*-/- mice

During the generation of *Sox15* knock-out mice, we found the deletion of 3' UTR of *Fxr2h* gene in the targeted construct. Because *Fxr2* and *Sox15* are narrowly clustered in the same

region of mouse chr. 11 (Miyashita et al. 1999), the construct for *Sox15* knock-out mice was interrupted by both neighbouring genes, *Sox15* and *Fxr2*.

Fxr2 is a homolog of Fmr1 protein which is responsible for fragile X syndrome and Fxr1 protein (Siomi et al. 1995; Zhang et al. 1995b). Since these proteins show a high sequence homology, and overlap in tissue distribution, analogous functions are suggested. It has been suggested that these proteins might partly complement one another. *Fxr2* knock-out mice are hyperactive (i.e. travel a greater distance, spent more time moving and moved faster) in open-field test, impaired on the rotarod test, had reduced levels of prepulse inhibition, displayed less contextual conditioned fear, impaired at locating the hidden platform (Bontekoe et al. 2002). *Sox15*-/- mice do not show such phenotypes, indicating *Sox15*-/- mice are not affected by deletion of 3' UTR of the *Fxr2*. However, the *Fxr2* gene does not have any evidence that it is involved in muscle differentiation. Because of low expression level of *Fxr2*, we could not detect the *Fxr2* transcripts in various tissues we examined by Northern blot in *Sox15*-/- mice tissues (data not shown).

To exclude the effect of *Fxr2* in myogenesis, we will generate new *Sox15* knock-out mice and investigate them.

5. SUMMARY

In this work, function of the murine genes, *MOCS1* and *Sox15* were investigated.

Human molybdenum cofactor deficiency is a rare and devastating autosomal-recessive disease for which no therapy is known. The absence of active sulfite oxidase, a molybdenum cofactor-dependent enzyme, results in neonatal seizures and early childhood death. Most patients harbor mutations in the *MOCS1* gene, whose murine homolog was disrupted by homologous recombination with a targeting vector. As in humans, heterozygous mice display no symptoms, but homozygous animals die between days 1 and 11 after birth. Biochemical analysis of these animals shows that molybdopterin and active cofactor are undetectable. They do not possess any sulfite oxidase or xanthine dehydrogenase activity. No organ abnormalities were observed and the synaptic localization of inhibitory receptors, which was found to be disturbed in molybdenum cofactor deficient-mice with Gephyrin mutation, appears normal. *MOCS*1-/- mice could be suitable animal model for biochemical and/or genetic therapy approaches.

Although the overall expression of the murine *MOCS1* gene is very low, prenatal *MOCS1* expression of the liver goes up during development. In addition, low activity of MoCo was found in amniotic fluid of *MOCS1*-/- embryos. Our investigations in liver and amniotic fluids of *MOCS1*-/- embryos show that *MOCS1*-/- embryos are able to uptake certain substances from their healthy mother which are essential for MoCo activity or the clearance for the toxic substances neutralization.

Sox genes encode a group of proteins that carry a DNA binding HMG domain implicated in transcriptional regulation. *Sox* genes are expressed in various phases of embryonic development and cell differentiation in a manner linked to cell specification. The *Sox15* gene is specifically expressed in proliferating myoblasts and ES cells. To elucidate the function of the *Sox15* gene and its role in muscle development, primary myoblast cultures from the *Sox15*-/- mice were established. Primary *Sox15*-/- myogenic cells exhibited a flattened morphology which is distinct from the compact morphology of wild-type myoblasts.

Under conditions that normally induce differentiation of myogenic cells, *Sox15*-/- cells exhibited strong reduction of differentiation potential to multinuclear myocytes as compared to wild-type cells. Northern blot analysis indicated that the expression of the

myogenic regulatory factor MyoD is down-regulated in *Sox15*-/- myoblasts, while Myf5 is up-regulated.

Electrophoretic mobility shift assays indicated that Sox15 protein was capable of binding to a DNA binding site for Sox proteins which is located on the distal regulatory region of *MyoD*. Following injury, *Sox15*-/- muscle was severely deficient in regenerative ability, which is similar to *MyoD*-/- muscle. Mice lacking both Sox15 and dystrophin displayed more extensive dystrophic change in skeletal muscle. Therefore we propose that the *Sox15* has a key role for muscle development through the myogenic program by regulation of *MyoD*.

6. REFERENCES

Allen, R.E., S.M. Sheehan, R.G. Taylor, T.L. Kendall, and G.M. Rice. 1995. Hepatocyte growth factor activates quiescent skeletal muscle satellite cells in vitro. *J Cell Physiol* **165**: 307-12.

Amalfitano, A. and J.S. Chamberlain. 1996. The mdx-amplification-resistant mutation system assay, a simple and rapid polymerase chain reaction-based detection of the mdx allele. *Muscle Nerve* **19**: 1549-53.

Asakura, A., M. Komaki, and M. Rudnicki. 2001. Muscle satellite cells are multipotential stem cells that exhibit myogenic, osteogenic, and adipogenic differentiation. *Differentiation* **68**: 245-53.

Barbot, C., E. Martins, L. Vilarinho, C. Dorche, and M.L. Cardoso. 1995. A mild form of infantile isolated sulphite oxidase deficiency. *Neuropediatrics* **26**: 322-4.

Beranger, F., C. Mejean, B. Moniot, P. Berta, and M. Vandromme. 2000. Muscle differentiation is antagonized by SOX15, a new member of the SOX protein family. *J Biol Chem* **275**: 16103-9.

Bischoff, R. and C. Heintz. 1994. Enhancement of skeletal muscle regeneration. *Dev Dyn* **201**: 41-54.

Boles, R.G., L.R. Ment, M.S. Meyn, A.L. Horwich, L.E. Kratz, and P. Rinaldo. 1993. Short-term response to dietary therapy in molybdenum cofactor deficiency. *Ann Neurol* **34**: 742-4.

Bolkenius, F.N. and D. Monard. 1995. Inactivation of protease nexin-1 by xanthine oxidase-derived free radicals. *Neurochem Int* **26**: 587-92.

Bondurand, N., A. Kobetz, V. Pingault, N. Lemort, F. Encha-Razavi, G. Couly, D.E. Goerich, M. Wegner, M. Abitbol, and M. Goossens. 1998. Expression of the SOX10 gene during human development. *FEBS Lett* **432**: 168-72.

Bontekoe, C.J., K.L. McIlwain, I.M. Nieuwenhuizen, L.A. Yuva-Paylor, A. Nellis, R. Willemsen, Z. Fang, L. Kirkpatrick, C.E. Bakker, R. McAninch, N.C. Cheng, M. Merriweather, A.T. Hoogeveen, D. Nelson, R. Paylor, and B.A. Oostra. 2002. Knockout mouse model for Fxr2: a model for mental retardation. *Hum Mol Genet* **11**: 487-98.

Bowles, J., G. Schepers, and P. Koopman. 2000. Phylogeny of the SOX family of developmental transcription factors based on sequence and structural indicators. *Dev Biol* **227**: 239-55.

Braun, T., M.A. Rudnicki, H.H. Arnold, and R. Jaenisch. 1992. Targeted inactivation of the muscle regulatory gene Myf-5 results in abnormal rib development and perinatal death. *Cell* **71**: 369-82.

Bushby, K. 2000. Genetics and the muscular dystrophies. *Dev Med Child Neurol* **42**: 780-4.

Carnac, G., M. Primig, M. Kitzmann, P. Chafey, D. Tuil, N. Lamb, and A. Fernandez. 1998. RhoA GTPase and serum response factor control selectively the expression of MyoD without affecting Myf5 in mouse myoblasts. *Mol Biol Cell* **9**: 1891-902.

Chalaux, E., T. Lopez-Rovira, J.L. Rosa, R. Bartrons, and F. Ventura. 1998. JunB is involved in the inhibition of myogenic differentiation by bone morphogenetic protein-2. *J Biol Chem* **273**: 537-43.

Chan, M.K., S. Mukund, A. Kletzin, M.W. Adams, and D.C. Rees. 1995. Structure of a hyperthermophilic tungstopterin enzyme, aldehyde ferredoxin oxidoreductase. *Science* **267**: 1463-9.

Cohen, H.J., R.T. Drew, J.L. Johnson, and K.V. Rajagopalan. 1973. Molecular basis of the biological function of molybdenum: the relationship between sulfite oxidase and the acute toxicity of bisulfite and SO2. *Proc Natl Acad Sci U S A* **70**: 3655-9.

Cohn, R.D. and K.P. Campbell. 2000. Molecular basis of muscular dystrophies. *Muscle Nerve* **23**: 1456-71.

Cole, D.E. and C.R. Scriver. 1981. Microassay of inorganic sulfate in biological fluids by controlled flow anion chromatography. *J Chromatogr* **225**: 359-67.

Cornelison, D.D. and B.J. Wold. 1997. Single-cell analysis of regulatory gene expression in quiescent and activated mouse skeletal muscle satellite cells. *Dev Biol* **191**: 270-83.

Coulton, G.R., J.E. Morgan, T.A. Partridge, and J.C. Sloper. 1988. The mdx mouse skeletal muscle myopathy: I. A histological, morphometric and biochemical investigation. *Neuropathol Appl Neurobiol* **14**: 53-70.

Feng, G., H. Tintrup, J. Kirsch, M.C. Nichol, J. Kuhse, H. Betz, and J.R. Sanes. 1998. Dual requirement for gephyrin in glycine receptor clustering and molybdoenzyme activity. *Science* **282**: 1321-4.

Floss, T., H.H. Arnold, and T. Braun. 1997. A role for FGF-6 in skeletal muscle regeneration. *Genes Dev* **11**: 2040-51.

Foster, J.W. 1996. Mutations in SOX9 cause both autosomal sex reversal and campomelic dysplasia. *Acta Paediatr Jpn* **38**: 405-11.

Fujii, M., K. Takeda, T. Imamura, H. Aoki, T.K. Sampath, S. Enomoto, M. Kawabata, M. Kato, H. Ichijo, and K. Miyazono. 1999. Roles of bone morphogenetic protein type I receptors and Smad proteins in osteoblast and chondroblast differentiation. *Mol Biol Cell* **10**: 3801-13.

George-Weinstein, M., R.F. Foster, J.V. Gerhart, and S.J. Kaufman. 1993. In vitro and in vivo expression of alpha 7 integrin and desmin define the primary and secondary myogenic lineages. *Dev Biol* **156**: 209-29.

Grady, R.M., H. Teng, M.C. Nichol, J.C. Cunningham, R.S. Wilkinson, and J.R. Sanes. 1997. Skeletal and cardiac myopathies in mice lacking utrophin and dystrophin: a model for Duchenne muscular dystrophy. *Cell* **90**: 729-38.

Graf, W.D., O.E. Oleinik, R.M. Jack, A.H. Weiss, and J.L. Johnson. 1998. Ahomocysteinemia in molybdenum cofactor deficiency. *Neurology* **51**: 860-2.

Gray, R.G., A. Green, S.N. Basu, G. Constantine, R.G. Condie, C. Dorche, C. Vianey-Liaud, and P. Desjacques. 1990. Antenatal diagnosis of molybdenum cofactor deficiency. *Am J Obstet Gynecol* **163**: 1203-4.

Gray, T.A. and R.D. Nicholls. 2000. Diverse splicing mechanisms fuse the evolutionarily conserved bicistronic MOCS1A and MOCS1B open reading frames. *Rna* **6**: 928-36.

Grounds, M.D. and Z. Yablonka-Reuveni. 1993. *Molecular and cellular biology of muscle regeneration in Molecular and cellualr biology of muscular dystrphy*. Chapman and Hall, London, UK.

Gubbay, J., J. Collignon, P. Koopman, B. Capel, A. Economou, A. Munsterberg, N. Vivian, P. Goodfellow, and R. Lovell-Badge. 1990. A gene mapping to the sex-determining region of the mouse Y chromosome is a member of a novel family of embryonically expressed genes. *Nature* **346**: 245-50.

Gussoni, E., H.M. Blau, and L.M. Kunkel. 1997. The fate of individual myoblasts after transplantation into muscles of DMD patients. *Nat Med* **3**: 970-7.

Gussoni, E., Y. Soneoka, C.D. Strickland, E.A. Buzney, M.K. Khan, A.F. Flint, L.M. Kunkel, and R.C. Mulligan. 1999. Dystrophin expression in the mdx mouse restored by stem cell transplantation. *Nature* **401**: 390-4.

Hansen, L.K., K. Wulff, C. Dorche, and E. Christensen. 1993. Molybdenum cofactor deficiency in two siblings: diagnostic difficulties. *Eur J Pediatr* **152**: 662-4.

Hanzelmann, P., G. Schwarz, and R.R. Mendel. 2002. Functionality of alternative splice forms of the first enzymes involved in human molybdenum cofactor biosynthesis. *J Biol Chem* **277**: 18303-12.

Harley, V.R., R. Lovell-Badge, and P.N. Goodfellow. 1994. Definition of a consensus DNA binding site for SRY. *Nucleic Acids Res* **22**: 1500-1.

Hasty, P., A. Bradley, J.H. Morris, D.G. Edmondson, J.M. Venuti, E.N. Olson, and W.H. Klein. 1993. Muscle deficiency and neonatal death in mice with a targeted mutation in the myogenin gene. *Nature* **364**: 501-6.

Hiraoka, Y., M. Ogawa, Y. Sakai, K. Taniguchi, T. Fujii, A. Umezawa, J. Hata, and S. Aiso. 1998. Isolation and expression of a human SRY-related cDNA hSOX20. *Biochim Biophys Acta* **1396**: 132-7.

Johnson, J.L., K.E. Coyne, K.V. Rajagopalan, J.L. Van Hove, M. Mackay, J. Pitt, and A. Boneh. 2001. Molybdopterin synthase mutations in a mild case of molybdenum cofactor deficiency. *Am J Med Genet* **104**: 169-73.

Johnson, J.L., Duran, M. 2001. *Molybdunum cofactor deficiency and isolated sulfite oxidase deficiency*. McGraw-Hill, New York.

Johnson, J.L. and K.V. Rajagopalan. 1976. Human sulfite oxidase deficiency. Characterization of the molecular defect in a multicomponent system. *J Clin Invest* **58**: 551-6.

Johnson, J.L. and K.V. Rajagopalan. 1982. Structural and metabolic relationship between the molybdenum cofactor and urothione. *Proc Natl Acad Sci U S A* **79**: 6856-60.

Johnson, J.L., K.V. Rajagopalan, and H.J. Cohen. 1974. Molecular basis of the biological function of molybdenum. Effect of tungsten on xanthine oxidase and sulfite oxidase in the rat. *J Biol Chem* **249**: 859-66.

Johnson, J.L., K.V. Rajagopalan, J.T. Lanman, R.B. Schutgens, A.H. van Gennip, P. Sorensen, and D.A. Applegarth. 1991. Prenatal diagnosis of molybdenum cofactor deficiency by assay of sulphite oxidase activity in chorionic villus samples. *J Inherit Metab Dis* **14**: 932-7.

Johnson, J.L., Waldman, S.K. 1995. *Moybdenum cofator deficiency and isolated sulfite oxidase deficiency*. McGraw Hill, New York.

Johnson, J.L., W.R. Waud, K.V. Rajagopalan, M. Duran, F.A. Beemer, and S.K. Wadman. 1980. Inborn errors of molybdenum metabolism: combined deficiencies of sulfite oxidase and xanthine dehydrogenase in a patient lacking the molybdenum cofactor. *Proc Natl Acad Sci U S A* **77**: 3715-9.

Johnson, J.L., M.M. Wuebbens, R. Mandell, and V.E. Shih. 1989. Molybdenum cofactor biosynthesis in humans. Identification of two complementation groups of cofactor-deficient patients and preliminary characterization of a diffusible molybdopterin precursor. *J Clin Invest* **83**: 897-903.

Jorde, L., J. Carey, M. Bamshad, and R. White. 2000. *Medical genetics*. Mosby, St. Louis.

Kablar, B., K. Krastel, C. Ying, A. Asakura, S.J. Tapscott, and M.A. Rudnicki. 1997. MyoD and Myf-5 differentially regulate the development of limb versus trunk skeletal muscle. *Development* **124**: 4729-38.

Kamachi, Y., M. Uchikawa, J. Collignon, R. Lovell-Badge, and H. Kondoh. 1998. Involvement of Sox1, 2 and 3 in the early and subsequent molecular events of lens induction. *Development* **125**: 2521-32.

Katagiri, T., A. Yamaguchi, M. Komaki, E. Abe, N. Takahashi, T. Ikeda, V. Rosen, J.M. Wozney, A. Fujisawa-Sehara, and T. Suda. 1994. Bone morphogenetic protein-2 converts the differentiation pathway of C2C12 myoblasts into the osteoblast lineage. *J Cell Biol* **127**: 1755-66.

Ketchum, P.A., H.Y. Cambier, W.A. Frazier, 3rd, C.H. Madansky, and A. Nason. 1970. In vitro assembly of Neurospora assimilatory nitrate reductase from protein subunits of a Neurospora mutant and the xanthine oxidizing or aldehyde oxidase systems of higher animals. *Proc Natl Acad Sci U S A* **66**: 1016-23.

Kirsch, J., I. Wolters, A. Triller, and H. Betz. 1993. Gephyrin antisense oligonucleotides prevent glycine receptor clustering in spinal neurons. *Nature* **366**: 745-8.

Kneussel, M., J.H. Brandstatter, B. Laube, S. Stahl, U. Muller, and H. Betz. 1999. Loss of postsynaptic GABA(A) receptor clustering in gephyrin-deficient mice. *J Neurosci* **19**: 9289-97.

Kucharczuk, K.L., C.M. Love, N.M. Dougherty, and D.J. Goldhamer. 1999. Fine-scale transgenic mapping of the MyoD core enhancer: MyoD is regulated by distinct but overlapping mechanisms in myotomal and non-myotomal muscle lineages. *Development* **126**: 1957-65.

Laudet, V., D. Stehelin, and H. Clevers. 1993. Ancestry and diversity of the HMG box superfamily. *Nucleic Acids Res* **21**: 2493-501.

Mansour, S.L., K.R. Thomas, and M.R. Capecchi. 1988. Disruption of the proto-oncogene int-2 in mouse embryo-derived stem cells: a general strategy for targeting mutations to non-selectable genes. *Nature* **336**: 348-52.

Maxwell, S.R., H. Thomason, D. Sandler, C. Leguen, M.A. Baxter, G.H. Thorpe, A.F. Jones, and A.H. Barnett. 1997. Antioxidant status in patients with uncomplicated insulin-dependent and non-insulin-dependent diabetes mellitus. *Eur J Clin Invest* **27**: 484-90.

Megeney, L.A., B. Kablar, K. Garrett, J.E. Anderson, and M.A. Rudnicki. 1996. MyoD is required for myogenic stem cell function in adult skeletal muscle. *Genes Dev* **10**: 1173-83.

Mendel, R.R. 1997. Molybdenum cofactor of higher plants: biosynthesis and molecular biology. *Planta* **203**: 399-405.

Meyer, J., P. Sudbeck, M. Held, T. Wagner, M.L. Schmitz, F.D. Bricarelli, E. Eggermont, U. Friedrich, O.A. Haas, A. Kobelt, J.G. Leroy, L. Van Maldergem, E. Michel, B. Mitulla, R.A. Pfeiffer, A. Schinzel, H. Schmidt, and G. Scherer. 1997. Mutational analysis of the SOX9 gene in campomelic dysplasia and autosomal sex reversal: lack of genotype/phenotype correlations. *Hum Mol Genet* **6**: 91-8.

Meyer, J., J. Wirth, M. Held, W. Schempp, and G. Scherer. 1996. SOX20, a new member of the SOX gene family, is located on chromosome 17p13. *Cytogenet Cell Genet* **72**: 246-9.

Miller, J.B., L. Schaefer, and J.A. Dominov. 1999. Seeking muscle stem cells. *Curr Top Dev Biol* **43**: 191-219.

Miyashita, A., N. Shimizu, N. Endo, T. Hanyuu, N. Ishii, K. Ito, Y. Itoh, M. Shirai, T. Nakajima, S. Odani, and R. Kuwano. 1999. Five different genes, Eif4a1, Cd68, Supl15h, Sox15 and Fxr2h, are clustered in a 40 kb region of mouse chromosome 11. *Gene* **237**: 53-60.

Nabeshima, Y., K. Hanaoka, M. Hayasaka, E. Esumi, S. Li, and I. Nonaka. 1993. Myogenin gene disruption results in perinatal lethality because of severe muscle defect. *Nature* **364**: 532-5.

Nason, A., K.Y. Lee, S.S. Pan, P.A. Ketchum, A. Lamberti, and J. DeVries. 1971. Invitro formation of assimilatory reduced nicotinamide adenine dinucleotide phosphate: nitrate reductase from a Neurospora mutant and a component of molybdenum-enzymes. *Proc Natl Acad Sci U S A* **68**: 3242-6.

Ng, L.J., S. Wheatley, G.E. Muscat, J. Conway-Campbell, J. Bowles, E. Wright, D.M. Bell, P.P. Tam, K.S. Cheah, and P. Koopman. 1997. SOX9 binds DNA, activates transcription, and coexpresses with type II collagen during chondrogenesis in the mouse. *Dev Biol* **183**: 108-21.

Nishiguchi, S., H. Wood, H. Kondoh, R. Lovell-Badge, and V. Episkopou. 1998. Sox1 directly regulates the gamma-crystallin genes and is essential for lens development in mice. *Genes Dev* **12**: 776-81.

Nishimura, R., Y. Kato, D. Chen, S.E. Harris, G.R. Mundy, and T. Yoneda. 1998. Smad5 and DPC4 are key molecules in mediating BMP-2-induced osteoblastic differentiation of the pluripotent mesenchymal precursor cell line C2C12. *J Biol Chem* **273**: 1872-9.

Oda, T., A.T. Miyamoto, Y. Okamoto, and T. Ban. 1993. Skeletal muscle-powered ventricle. Effects of size and configuration on ventricular function. *J Thorac Cardiovasc Surg* **105**: 68-77.

Ogier, H., S.K. Wadman, J.L. Johnson, J.M. Saudubray, M. Duran, J. Boue, A. Munnich, and C. Charpentier. 1983. Antenatal diagnosis of combined xanthine and sulphite oxidase deficiencies. *Lancet* **2**: 1363-4.

Patapoutian, A., B.J. Wold, and R.A. Wagner. 1995. Evidence for developmentally programmed transdifferentiation in mouse esophageal muscle. *Science* **270**: 1818-21.

Pateman, J., D. Cove, B. Rever, and D. Roberts. 1964. A common co-factor for nitrate reductase and xanthine dehydrogenase which also regulates the synthesis fro nitrate reductase. *Nature* **201**: 58-60.

Pevny, L.H. and R. Lovell-Badge. 1997. Sox genes find their feet. *Curr Opin Genet Dev* **7**: 338-44.

Pfeiffer, F., R. Simler, G. Grenningloh, and H. Betz. 1984. Monoclonal antibodies and peptide mapping reveal structural similarities between the subunits of the glycine receptor of rat spinal cord. *Proc Natl Acad Sci U S A* **81**: 7224-7.

Pingault, V., N. Bondurand, K. Kuhlbrodt, D.E. Goerich, M.O. Prehu, A. Puliti, B. Herbarth, I. Hermans-Borgmeyer, E. Legius, G. Matthijs, J. Amiel, S. Lyonnet, I. Ceccherini, G. Romeo, J.C. Smith, A.P. Read, M. Wegner, and M. Goossens. 1998. SOX10 mutations in patients with Waardenburg-Hirschsprung disease. *Nat Genet* **18**: 171-3.

Rajagopalan, K.V. 1980. *Sulfieoxidase, in Coughlan MP (ed); Molybdenum and Molybdenum-Conining Enzymes*. Oxford, Pegamon.

Rajagopalan, K.V. and J.L. Johnson. 1992. The pterin molybdenum cofactors. *J Biol Chem* **267**: 10199-202.

Reiss, J. 2000. Genetics of molybdenum cofactor deficiency. *Hum Genet* **106**: 157-63.

Reiss, J., E. Christensen, G. Kurlemann, M.T. Zabot, and C. Dorche. 1998a. Genomic structure and mutational spectrum of the bicistronic MOCS1 gene defective in molybdenum cofactor deficiency type A. *Hum Genet* **103**: 639-44.

Reiss, J., N. Cohen, C. Dorche, H. Mandel, R.R. Mendel, B. Stallmeyer, M.T. Zabot, and T. Dierks. 1998b. Mutations in a polycistronic nuclear gene associated with molybdenum cofactor deficiency. *Nat Genet* **20**: 51-3.

Reiss, J., C. Dorche, B. Stallmeyer, R.R. Mendel, N. Cohen, and M.T. Zabot. 1999. Human molybdopterin synthase gene: genomic structure and mutations in molybdenum cofactor deficiency type B. *Am J Hum Genet* **64**: 706-11.

Reiss, J., S. Gross-Hardt, E. Christensen, P. Schmidt, R.R. Mendel, and G. Schwarz. 2001. A mutation in the gene for the neurotransmitter receptor-clustering protein gephyrin causes a novel form of molybdenum cofactor deficiency. *Am J Hum Genet* **68**: 208-13.

Romero-Ramos, M., P. Vourc'h, H.E. Young, P.A. Lucas, Y. Wu, O. Chivatakarn, R. Zaman, N. Dunkelman, M.A. el-Kalay, and M.F. Chesselet. 2002. Neuronal differentiation of stem cells isolated from adult muscle. *J Neurosci Res* **69**: 894-907.

Rudnicki, M.A., T. Braun, S. Hinuma, and R. Jaenisch. 1992. Inactivation of MyoD in mice leads to up-regulation of the myogenic HLH gene Myf-5 and results in apparently normal muscle development. *Cell* **71**: 383-90.

Rudnicki, M.A., P.N. Schnegelsberg, R.H. Stead, T. Braun, H.H. Arnold, and R. Jaenisch. 1993. MyoD or Myf-5 is required for the formation of skeletal muscle. *Cell* **75**: 1351-9.

Sabourin, L.A., A. Girgis-Gabardo, P. Seale, A. Asakura, and M.A. Rudnicki. 1999. Reduced differentiation potential of primary MyoD-/- myogenic cells derived from adult skeletal muscle. *J Cell Biol* **144**: 631-43.

Saito, Y. and I. Nonaka. 1994. Initiation of satellite cell replication in bupivacaine-induced myonecrosis. *Acta Neuropathol (Berl)* **88**: 252-7.

Salman, M.S., C. Ackerley, C. Senger, and L. Becker. 2002. New insights into the neuropathogenesis of molybdenum cofactor deficiency. *Can J Neurol Sci* **29**: 91-6.

Schilham, M.W., M.A. Oosterwegel, P. Moerer, J. Ya, P.A. de Boer, M. van de Wetering, S. Verbeek, W.H. Lamers, A.M. Kruisbeek, A. Cumano, and H. Clevers. 1996. Defects in cardiac outflow tract formation and pro-B-lymphocyte expansion in mice lacking Sox-4. *Nature* **380**: 711-4.

Schultz, E. 1976. Fine structure of satellite cells in growing skeletal muscle. *Am J Anat* **147**: 49-70.

Siomi, M.C., H. Siomi, W.H. Sauer, S. Srinivasan, R.L. Nussbaum, and G. Dreyfuss. 1995. FXR1, an autosomal homolog of the fragile X mental retardation gene. *Embo J* **14**: 2401-8.

Sock, E., K. Schmidt, I. Hermanns-Borgmeyer, M.R. Bosl, and M. Wegner. 2001. Idiopathic weight reduction in mice deficient in the high-mobility-group transcription factor Sox8. *Mol Cell Biol* **21**: 6951-9.

Stallmeyer, B., G. Drugeon, J. Reiss, A.L. Haenni, and R.R. Mendel. 1999a. Human molybdopterin synthase gene: identification of a bicistronic transcript with overlapping reading frames. *Am J Hum Genet* **64**: 698-705.

Stallmeyer, B., G. Schwarz, J. Schulze, A. Nerlich, J. Reiss, J. Kirsch, and R.R. Mendel. 1999b. The neurotransmitter receptor-anchoring protein gephyrin reconstitutes molybdenum cofactor biosynthesis in bacteria, plants, and mammalian cells. *Proc Natl Acad Sci U S A* **96**: 1333-8.

Stover, J.F., K. Lowitzsch, and O.S. Kempski. 1997. Cerebrospinal fluid hypoxanthine, xanthine and uric acid levels may reflect glutamate-mediated excitotoxicity in different neurological diseases. *Neurosci Lett* **238**: 25-8.

Tapscott, S.J., A.B. Lassar, and H. Weintraub. 1992. A novel myoblast enhancer element mediates MyoD transcription. *Mol Cell Biol* **12**: 4994-5003.

Teboul, L., D. Gaillard, L. Staccini, H. Inadera, E.Z. Amri, and P.A. Grimaldi. 1995. Thiazolidinediones and fatty acids convert myogenic cells into adipose-like cells. *J Biol Chem* **270**: 28183-7.

van de Wetering, M., M. Oosterwegel, K. van Norren, and H. Clevers. 1993. Sox-4, an Sry-like HMG box protein, is a transcriptional activator in lymphocytes. *Embo J* **12**: 3847-54.

van der Klei-van Moorsel, J.M., L.M. Smit, M. Brockstedt, C. Jakobs, C. Dorche, and M. Duran. 1991. Infantile isolated sulphite oxidase deficiency: report of a case with negative sulphite test and normal sulphate excretion. *Eur J Pediatr* **150**: 196-7.

van Gennip, A.H., N.G. Abeling, A.E. Stroomer, H. Overmars, and H.D. Bakker. 1994. The detection of molybdenum cofactor deficiency: clinical symptomatology and urinary metabolite profile. *J Inherit Metab Dis* **17**: 142-5.

Venuti, J.M., J.H. Morris, J.L. Vivian, E.N. Olson, and W.H. Klein. 1995. Myogenin is required for late but not early aspects of myogenesis during mouse development. *J Cell Biol* **128**: 563-76.

Vujic, M., T. Rajic, P.N. Goodfellow, and M. Stevanovic. 1998. cDNA characterization and high resolution mapping of the human SOX20 gene. *Mamm Genome* **9**: 1059-61.

Wagner, T., J. Wirth, J. Meyer, B. Zabel, M. Held, J. Zimmer, J. Pasantes, F.D. Bricarelli, J. Keutel, E. Hustert, and et al. 1994. Autosomal sex reversal and campomelic dysplasia are caused by mutations in and around the SRY-related gene SOX9. *Cell* **79**: 1111-20.

Wegner, M. 1999. From head to toes: the multiple facets of Sox proteins. *Nucleic Acids Res* **27**: 1409-20.

Wuebbens, M.M. and K.V. Rajagopalan. 1993. Structural characterization of a molybdopterin precursor. *J Biol Chem* **268**: 13493-8.

Yamamoto, N., S. Akiyama, T. Katagiri, M. Namiki, T. Kurokawa, and T. Suda. 1997. Smad1 and smad5 act downstream of intracellular signalings of BMP-2 that inhibits myogenic differentiation and induces osteoblast differentiation in C2C12 myoblasts. *Biochem Biophys Res Commun* **238**: 574-80.

Yu, Z.F., A.J. Bruce-Keller, Y. Goodman, and M.P. Mattson. 1998. Uric acid protects neurons against excitotoxic and metabolic insults in cell culture, and against focal ischemic brain injury in vivo. *J Neurosci Res* **53**: 613-25.

Yun, K. and B. Wold. 1996. Skeletal muscle determination and differentiation: story of a core regulatory network and its context. *Curr Opin Cell Biol* **8**: 877-89.

Zhang, W., R.R. Behringer, and E.N. Olson. 1995a. Inactivation of the myogenic bHLH gene MRF4 results in up-regulation of myogenin and rib anomalies. *Genes Dev* **9**: 1388-99.

Zhang, Y., J.P. O'Connor, M.C. Siomi, S. Srinivasan, A. Dutra, R.L. Nussbaum, and G. Dreyfuss. 1995b. The fragile X mental retardation syndrome protein interacts with novel homologs FXR1 and FXR2. *Embo J* **14**: 5358-66.

Curriculum vitae

I.   Personal Data

Full Name: Lee, Heon-Jin

E-mail: protist@hitel.net; hlee3@gwdg.de

Date of Birth: 5th August, 1971.

Sex: male

Present Address: Annastr. 17. App.38 D-37075, Goettingen, Germany

Nationality: Korea

Marital Status: Single

II.   Educational Background:

Mar. 1990 - Feb. 1997   Department of Microbiology, Pusan National University

Jan. 1992 - May. 1994   Military Service (Army)

Mar. 1997 - Feb. 1999   Department of Biochemistry of Medical School, Pusan National University (Master of Medicine)

Thesis Topics: "Role of NF-kappaB in the autooxidized dopamine-induced apoptosis of PC12 cells"

Jun. 2000 - Jul. 2003   Doctorate of Philosophy (Ph.D)

Institute of Human Genetics, Georg-August-Universität, Göttingen, Germany.

III.   Occupation:

Employed by the Korea Research Institute of Bioscience and Biotechnology, from January 1999 to February 2000.

IV.   Publication:

1. Kang, C. D., Jang, J. H., Kim, K. W., **Lee, H. J**., Jeong, C. S., Kim, C. M., Kim, S. H., and Chung, B. S. (1998) Activation of c-jun N-terminal kinase/stress-activated protein kinase and the decreased ratio of Bcl-2 to Bax are associated with the autooxidized dopamine-induced apoptosis in PC12 Cells. *Neurosceince Letters* **256**, 37-40.

2. Kang CD, Ahn BK, Jeong CS, Kim KW, **Lee HJ**, Yoo SD, Chung BS, Kim SH Downregulation of JNK/SAPK Activity Is Associated with the Cross-Resistance to P-Glycoprotein-Unrelated Drugs in Multidrug-Resistant FM3A/M Cells Overexpressing P-Glycoprotein. *ExpCell Res* 2000 Apr 10, **256(1),** 300-307.

3. Lee HJ, Kim SH, Kim KW, Um JH, Lee HW, Chung BS, Kang CD Antiapoptotic role of NF-kappaB in the auto-oxidized dopamine-induced apoptosis of PC12 cells. *J Neurochem* 2001 Jan, **76(2)**, 602-9.

4. Lee HJ, Adham IM, Schwarz G, Kneussel M, Sass JO, Engel W, Reiss J Molybdenum cofactor-deficient mice resemble the phenotype of human patients *Hum Mol Genet* 2002 Dec 15, **11(26)**, 3309-17.

Lee, Heon Jin

Lebenslauf

Persönliche Daten: Heon-Jin Lee

Geboren am 5.August 1971 in Pusan, Süd-Korea

Als Sohn von Yoon-Doo Lee und Il-Rae Lee, geb. Roh

Staatsangehörigkeit: koreanisch

Ausbildung:

März 1978 – Februar 1984: Grundschule in Pusan, Süd-Korea

März 1984 – Februar 1990: Gymnasium in Pusan, Süd-Korea

März 1990 – Februar 1997: Department of Microbiology, Pusan National Universität, Süd-Korea

Januar 1992 – Mai 1994: Militärdienst in Süd-Korea

März 1997 – Februar 1999: Department of Biochemistry of Medical school, Pusan National Universität, Süd-Korea mit Master of Medicine Abschluss (Thema: "Role of NF-kappaB in the autooxidized dopamine- induced apoptosis of PC12 cells")

Juni 2000 – Juli 2003: Beginn der Doktorarbeit unter der Leitung von Prof. Dr. med. W. Engel in der Institut für Humangenetik, Georg-August-Universität Göttingen.

ACKNOWLEDGEMENTS